Interfacial Viscoelastic moduli of bare, surfactant-laden and nanoparticle-laden interfaces oscillating in a weak gel

Ahmad Jaber

Ecole Doctorale SIMPPé

Laboratoire Réactions et Génie des Procédés

Thèse

Présentée et soutenue publiquement pour l'obtention du titre de

DOCTEUR DE l'UNIVERSITE DE LORRAINE

Mention: Génie des Procédés, des Produits et des Molécules

par **Ahmad JABER**

Sous la co-direction de **THIBAULT ROQUES-CARMES ET TAYSSIR HAMIEH**

Interfacial Viscoelastic moduli of bare, surfactant-laden and nanoparticle-laden interfaces oscillating in a weak gel.

Le 23 Juin 2023

Membres de Jury :

Rapporteurs	Nicolas HUANG	Professeur, CNRS, Université Paris-Saclay, Paris.
	Delphine HUC-MATHIS	Maitre de Conférence, Institut AgroParisTech, Paris.
Examinateurs	Joumana TOUFAILY (Présidente de jury)	Professeur, Université Libanaise, Beyrouth, Liban.
	Isabelle HENAUT	Ingénieure de recherche, Institut Français du Pétrole, Paris.
Directeurs de thèse	Thibault ROQUES-CARMES	Maitre de Conférences, Directeur de thèse, Université de Lorraine, Nancy.
	Tayssir HAMIEH	Professeur, Codirecteur de thèse, Université Libanaise, Beyrouth, Liban.
Invités	Lazhar BENYAHIA	Professeur, Université du Mans, IMMM, Le Mans.
	Alain DURAND	Professeur, Université de Lorraine, Nancy.
	Philippe MARCHAL	Ingénieur de recherche, CNRS, Université de Lorraine, Nancy
	Marianne PARENT	Maitre de conférences, Université de Lorraine, Nancy.

Remerciements

Au nom de Dieu, le miséricordieux

Je suis reconnaissant pour cette opportunité unique dans ce travail de recherche, je remercie mes co-directeurs de thèse Pr. Tayssir Hamieh et Dr. Thibault Roques-Carmes pour leur confiance et leur suivi durant ces années, puis en particulier Pr. Lazhar Benyahia qui m'a accueilli et guidé durant mes manipulations et mon séjour au sein de l'IMMM à Le Mans, nos échanges m'ont enrichi au niveau professionnel et personnel.

Je suis reconnaissant aussi à ma famille, au Liban ou en Europe, surtout mes parents qui m'ont accompagné durant cette aventure dans la joie que dans le doute en partageant leurs expériences comme chercheurs, la sagesse et les connaissances de mon père demeurent mon inspiration et ma mère qui a toujours veillé sur mon bien être et sur mon progrès. Mon frère Mahdi et ma tante qui m'ont tant aidé durant mon séjour et m'ont rappelé le sentiment de familiarité ici en europe, et ma sœur et mon frère au Liban, Sarah et M. Ali.

J'ai eu le plaisir de faire la connaissance de nombreux amis et collègues au fil de ces années: Yuwen, merci pour ton humour et ton support, notre groupe fut animé grâce à toi. Théo mon camarade de bureau qui m'a aidé à m'intégrer aisément dans cette belle équipe et nos discussions fument enrichissantes. Pareil pour « monsieur » Gireesh, avec qui j'ai pu échanger sur des sujets divers et assez « lourds », faisant preuve d'humilité et d'humour. Lingsam, la favorie et la « cheffe » de l'équipe. Marisol et nos drôles interactions, Elie, Sandra, Ahmad, Joao, Chayanan, Trang, Tharin, Paul, Jiafeng et pleins d'autres... merci pour les belles souvenir au Mans. Diego, qui a été ma référence à Nancy, Mohammad sur qui on compte pour prendre le relais après moi, Dayan, Felipe, Adilson, Yu. Je tiens aussi à remercier les techniciens et permanents des équipes PCI et GEMICO au Mans et Nancy respectivement.

Je clôture ce message avec un sentiment profond de gratitude et de fierté, en exprimant toute ma reconnaissance à Dieu, c'est mon espoir de rester sur la bonne Voie de la sagesse et de la vertu, c'est grâce à Votre pouvoir et Votre volonté que je suis arrivé à finir ce projet, Al Hamdulillah.

Résumé

Mots clés : Rhéologie interfaciale, Goutte oscillante, gel thermosensible, tensioactif, nanoparticules

Dans les pays industrialisés, on voit apparaître une forte demande pour des produits à propriété d'usages. Les industries, notamment chimiques, doivent répondre à de nombreux challenges. Les technologies et produits qui se développent concernent le design, la formulation et les procédés de fabrication dans un contexte de développement durable et d'économie circulaire. En fait, il devient nécessaire de mettre en place des recherches portant simultanément sur la formulation et le procédé de fabrication de produits formulés. Ces produits nano ou micro-structurés qui combinent plusieurs fonctions concernent principalement des milieux et fluides complexes tels que les fluides non-Newtonien (gels, solution de polymères, poudres, dispersions colloïdales, et les émulsions. Dans ce contexte, la compréhension des phénomènes interfaciaux, et plus particulièrement de la physico-chimie des phénomènes se produisant à toutes les interfaces, devient nécessaire pour appréhender à la fois la formulation, le design, la fabrication et l'utilisation de ces produits formulés. Le concept utilisé pour caractériser les interfaces est la tension superficielle ou interfaciale. Elle est reliée à la probabilité de compatibilité entre deux phases. Il s'agit également de l'énergie à fournir pour augmenter la surface d'une interface mais également de la force qui s'oppose à l'accroissement de l'interface. Cette notion est très importante mais elle caractérise l'interface à l'équilibre ce qui n'est pas toujours suffisant pour connaitre l'organisation des molécules adsorbées aux interfaces (particules, polymères, protéines et tensioactifs). C'est une des raisons pour lesquelles la rhéologie interfaciale a été développée. Le principe de la rhéologie interfaciale est basé sur l'analyse de la réponse de l'interface soumise à une sollicitation ou déformation. La déformation de l'interface peut être produite par dilatation ou cisaillement. Dans le cas de la rhéologie interfaciale par dilatation, la goutte oscillante et la balance de Langmuir sont les deux techniques couramment utilisées. Elles sont généralement utilisées avec des polymères et tensioactifs adsorbées. Dans le cas de la rhéologie interfaciale par

cisaillement, l'interface est directement cisaillée par un anneau. Ce type d'appareil est principalement utilisé avec des particules adsorbées à l'interface. Dans le cadre de ce travail de thèse, la méthode de la goutte oscillante a été sectionné pour effectuer les mesures de rhéologie interfaciale.

Les mesures de rhéologie interfaciale donnent accès à la viscoélasticité interfaciale qui peut être divisé en deux modules: module élastique et module visqueux interfaciaux. De nombreuses données sont disponibles dans la littérature avec des couches de tensioactifs, polymères et protéines adsorbées à l'interface. Les mesures semblent pertinentes quand la goutte et la phase continue ont des viscosités faibles et sont des fluides Newtoniens. Cependant, la majorité des produits formulés sont non Newtoniens et possèdent un comportement rhéologique complexe basé sur la thixotropie, des seuils d'écoulement et la viscoélasticité. Cet aspect est le point clef de cette thèse. Que se passe-t-il en termes de rhéologie interfaciale dans le cas d'une goutte oscillante qui oscille dans un fluide complexe. Peut-on ignorer la contribution de la phase continue quand on estime la viscoélasticité interfaciale? La philosophie suivie dans ce travail est de comprendre comment utiliser les appareils de rhéologie interfaciale de façon intelligente et pertinente. Est-ce que la contribution de la phase continue peut devenir importante quand on utilise des fluides non-Newtoniens sous forme de gel faible? Seul des gels faibles seront considérés dans ce travail car un gel fort empêcherait la goutte d'osciller.

En termes de méthodologie suivie dans ce travail, la sélection du bon système chimique a été une étape importante. Il a été décidé de travailler avec une goutte oscillant dans une phase continue aqueuse complexe. En termes d'huile, celle-ci devait avoir une faible viscosité afin de pouvoir facilement se compresser et se dilater. Une huile appelée indopol a été finalement sélectionnée comme huile modèle. Elle présente une viscosité de l'ordre de 10 mPa.s. Pour la phase continue, l'objectif était d'identifier un composé permettant d'obtenir un système sous forme liquide ou gel mais sans activité interfaciale. Il s'agissait d'obtenir un gel faible avec un seuil d'écoulement pour une contrainte de l'ordre de 1 Pa. Le κ-carraghénane (biopolymère) a été finalement retenu dans le cadre de cette thèse. Il s'agit d'un biopolymère linéaire à base de polysaccharide sulfaté provenant d'algue rouge, ce biopolymère peut former de manière réversible des gels faibles selon l'histoire thermique et la concentration en solution. Ces deux paramètres définissent la force du gel.

Dans une première partie, nous avons travaillé avec des systèmes sans additifs interfaciaux de type tensioactif ou particule. La mesure de la viscoélasticité interfaciale donne de nombreuses informations sur la possibilité des agents de surface (tensioactif, particules, protéines) à texturer une interface. Cependant, nous avons mis en évidence que la contribution de la rhéologie de la phase continue ne peut pas être négligée quand la phase continue est sous la forme d'un gel faible. Pour cela, des mesures de gouttes oscillantes de solution d'indopol apolaire (huile de polyisobutène) dans des solutions aqueuses contenant du κ-carraghénane (KC) ont été conduites. Le point clef de cette étude est que le κ-carraghénane n'a aucune activité interfaciale. En jouant sur la température (T = 30 – 15°C) et la concentration en biopolymère (2 – 6 g/L), il a été possible de contrôler la transition sol-gel de la solution contenant le κ-carraghénane. Lorsque la goutte d'indopol oscille dans une solution de κ-carraghénane sous forme de gel faible (T = 15 et 20°C, et [κ-carraghénane] = 5-6 g/L), un comportement élastique de l'interface apparaît et augmente avec la force du gel (Figure 1). L'autre résultat majeur, est que la méthode de goutte oscillante peut être un indicateur très sensible de la présence de gel faibles dans des solutions, ce qui est très dur à détecter via des rhéomètres classiques.

Dans le chapitre suivant, un tensioactif est introduit dans le système afin de sonder l'interface et surtout le comportement rhéologique en présence d'une couche de tensioactif adsorbée à l'interface liquide/liquide. La présence de cette couche de tensioactif a pour objectif d'introduire un comportement viscoélastique au niveau de l'interface. Il s'agit ici, d'étudier comment de la solution dans la phase continue, sous la forme d'un gel faible, impacte les propriétés interfaciales des modules viscoélastiques interfaciaux d'une goutte oscillante en présence d'un tensioactif. Dans un premier temps, le choix du tensioactif s'avère important. Dans notre système, une goutte montante d'indopol est mise en contact d'une phase aqueuse contenant du κ-carraghénane, nous avons voulu éviter de possibles interactions entre les deux espèces. De ce fait, on a opté à ce que le tensioactif soit introduit dans la phase huileuse d'indopol dans la goutte ce qui requiert un tensioactif qui a une meilleure affinité pour l'huile que pour l'eau. En conséquence, le tensioactif doit posséder une équilibre hydrophile-lipophile (HLB) inférieure à 10. Des tensioactifs de type monoléate de sorbitan, appelé plus couramment, Span® 80 ont été sélectionnés dans cette étude.

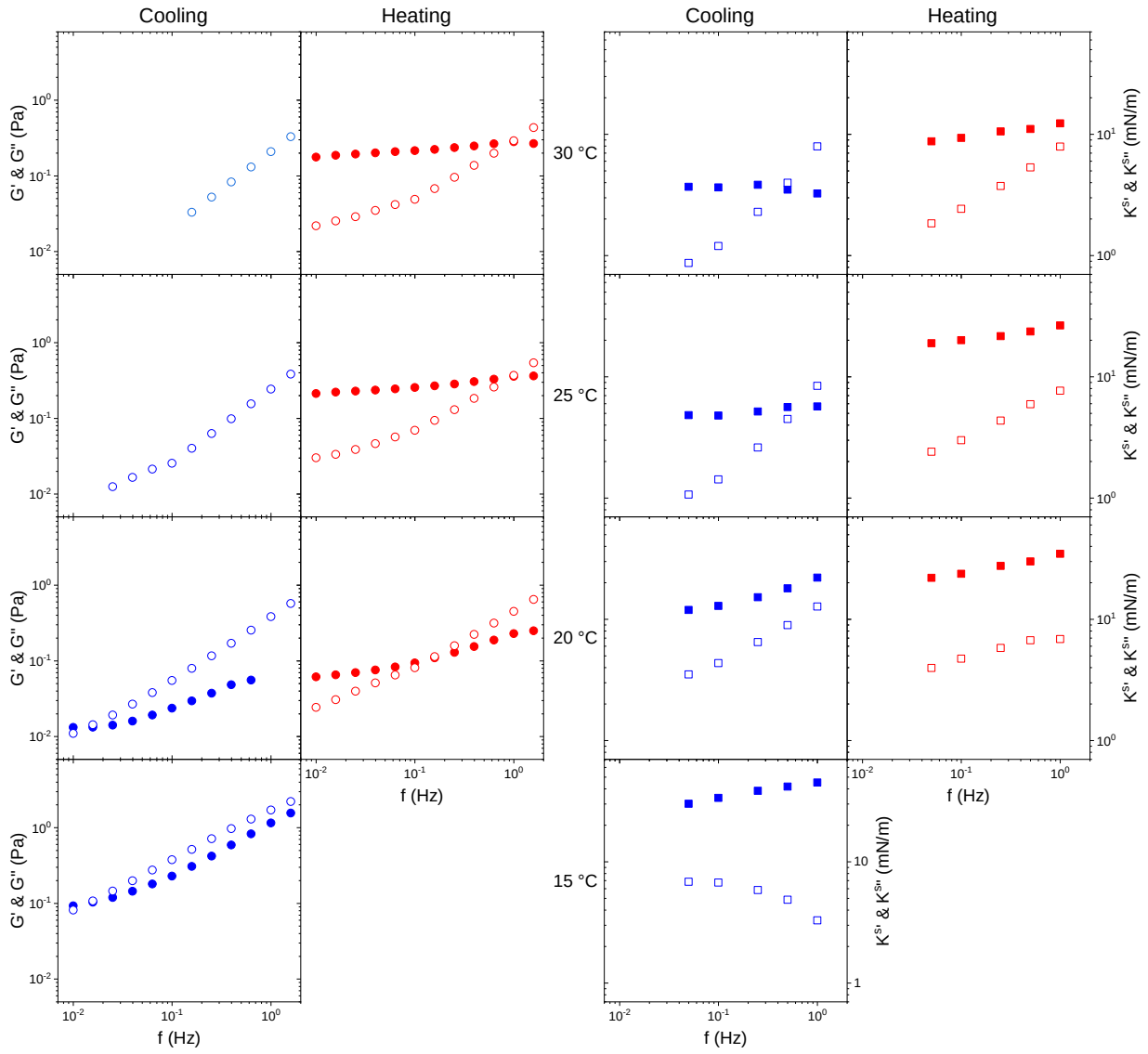

Figure 1: Variation de G' (●), G'' (○), et du module interfacial élastique K^{s}' (■) et visqueux K^{s}'' (□) pour une concentration de 5 g/L de κ-carrageenan à différentes températures durant le refroidissement et le réchauffage.

Dans le chapitre suivant, un tensioactif est introduit dans le système afin de sonder l'interface et surtout le comportement rhéologique en présence d'une couche de tensioactif adsorbée à l'interface liquide/liquide. La présence de cette couche de tensioactif a pour objectif d'introduire un comportement viscoélastique au niveau de l'interface. Il s'agit ici, d'étudier comment de la solution dans la phase continue, sous la forme d'un gel faible, impacte les propriétés interfaciales

Logiquement, la tension interfaciale indopol/eau diminue avec la concentration en tensioactif et se stabilise autour de quantité de 0,05 et 0,1% en Span. La quantité de span adsorbée, i.e. l'excès de surface, est de $\Gamma = 2.13.10^{-6}$ mol/m^2. Cette valeur indique la présence d'une couche de tensioactif à l'interface liquide/liquide. Ces deux dernières concentrations de Span (0,05 et 0,1%) sont utilisées pour les expériences de rhéologie interfaciale. Nos résultats de mesures de rhéologie interfaciale, mettent en avant que l'effet de la couche de tensioactif adsorbée sur les propriétés viscoélastique interfaciale dépend fortement de l'état dans lequel se trouve la phase aqueuse contenant le κ-carrageenan. Quand la phase aqueuse est sous forme liquide, la présence de Span augmente l'élasticité de l'interface (Figure 2, T = 30 et 25°C). L'élasticité de l'interface en présence de span avec et sans KC est identique, et supérieure à celle du KC seul. On déduit que la couche de Span joue le rôle le plus important dans l'élasticité de l'interface. Autrement dit, l'élasticité de l'interface vient principalement de la couche de tensioactif adsorbée.

A l'opposé, quand le KC devient un gel, un comportement inattendu est observé (Figure 2, 15 et 20°C). L'élasticité interfaciale est plus grande en absence de Span qu'en présence de Span. De plus, l'élasticité interfaciale en présence de KC seul est plus grande que celle en présence de Span sans KC. Ces données mettent en évidence que le gel de la phase continue joue un rôle majeur dans la viscoélasticité de l'interface en comparaison de celle du tensioactif. Cela confirme que lorsque la phase continue est sous forme de gel, elle ne peut pas être négligée lors de la mesure de rhéologie interfaciale. L'élasticité interfaciale est plus faible en présence de Span lorsque la phase continue aqueuse est sous forme de gel. L'origine de cette diminution de la viscoélasticité en présence de span à l'interface reste encore non élucidée de façon claire. L'élasticité finale semble dépendre des interactions entre la couche de tensioactif molle à l'interface et le gel dur de la phase continue. Le gel de la phase continue semble fragiliser l'interface recouverte de tensioactif.

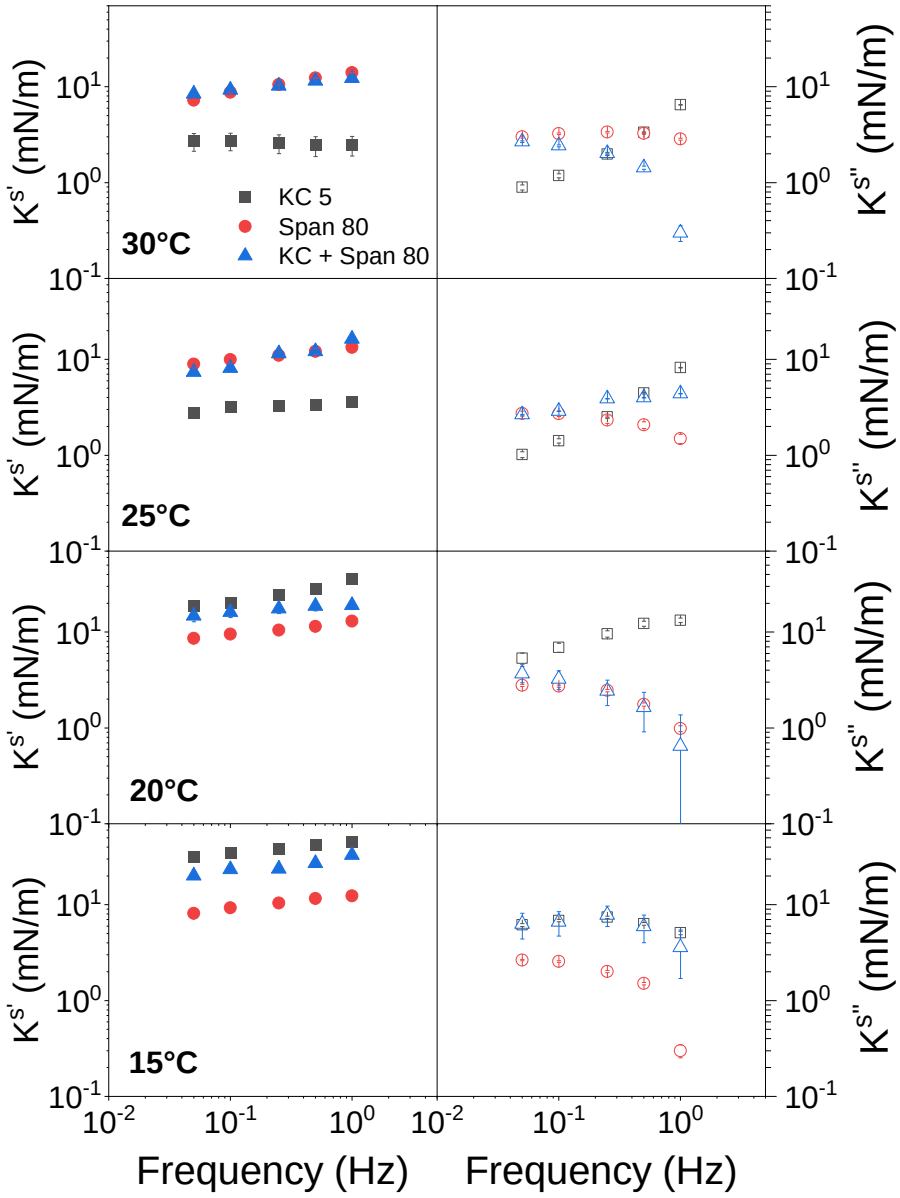

Figure 2: Variation du module interfacial élastique Ks' (■) et visqueux Ks'' (□) en présence de KC 5g/L dans la solution aqueuse sans Span ("KC 5"), ou en présence de Span 80 0.05%w/w adsorbé à l'interface dans l'eau sans KC ("Span 80"), et une combinaison des 2, i.e. KC 5g/L dans la phase continue aqueuse et 0.05%w/w Span 80 dans l'indopol ("KC + Span 80").

Une interprétation possible de ce phénomène est le glissement « slippage » entre la couche de tensioactif adsorbée et l'hydrogel donnant lieu à un phénomène appelé shear banding ou bande de cisaillement. Quand la goutte oscille, des bandes de cisaillement sont créés et le gel dur cisaille l'interface. Par conséquent, la goutte se déforme plus facilement. Dans ce cas, la couche de span adsorbée joue le rôle de lubrifiant à l'interface entre la goutte d'indopol et la phase continue. Une autre approche consiste à considérer que la dilatation de l'interface est opposée à la déformation élastique de la phase continue, réduisant la réponse du gel autour de la goutte.

Les tendances observées en présence et en absence de gel ont été confirmés par d'autres expériences à différentes concentrations de KC (3-6 g/L), span (0,05 et 0,1%) et différentes températures (15-30 °C).

Dans une seconde étape, des émulsions ont été préparées avec ces formulations. Afin de mettre en avant les phénomènes interfaciaux, des émulsions concentrées avec des fractions volumiques de gouttelettes plus élevées que 60% doivent être préparées. Cependant, la présence de span conduit à formuler des émulsions inverses E/H ce qui indique que la phase gel due au KC se situe dans les gouttes d'eau plutôt que dans la phase continue huileuse. En dépit de ces contraintes, une tentative d'exploration de relations entre les propriétés rhéologiques volumiques et interfaciales est conduite. Les mesures de rhéologies de l'émulsion révèlent qu'en absence de KC, le module élastique est plus élevé que le module visqueux dans toute la gamme de fréquence étudiée. L'addition de gel faible de KC (KC = 5 g/L) ne change pas de façon significative le comportement rhéologique de l'émulsion. Une faible mais régulière augmentation du module élastique de l'émulsion se produit lorsque la température est diminuée de 30 °C à 15 °C (de liquide à gel). Cela indique que G' augmente quand la phase dispersée passe d'un état liquide à un gel. Cependant, cette variation de G' apparaît mesurée et n'est pas significative en comparaison de la contribution interfaciale du film de tensioactif autour des gouttes d'eau. Il est donc difficile de conclure quant à une possible corrélation entre les propriétés rhéologiques volumiques et interfaciales de l'émulsion étant donné que la phase gel se situe dans les gouttes dans les émulsions alors que le gel était dans la phase continue lors des analyses de rhéologie interfaciale. Il aurait fallu travailler avec des émulsions H/E.

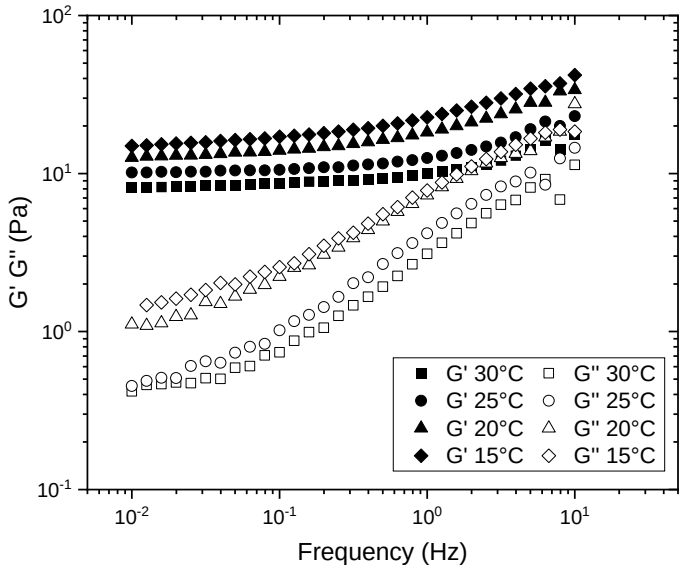

Figure 3: Module élastique G' et visqueux G'' de l'émulsions en présence de Span 80 à des températures de 30°C, 25, 20 et 15°C.

Dans le chapitre suivant, l'effet de la présence de nanoparticules à l'interface liquide/liquide sur les propriétés de rhéologie interfaciale de gouttes d'indopol oscillants dans des solutions aqueuses contenant du KC sous la forme de gel ou de liquide a été étudié. Il s'agit d'une configuration équivalente à celle du chapitre précédent mais la couche de tensioactif est remplacée par une couche de particules attachée à l'interface. Les mesures de rhéologie interfaciale utilisant la goutte oscillante avec des particules ne sont pas une tâche aisée et reste un challenge. Par exemple, des essais précédant dans l'équipe lors d'une thèse ont mis en avant la difficulté de ce type de mesure notamment en raison de la formation de « croute » de particules à la surface de la goutte qui perturbent fortement le signal. Il apparaît également que ce type de mesure avec des particules est rarement reportée dans la littérature. Dans le cadre de cette étude, le choix des particules et de leurs positions initiales dans la phase continue ou dans la goutte nous a semblé jouer un rôle non-négligeable. Dans une première partie, cet aspect a été étudié. La silice sera utilisée comme particule modèle. L'objectif est de trouver des particules de silice qui s'adsorbent à l'interface des gouttes d'indopol et de disperser les particules initialement dans l'indopol pour éviter les interactions entre le KC et les particules. Cela permet également de n'avoir que du KC dans la phase continue comme dans les chapitres précédents. Le critère principal de sélection a été basé sur l'apparition de viscoélasticité interfaciale en présence de

silice. Ces mesures préliminaires d'élasticité ont été effectuée sans KC dans la phase continue. Des silices fumées Aérosil® modifiée en surface ont été testées. L'objectif a été de trouver le ou les types de silice qui permettent d'obtenir une valeur détectable du module élastique interfacial permettant d'attester de l'adsorption des particules à la surface des gouttes d'indopol. En effet, pour s'adsorber à l'interface, les particules doivent diffuser du cœur de la goutte vers l'interface, franchir une barrière énergétique pour ensuite s'adsorbée. Pour l'ensemble des particules, il est important de noter l'absence d'élasticité de l'interface. Ceci indique l'absence d'adsorption des particules à l'interface. Ce résultat est surprenant, de prime abord, car ces particules ont déjà été utilisées pour stabiliser des émulsions de Pickering avec des huiles assez similaires. De plus, les photographies en microscopie confocale confirmaient l'adsorption de ces particules à la surface des gouttes après émulsification par des ultra-sons. Ceci établit que l'adhésion des particules à l'interface liquide/liquide peut-être différente entre les émulsions et en rhéologie interfaciale car le mélange ou l'énergie d'agitation est fondamentale pour adsorber les particules. Durant le procédé d'émulsification, la migration et l'adsorption des particules à l'interface liquide/liquide est favorisée par le flux et l'écoulement produit par le mobile d'agitation. A l'opposé, avec la goutte oscillante, la seule façon pour les particules pour aller à l'interface est le mécanisme de diffusion. Le temps de diffusion est long. De plus, pour traverser la barrière d'activation pour s'adsorber, de l'énergie mécanique est nécessaire. Pour toutes ces raisons, nous voyons qu'il est plus facile pour les particules d'aller à l'interface durant l'émulsification. Pour favoriser l'adsorption des particules à l'interface liquide/liquide durant les analyses de rhéologie interfaciale l'isopropanol (IPA) est ajouté comme co-solvant dans l'indopol. Les particules de silice se dispersent mieux en présence d'IPA puisqu'il modifie les interactions stériques de la silice avec la phase huileuse d'indopol. De plus, l'IPA est volatile, ce qui permet une rapide évaporation de ce dernier. Dans notre système, l'IPA diminue la tension interfaciale et favorise et la diffusion à l'interface avant de s'évaporer. En présence d'IPA, des modules élastiques de l'ordre de 40-50 mN/m sont obtenus. Le même type d'expérience avec du PDMS en remplacement de l'indopol permet d'obtenir également des modules élastiques non-négligeables proches de 20 mN/m. Tous ces résultats mettent en évidence la présence de particules de silice à la surface des gouttes via l'ajout d'IPA.

Les mesures de rhéologie interfaciale sont conduites à l'aide d'une goutte oscillante d'indopol contenant de l'isopropanol. La phase aqueuse continue contient du KC à une concentration de 5

g/L. La concentration de silice est fixée à 0,5% par rapport à l'indopol. Durant l'expérience, la température est variée de 30°C à 15°C pour que le KC passe de l'état liquide à gel (Figure 4). Lorsque la phase continue aqueuse contenant le KC est sous forme liquide (T = 30 et 25°C), le module visqueux interfacial suit une loi de puissance avec la fréquence alors que le module élastique reste faible et constant. La valeur de l'élasticité augmente d'un ordre de grandeur en présence de particules adsorbées à l'interface. Cela met en évidence a forte adsorption des particules à l'interface. Cependant, l'évolution du module visqueux avec la fréquence est différente en absence et en présence de particules. Sans particules, le module visqueux augmente de façon importante avec la fréquence, alors qu'en présence de particules ce module parait indépendant de la fréquence. Le module visqueux est également plus élevé en présence de silice. Il est également intéressant d'analyser les data lorsque la phase continue aqueuse contenant le KC est sous forme de gel (T = 15°C), la présence des particules ne modifie pas la forme des courbes K^s' and K^s'' en fonction de la fréquence. Cela met en avant que la forme des courbes dépend principalement du gel de la phase continue. Cependant, la présence de silice adsorbée augmente le caractère élastique de l'interface. Cela implique que l'élasticité du système est la « somme » des contributions élastiques de l'interface due aux particules adsorbées et celle du gel, autrement dit, l'interaction entre les particules de silice dures et le gel « dur » de la phase continue augmente l'élasticité du système.

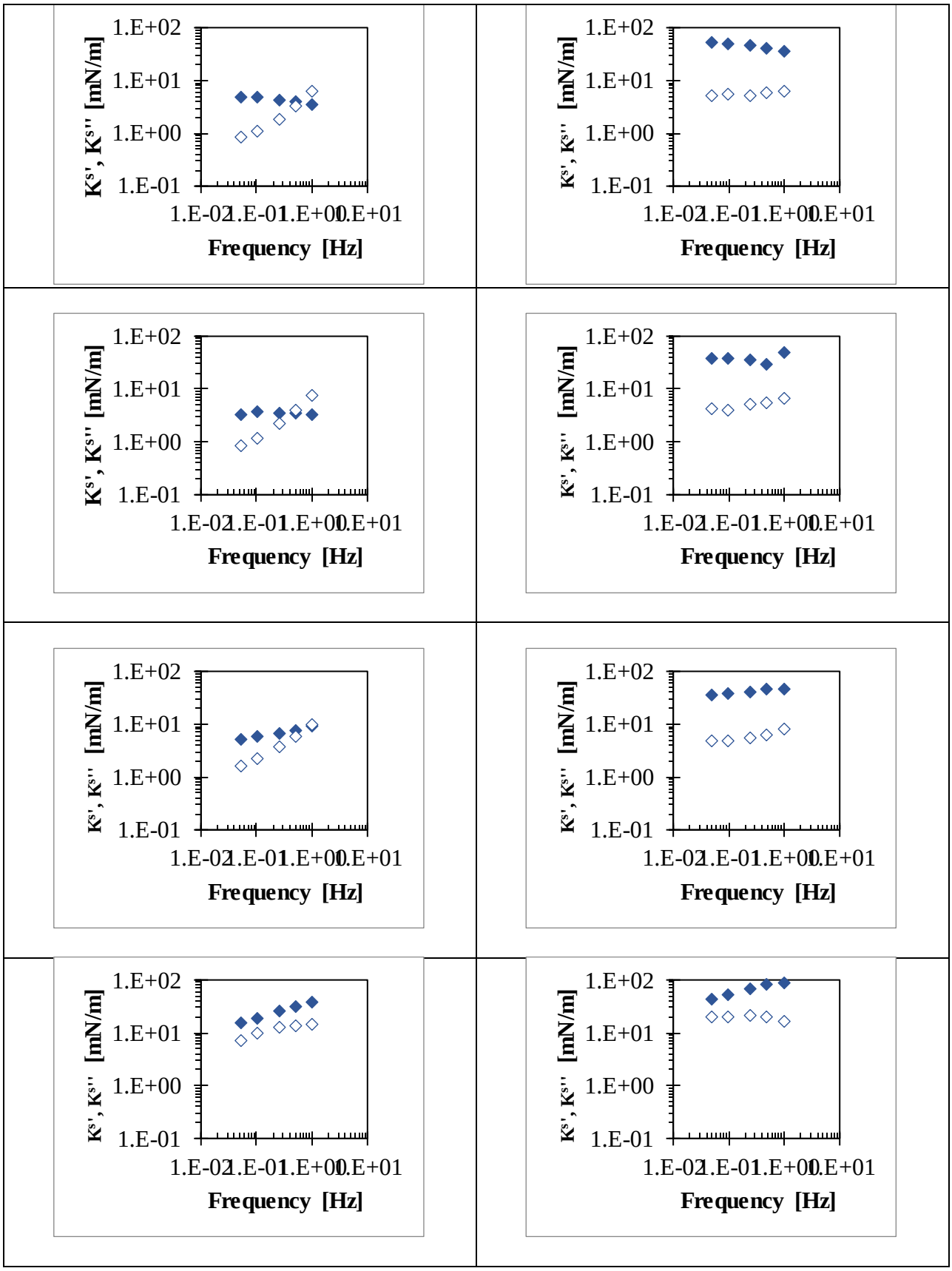
1.E+02
1.E+01
1.E+00
1.E-01
Ks', Ks'' [mN/m]
1.E-02
1.E-01
1.E+00
1.E+01
Frequency [Hz]

Figure 4: Variation du module interfacial élastique Ks' (■) et visqueux Ks" (□) en presence de KC 5g/L in the bulk phase without silica particles (left-hand column) and with 0.5% of silica particles monolayer adsorbed at the interface (right-hand column). In all the cases, the KC concentration is equal to 5 g/L and the isopropanol concentration reads as 10% in the indopol/isopropanol/silica drop phase.

Il nous a paru intéressant de comparer les résultats avec du span et de la silice. Dans les deux cas, la concentration de KC dans la phase continue est identique (5g/L) et la gamme de température reste similaire (T = 15 – 30°C). La seule différence est donc la présence de tensioactifs ou de particules à l'interface indopol/eau-KC. Lorsque la phase continue aqueuse contenant le KC est sous forme liquide (T = 30 et 25°C), la présence de span et de silice augmente l'élasticité de l'interface. Les deux couches adsorbées de particules et tensioactifs augmentent le module élastique interfacial. La valeur du module est plus élevée avec la silice qu'avec le span. Dit différemment, la couche dure de particules produit un module élastique plus élevé que la couche molle de tensioactif. A l'opposé, lorsque la phase continue aqueuse contenant le KC est sous forme de gel (T = 15 °C), la dureté de la couche adsorbée (molle ou dure) impacte de façon importante l'élasticité finale mesurée. L'interaction entre le film adsorbé à l'interface et la phase continue joue le rôle majeur. Quand le gel solide est mis en contact avec l'interface molle recouverte de tensioactif, une interaction dure/mou se produit. Cela produit une diminution du module élastique mesuré en raison de la formation de bande de cisaillement « shear-banding ». Le module interfacial apparent semble tenir compte de la contribution du gel dans la phase continue réduit de la contribution de la couche de span adsorbée. L'inverse se produit quand la goutte recouverte d'une couche de silice dure oscille dans une phase continue sous forme de gel. Une interaction dure/dure se produit. Une augmentation du module élastique apparent se produit. Le module élastique apparent inclue la contribution du gel dans la phase continue et de la contribution de la couche de silice adsorbée.

Summary

Keywords: Interfacial Rheology, Oscillating Drop, Thermo-sensible gel, surfactant, nanoparticles

We present a study implementing the oscillating drop method to probe the oil/water interface, modifiable by surfactants or nanoparticles, while surrounded by a continuous phase of controllable rheology. The key question posed in this work concerns the effect of the rheological properties of the continuous phase on the measurements of interfacial viscoelastic moduli extracted from the compression/expansion of an oscillating drop. With this in mind, the continuous phase consists of a thermo-reversible hydrogel K-carrageenan, selected for its interfacial inactivity but also for its hysteresis after the sol/gel transition which allows to have a gel or liquid at the same temperature according to the thermal history.

In the case of a pure oil/water interface and under conditions where the KC solution is liquid, the elastic modulus of the interface remains weak. When the KC solution becomes a gel, even if it is weak to the point that the solution flows under its own weight, we witness the appearance of an elastic signature in interfacial viscoelastic measures attesting to the contribution of the rheology of the continuous phase being not negligible.

The presence of a surfactant at the oil/water interface, generating an interfacial elastic modulus that increases with the concentration of surfactant in the case of a liquid surrounding medium. In the presence of a weak gel, the interfacial modulus decreases despite that the modulus of the KC gel increases, this is attributed to a pseudo-localization of deformation at the interface. This phenomenon disappears in the case of an interface laden with solid nanoparticles (Pickering effect).

All of this work reveals the importance of deconvoluting interfacial and volume contributions in an interfacial viscoelasticity test of the pendant drop.

Contents

Chapter I: Introduction

Industrialized countries are experiencing rapid growth in customer demand for products with targeted use properties[1,2]. The chemical industries are therefore faced with many challenges. The technologies that are being developed concern both the design of the product and its manufacturing process in a context of sustainable development, bio-compatibility and its future after use[3,4]. In fact, it becomes necessary to mobilize on research concerning simultaneously the formulation and the production engineering of the product. These sophisticated nano and micro-structured products, which combine several functions, mainly concern complex media such as non-Newtonian liquids (gels, water-soluble polymers), powders, colloidal dispersions and emulsions.

In this context, the understanding of the interfacial phenomena and more particularly of the surface properties remains essential to apprehend at the same time the formulation, the design, the manufacture and the use of the highly specialized product. Let us quote two examples. In the field of divided solids, it appears fundamental to control the formulation of powders which is governed by the physicochemical aspects of surface. The solid/liquid interactions, which depend mainly on the surface properties, are notably observed during the impregnation of the solid by the liquid phase and during the dispersion of the divided solid in a liquid. The passage of the liquid/vapor interface through the powder depends strongly on the solid/liquid interactions. After dispersion, solid/liquid interactions are added to solid/solid interactions, the whole governing the phenomena of aggregation and flocculation. Let's take another example from everyday life. Let's take another example from everyday life. Chemical products based on emulsions are encountered in a lot of applications such as foods (milk, mayonnaise, vinaigrette, and ice creams), cosmetic and pharmaceutics (cosmetic creams, sun cream), petroleum oil recovery and bituminous. In these applications, these chemical products are polyphasic systems where several phases (liquid, solid, gas) have to coexist leading to various interfaces. The liquid/liquid interface plays the main role during the fabrication and stabilization since the surface areas can reach values larger than 1000 m^2.

The concept used to characterize the interface is the surface tension or interfacial tension. The surface energy is related to the probability of compatibility between the two species which can be two liquids, a liquid and a gas, a solid and a liquid, or a solid and a gas phase. The exact definition of the interfacial tension reads as the energy needed to increase the surface of the interface. It is expressed, generally, in mJ/m^2 or mN/m. The interfacial tension is traditionally the most widely studied characteristic of the interfacial phenomena. However, this method based on system at equilibrium is not always sufficient to follow the organization of the adsorbed molecules in the adsorption layers at the interfaces[5]. This is the reason why interfacial rheology has been developed[6,7].

The principle of interfacial rheology is to probe the response of the interface (liquid/liquid or liquid/gas) to solicitation. It works out of equilibrium but gives access to the organization of the molecules (surfactants, proteins, and polymers) or particles at the interface. The deformation of the interface can be produced by dilatation or shearing[6,8] [Mendoza 2014, Jaensson 2018]. On the one hand, for interfacial dilatational rheology, drop tensiometry and Langmuir film balance are currently encountered[8–11]. They are mainly used with surfactants and polymers. On the other hand, for interfacial shear rheology, the interface is directly sheared[12–16]. In the framework of this thesis, oscillating drop method has been selected to perform the whole interfacial rheological measurements. This apparatus was available in the two laboratories (Le Mans and Nancy). In addition, one of the aims of this thesis is to set up and implement this apparatus and try to make this type of device as easy to use as a classical rheometer.

The interfacial rheology measurements give access to interfacial viscoelasticity. The latter can be divided into the interfacial elastic contribution and the interfacial viscous component. A lot of data are available in the literature with simple systems such as oil/air, water/air, oil/water interfaces with surfactants, polymers and proteins as well as particles. The results appear relevant when the drop and the continuous phase have low viscosities and, mainly, are Newtonian fluids. However, for real or industrial applications, the fluids are generally non longer Newtonian and display a complex rheological behavior such as thixotropy, yield point fluid, and viscoelasticity. As an example, for Pickering emulsions, which are emulsions stabilized with particles[17,18], a

network of particles can be formed in the continuous phase[15,19–22]. In addition, the presence of proteins and polymers in the continuous phase is also expected to switch the rheological behavior from Newtonian pure liquid to complex fluids in the presence of macromolecules. This aspect is the key point of the thesis. What happens in terms of interfacial rheology when a drop of fluid is oscillating in a complex medium? Can we ignore the contribution of the continuous phase when estimating the interfacial viscoelasticity? The underlying idea and philosophy of this thesis is to understand how to use interfacial rheology apparatus intelligently. Is the contribution of the bulk becoming important when using complex non-Newtonian continuous phase such as a gel? Obviously, only weak gels are considered since a strong gel hinders the oscillation of the drops.

In terms of the methodology followed in this work, the selection of the right chemical system was an important step. It was decided to work with a drop of oil oscillating in an aqueous continuous complex phase. In terms of oil, the oil needs to have a low viscosity in order to be able to oscillate in the system. Dodecane was first considered and tested but it was too sensitive to oxidation under our temperature ramps of 60-30 to 15 °C. Indopol oil, an aliphatic oil of small molecular weight, with a weak viscosity was finally selected as a model oil. Its viscosity is lower than 10 mPa.s. For the continuous phase, the objective was to obtain a system liquid or gel without interfacial activity and forming a weak gel with a flow threshold or yield point lower than 1 Pa. For non-rheological specialist, a yield point of 1 Pa means that the liquid flow under the effect of gravity when you return the bottle. Some preliminary tests were conducted with Carbopol which is composed of high molecular weight crosslinked polyacrylic acid polymers. However, K-carrageenan was finally selected. It is a natural linear sulfated polysaccharide coming from the red algae. This biopolymer was already thoroughly studied and used in the laboratory[23,24]. In water, this biopolymer can form weak gel with a 3-dimensional structure in the continuous aqueous phase []. In addition, we deal with a physical gel since the connections between the biopolymers can be detached when varying some operating conditions. The biopolymer creates a reversible gelation. The liquid-gel transition depends on both the temperature and the concentration of K-carrageenan. These two parameters will then define the strength and the form of the gel.

In this study, this system is used in three successive steps. In a first step, we measure the interfacial viscoelasticity with pure interface with only indopol/water-K-carrageenan. We have a pure interface inside a complex media (water-K-carrageenan). Then, an adsorbed layer is created at this interface. To this aim, surfactant such as Span 80 and silica particles are successively utilized here. In these cases, complex interfacial films are used inside complex medium.

The description of my work will be articulated around three complementary axes briefly presented here.

Chapter II gives the state of the art while the chapter III present the materials and the methods used in this thesis. These two chapters focus mainly on interfacial rheology devoted to oscillating drops.

In chapter IV, the interfacial viscoelasticity of indopol drop oscillating in water containing K-carrageenan is studied. The κ-carrageenan concentration and temperature are varied in order to modulate the liquid and gel behavior as well as the gel properties. The impact of an extremely weak gel on the interfacial rheology of an oil/water interface is addressed. In the case of a solution with no interfacial activity, we have shown that interfacial viscoelasticity measurements still display rheological signatures that would suggest, incorrectly, the presence of an elastic interface. Indeed, the viscoelastic signature of the interface seems to be clearly correlated with the rheology of the volume.

In chapter V, a surfactant is introduced into the system in order to probe the interface and the rheological behavior in the presence of a monolayer of surfactant adsorbed at the interface. The presence of this monolayer of surfactant ensures a viscoelastic behavior of the liquid/liquid interface. In this chapter, we would like to follow how the effect of the bulk, under the form of liquid or weak gel, impacts the interfacial properties of the viscoelastic moduli of an oscillating drop in the presence of surfactant. In a second step, emulsions are prepared with these formulations. A tentative of exploration of the relationships between bulk and interfacial rheological properties is conducted.

In chapter VI, the effect of nanoparticles on the interfacial rheological properties of indopol oil droplets oscillating in aqueous solution of KC under the form of a gel or a liquid is studied. It is equivalent to the configuration of the previous chapter, but the surfactant adsorbed layer is replaced by a layer of nanoparticles at the interface. Interfacial rheology experiments are conducted with indopol-isopropanol droplets containing R816 and fumed silica "FS" silica oscillating in water medium containing KC at a concentration of 5 g/L. The silica concentration in oil is fixed to 0.5 %. During the experiments, the temperature is varied from 30 °C to 15 °C. Finally, the results obtained with span and silica in the presence of KC are compared and discussed. The two systems adsorb at the interface and create hard solid interfacial layer for silica and soft interfacial layer with span.

References

(1) Hill, M. Chemical Product Engineering—the Third Paradigm. *Comput. Chem. Eng.* **2009**, *33* (5), 947–953.

(2) Charpentier, J.-C. Among the Trends for a Modern Chemical Engineering, the Third Paradigm: The Time and Length Multiscale Approach as an Efficient Tool for Process Intensification and Product Design and Engineering. *Chem. Eng. Res. Des.* **2010**, *88* (3), 248–254.

(3) Favre, E.; Marchal-Heusler, L.; Kind, M. Chemical Product Engineering: Research and Educational Challenges. *Chem. Eng. Res. Des.* **2002**, *80* (1), 65–74.

(4) Cussler, E. L.; Wagner, A.; Marchal-Heussler, L. Designing Chemical Products Requires More Knowledge of Perception. *AIChE J.* **2010**, *56* (2), 283–288.

(5) Kovtun, A. I.; Kartashynska, E. S.; Vollhardt, D. Adsorption and Viscoelastic Properties of Chitosan Lactate at the Liquid-Gas Interface. *JCIS Open* **2021**, *1*, 100001.

(6) Mendoza, A. J.; Guzmán, E.; Martínez-Pedrero, F.; Ritacco, H.; Rubio, R. G.; Ortega, F.; Starov, V. M.; Miller, R. Particle Laden Fluid Interfaces: Dynamics and Interfacial Rheology. *Adv. Colloid Interface Sci.* **2014**, *206*, 303–319. https://doi.org/10.1016/j.cis.2013.10.010.

(7) Deshmukh, O. S.; van den Ende, D.; Stuart, M. C.; Mugele, F.; Duits, M. H. G. Hard and Soft Colloids at Fluid Interfaces: Adsorption, Interactions, Assembly & Rheology. *Adv. Colloid Interface Sci.* **2015**, *222*, 215–227. https://doi.org/10.1016/j.cis.2014.09.003.

(8) Jaensson, N.; Vermant, J. Tensiometry and Rheology of Complex Interfaces. *Curr. Opin. Colloid Interface Sci.* **2018**, *37*, 136–150. https://doi.org/10.1016/j.cocis.2018.09.005.

(9) Sagis, L. M. C.; Fischer, P. Nonlinear Rheology of Complex Fluid–Fluid Interfaces. *Curr. Opin. Colloid Interface Sci.* **2014**, *19* (6), 520–529. https://doi.org/10.1016/j.cocis.2014.09.003.

(10) Marczak, W.; Rogalski, M.; Modarressi, A.; Rogalska, E. A Model of Compression Isotherms for Analyzing Particle Layers. *Colloids Surf. Physicochem. Eng. Asp.* **2016**, *489*, 128–135.

(11) Pradilla, D.; Simon, S.; Sjoblom, J.; Samaniuk, J.; Skrzypiec, M.; Vermant, J. Sorption and Interfacial Rheology Study of Model Asphaltene Compounds. *Langmuir* **2016**, *32* (12), 2900–2911.

(12) Krägel, J.; Derkatch, S. R. Interfacial Shear Rheology. *Curr. Opin. Colloid Interface Sci.* **2010**, *15* (4), 246–255. https://doi.org/10.1016/j.cocis.2010.02.001.

(13) Golemanov, K.; Tcholakova, S.; Denkov, N.; Pelan, E.; Stoyanov, S. D. Surface Shear Rheology of Saponin Adsorption Layers. *Langmuir* **2012**, *28* (33), 12071–12084. https://doi.org/10.1021/la302150j.

(14) Klein, C. O.; Theodoratou, A.; Rühs, P. A.; Jonas, U.; Loppinet, B.; Wilhelm, M.; Fischer, P.; Vermant, J.; Vlassopoulos, D. Interfacial Fourier Transform Shear Rheometry of Complex Fluid Interfaces. *Rheol. Acta* **2019**, *58* (1), 29–45.

(15) Velandia, S. F.; Ramos, D.; Lebrun, M.; Marchal, P.; Lemaitre, C.; Sadtler, V.; Roques-Carmes, T. Exploring the Link between Interfacial and Bulk Viscoelasticity in Reverse Pickering Emulsions. *Colloids Surf. Physicochem. Eng. Asp.* **2021**, *624*, 126785.

(16) Roques-Carmes, T.; Lebrun, M.; Wang, Y.; Ramos, D.; Marchal, P.; Sadtler, V. Comparison of Rheological Methods to Obtain a Sufficient Sensitivity with Shear Interfacial Rheology in the Presence of Nanoparticles at Liquid/Liquid Interfaces. *Silicon* **2022**. https://doi.org/10.1007/s12633-022-02138-z.

(17) Schmitt, V.; Destribats, M.; Backov, R. Colloidal Particles as Liquid Dispersion Stabilizer: Pickering Emulsions and Materials Thereof. *Comptes Rendus Phys.* **2014**, *15* (8–9), 761–774.

(18) Chevalier, Y.; Bolzinger, M.-A. Emulsions Stabilized with Solid Nanoparticles: Pickering Emulsions. *Colloids Surf. Physicochem. Eng. Asp.* **2013**, *439*, 23–34. https://doi.org/10.1016/j.colsurfa.2013.02.054.

(19) Dinkgreve, M.; Velikov, K. P.; Bonn, D. Stability of LAPONITE®-Stabilized High Internal Phase Pickering Emulsions under Shear. *Phys. Chem. Chem. Phys.* **2016**, *18* (33), 22973–22977.

(20) Villota, R.; Hawkes, J. G.; Cochrane, H. Food Applications and the Toxicological and Nutritional Implications of Amorphous Silicon Dioxide. *Crit. Rev. Food Sci. Nutr.* **1986**, *23* (4), 289–321.

(21) Barros, F. M. F.; Chassenieux, C.; Nicolai, T.; de Souza Lima, M. M.; Benyahia, L. Effect of the Hydrophobicity of Fumed Silica Particles and the Nature of Oil on the Structure and Rheological Behavior of Pickering Emulsions. *J. Dispers. Sci. Technol.* **2018**.

(22) Ganley, W. J.; van Duijneveldt, J. S. Controlling the Rheology of Montmorillonite Stabilized Oil-in-Water Emulsions. *Langmuir* **2017**, *33* (7), 1679–1686.

(23) Croguennoc, P.; Meunier, V.; Durand, D.; Nicolai, T. Characterization of Semidilute κ-Carrageenan Solutions. *Macromolecules* **2000**, *33* (20), 7471–7474.

(24) Meunier, V.; Nicolai, T.; Durand, D. Structure and Kinetics of Aggregating κ-Carrageenan Studied by Light Scattering. *Macromolecules* **2000**, *33* (7), 2497–2504.

Chapter II: State of the Art

2.1. Natural Phenomenon

Figure 1: A drop of rain on a lotus leaf (hydrophobic surface)

Two water drops in contact are the siege of many interfacial phenomena[1] or when a drop of rain falls on a leaf the drop takes a spherical shape (figure 1) instead of simply covering the leaf surface and "wetting" it, this is because of the mismatch of the two phases and the different interaction forces that could happen[2,3] the water phase is made up of polar water molecules with H-H bonding and the leaf surface is mostly made up of organic H-C chain polymer. For water molecules at the interface a fraction of the repulsive-attractive forces unequilibrated leaving free energy that is minimized by reducing the contact surface, thus the drop rises with a contact angle. A similar imbalance also gives the drop its top curvature.

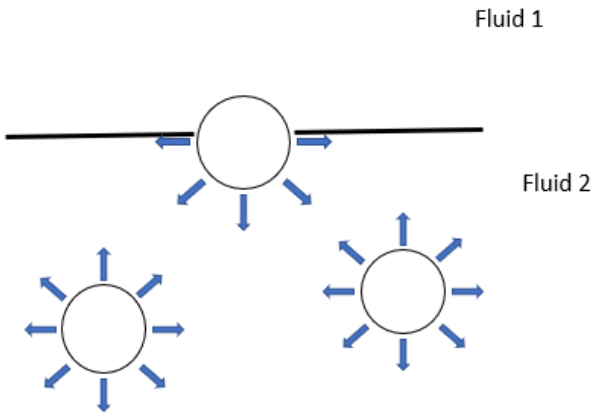

Figure 2: A schematic representation of the intermolecular forces (blue arrows) acting on fluid molecules. The drops in fluid 2 have their forces equilibrated while at the interface free energy is left unequilibrated.

The free energy shapes the boundary between the phases thus we define surface tension or interfacial tension as the work required to increase and reverse the surface area by a unit amount at isothermal conditions[4–6] and it is measured in dyne.cm^2 or mN/m in SI.

The other manifestation of interfacial tension appears in the coalescence mechanism of emulsions and foams, from a thermodynamic point of view the dispersed droplets in an incompatible fluid seek to find equilibrium due to their energy which translates to different mechanisms such as coalescence, ostwald ripening and flocculation, these mechanism ultimately lead to phase separation once the droplets fuse, here the viscoelastic properties come into play as only a thin liquid film of the continuous phase separates the two drops. As the pressure builds up the in the narrow space between the two droplets, the interfaces on both sides deforms and take a "dimple" shape until rupture of the film allowing the droplets to fuse, as reported by some authors[7–11] (figure 3).

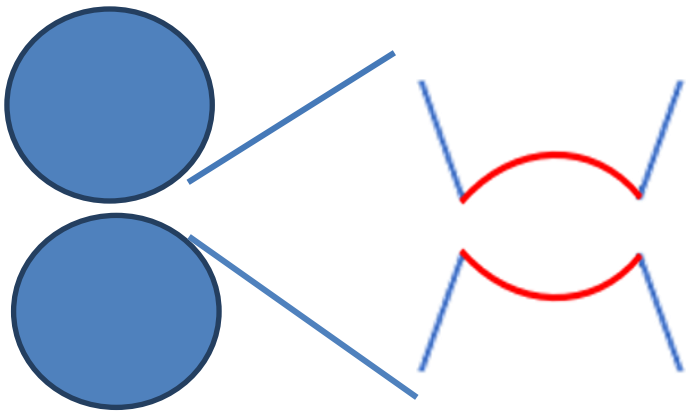

Figure 3: The “dimple” shape (red) deformation of the interface when two droplets approach each other before coalescence.

2.2. Surfactants and nanopraticles

Many emulsions in nature can be stabilized by amphiphilic molecular components like milk proteins[12], asphaltenes[13]. Other emulsions can be stabilized by more simple and synthetic molecules like SDS or sorbate monooleate (Span 80) that possess a polar group “head” and a hydrocarbon chain “tail”. Their amphiphilic nature leads to an affinity to the oil/water interface designed by a hydrophilic-lipophobic balance[14] (HLB). These amphiphilic molecules called surfactants can lower interfacial tension and act as a steric barrier against coalescence. Indeed, when the drainage of the continuous phase film begins and the interface stretches, surfactant gradient concentrations create Marangoni flows that oppose the rupture of the interface[15].

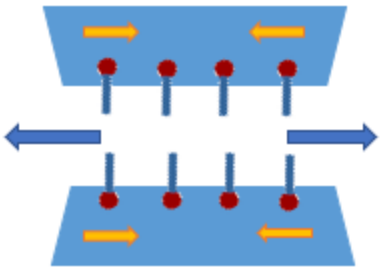

Figure 4: The effect of surfactant layers on the coalescence of two droplets, the stretching of the interface creates marangoni flows (yellow arrows) that oppose the rupture of the film (blue arrows).

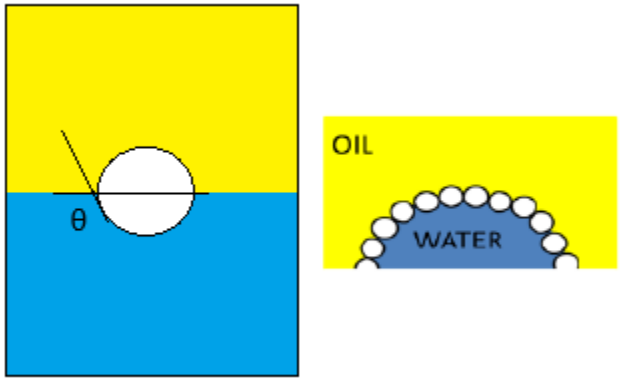

Figure 5: Wetting of nanoparticles at oil/water and water/oil interface. The contact angle θ reflects the wetting preference leading to direct or inverse emulsions, in this case $\theta > 90°$ meaning a preference for the oil phase.

Similarly, the Pickering effect[16–18] describes emulsions stabilized by soft or hard colloidal particles. As they adsorb to the interface amidst electrostatic[19] and capillary[20,21] interactions. The major difference between nanoparticles and molecular surfactants is the higher desorption energy for the former as it can reach an order of 10^3 k_BT (figure 6) making the adsorption almost irreversible as shown in the equation[22,23]:

$$E = \pi R^2 \gamma_{ow}^2 (1 \pm \cos\theta) \text{ (eq. 1)}$$

Where E is the desorption energy, R is the radius of the particle, γ_{ow} is the interfacial tension between the two phases (in the equation oil/water), θ is the contact angle (figure 5)

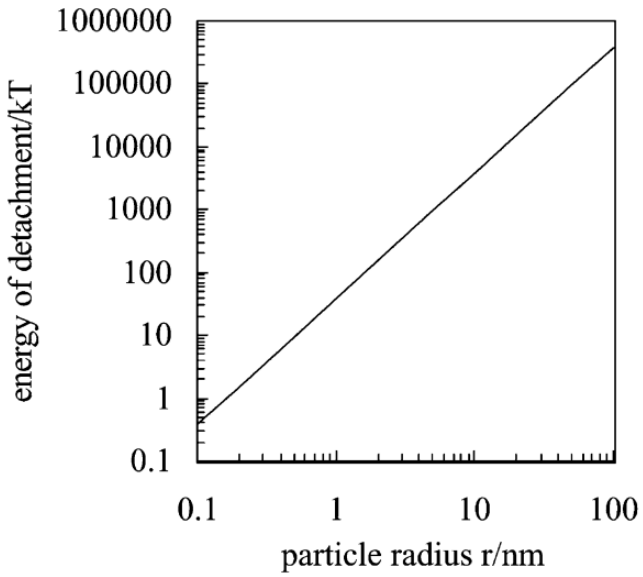

Figure 6: Energy of detachment of a particle adsorbed at the interface as a function of particle radius [B.P. Binks, 2000] as shown in equation 1.

2.3. Interfacial Rheology

The modification of interface's resistance to deformation both in shear and dilatational modes calls for mechanical and rheological tests that measure the interface's viscoelasticity and interfacial tension. Many methods probe the interface in static and dynamic modes such as the Du Nouy ring[24], Wilhelmy plate[25], Langmuir-Blodgett trough[26], drop profile tensiometry[27], maximum drop/bubble pressure[28] just to name a few.

Static measurements are useful to estimate the IFT between two fluids and more importantly to follow adsorption kinetics and surface coverage to find the critical micelle concentration (CMC)

of a surfactant. The experiments are either done with a force sensor that measures the capillary force at detachment of a geometry or plate from the interface. Other methods are based on bubble/drops formed at the tip of a needle capillary either by measuring the pressure within a closed cell or by fitting the Young Laplace equation on the image of a drop profile.

Dynamic measurements essentially consider interfaces as 2D continuums with their own viscoelasticity i.e. their ability to store (elasticity) and dissipate energy (viscosity) that can be tested in dilatational and shear modes[29,30]. In the former compression/expansion sequences are imposed without changing the shape of the interface while in the latter the shape of the interface is changed but not the area. The periodic variation in surface pressure can be attributed to mass transfer between the interface and the bulk phase and/or molecular reorientation, conformational changes or aggregation processes of the adsorbed surfactant/particle molecules.

2.4. Drop profile tensiometry

2.4.1. Theory

Drop profile tensiometry is the focus of this work, therefore it shall be discussed in more detail than the previous methods. Worthington[31–33] was the first to evaluate the pressure across a portion of the curved interface of a hanging drop, the measurement is done on a droplet formed at the tip of a capillary, either as a pendant drop (for a drop denser) or a rising drop (denser continuous phase). In both cases the drop is subject to only two forces: Gravity and IFT, the Young-Laplace reads:

$$\gamma\left(\frac{1}{R_1}+\frac{1}{R_2}\right) = \Delta P - \Delta\rho g z$$

γ is the interfacial tension, R_1 and R_2 the major and minor radii of the droplet, ΔP the pressure difference along the interface, $\Delta\rho$ the density difference between the two fluids, g the acceleration of gravity and z the drop radius at the apex.

We can see that the drop in this setup is deformed by gravity and the drop profile can be represented with a set of differential equations[34] with s (arc length of the curvature), x (horizontal coordinate) an z (vertical coordinate) as parameters, ϕ the tangent angle.

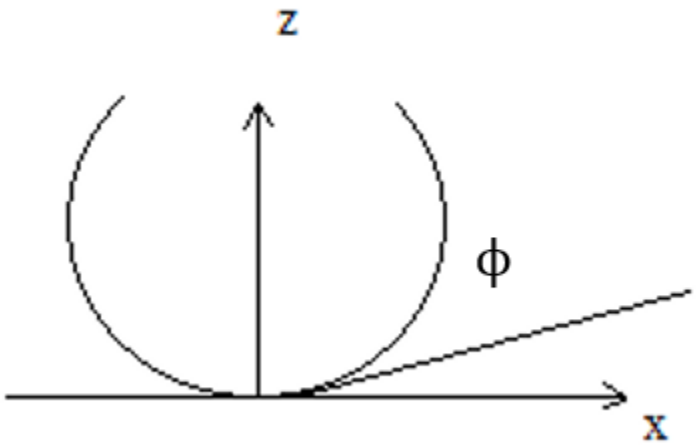

Figure 7: Drop profile in the 2D x,z plane, ϕ is the

$$\frac{d\phi}{d\tilde{s}} = 2 \pm \beta\tilde{z} - \frac{sin\phi}{\tilde{x}}$$

$$\frac{d\tilde{x}}{d\tilde{s}} = cos\phi$$

$$\frac{d\tilde{z}}{d\tilde{s}} = sin\phi$$

$\beta = \Delta\rho g b^2/\gamma$ is a shape factor that considers the balance between gravitational forces and interfacial tension, also written as B_o. It. DPT is best suited for fluids with a significant density difference and for droplets of tens of microliters in volume. Generally, a B_o of 0.1 or above is an indicator of an accurate measurement[35]. More recently, Berry et al.[36] have introduced another dimensionless factor called the Worthington number, W_o, which takes into account the internal needle diameter $Ø_n$ and maximum drop volume at detachment: $W_o = \frac{\Delta\rho g V_d}{\pi\gamma Ø_n}$

2.4.2. Experimental Setup

The experimental setup is quite simple. The drop/bubble is formed at the tip of a capillary and is illuminated by a light source. The silhouette of the drop is captured by a CDD camera which transmits the real-time image to a PC with a specialized image processing software. The edge points and the contour of the drop are detected thanks to a threshold between the grey levels of pixels From there an algorithm attempts to superpose a theoretical drop contour based on the Young-Laplace equation[27].

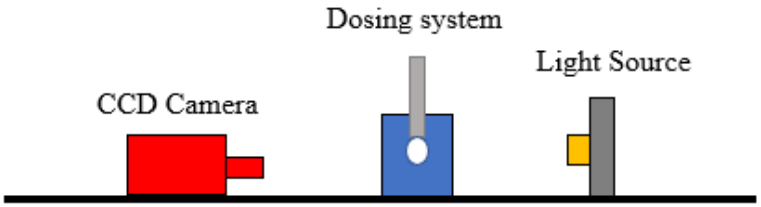

Figure 8: The experimental setup of the pendant drop tensiometer. A CCD camera films the pendant/rising drop or bubble and sends the image to software. A dosing system (motorized syringe) controls dynamic dilatation

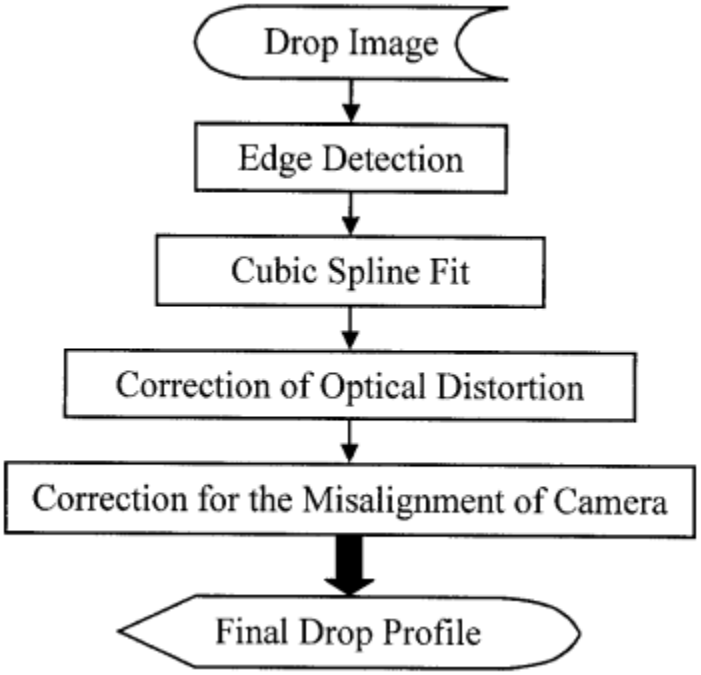

Figure 8: Proposed flow chart for the DPT fitting and computation procedure from edge detection to final drop profile.[27]

The advantage of this method is its simple setup and its accuracy for both air-liquid and liquid-liquid interfaces. The user needs little input (densities of the fluids) to obtain an accurate measurement (±0.1mN/m error) of the IFT as well as a good control of the temperature. The real-time imaging of the drop is also used to follow adsorption kinetics or the determination of Critical Micelle Concentration (CMC) [37].

$$A = A_0 + \check{A}\sin(2\pi v t) \text{ (Equation 2)}$$

$$V = V_0 + \check{V}\sin(2\pi v t) \text{ (Equation 3)}$$

$$\gamma = \gamma_0 + \check{\gamma}\sin(2\pi v t + \varphi) \text{ (Equation 4)}$$

$$K = \frac{d\gamma}{dA} \text{ (Equation 5)}$$

The sinusoidal variations of area (A) or volume (V) and IFT are listed in the above equations, with A_0 V_0 and $\check{A}$ $\check{V}$ the reference volume/area of the initial drop and the amplitude of deformation for the area/volume respectively. φ is a phase shift angle between the IFT and volume/area signals, it varies between 0 (purely elastic) and 90° (purely viscous).

2.4.3. Limitations

Although the method is very accurate in determining IFT and interfacial viscoelasticity some limitations are to be noticed. As mentioned earlier, pendant or rising drops need to be deformed by gravity thus a density difference is required. In dynamic measurements the Young-Laplace fit restricts drop deformation to small values to maintain mechanical equilibrium. So a frequency limit of 1Hz or less depending on the rigidity of the interface and viscous forces are accounted for by respecting a capillary number $C_a < 0.002$ to avoid bulk interferences[38–40].

2.5. Link between Bulk and interfacial Rheology

Only few works have recently explored the link between interfacial and bulk viscoelasticity[41–44]. The most recent work in this regard is Velandia et al.[44] looked into the interfacial rheology of the dodecane/water interface laden with fumed silica nanoparticle and it was found that a power law exists between the elastic moduli of the bulk dodecane/water, they used a conventional rheometer mounted with a double wall ring (DWR) geometry. The works of Mason and bibette[45] on mono- and polydisperse compressed emulsion are also interesting as they managed to link bulk emulsion stability to the volume fraction and radius of the drop phase and the interfacial tension.

References

1. Gennes, P.-G. de, Brochard-Wyart, F., Quéré, D., Fermigier, M. & Clanet, C. *Gouttes, bulles, perles et ondes*. (Belin, 2005).

2. Butt, H.-J. & Kappl, M. *Surface and interfacial forces*. (John Wiley & Sons, 2018).

3. Israelachvili, J. N. *Intermolecular and surface forces*. (Academic press, 2011).

4. Levine, S., Bowen, B. D. & Partridge, S. J. Stabilization of emulsions by fine particles I. Partitioning of particles between continuous phase and oil/water interface. *Colloids Surf.* **38**, 325–343 (1989).

5. Menon, V. B., Nikolov, A. D. & Wasan, D. T. Interfacial effects in solids-stabilized emulsions: measurements of film tension and particle interaction energy. *J. Colloid Interface Sci.* **124**, 317–327 (1988).

6. Menon, V. B., Nikolov, A. D. & Wasan, D. T. Interfacial effects in solids-stabilized emulsions: effect of surfactant and pH on film tension and particle interaction energy. *J. Dispers. Sci. ANDTECHNOLOGY* **9**, 575–593 (1988).

7. Yue, P., Feng, J. J., Liu, C. & Shen, J. Diffuse-interface simulations of drop coalescence and retraction in viscoelastic fluids. *J. Non-Newton. Fluid Mech.* **129**, 163–176 (2005).

8. Zdravkov, A. N., Peters, G. W. M. & Meijer, H. E. H. Film drainage between two captive drops: PEO–water in silicon oil. *J. Colloid Interface Sci.* **266**, 195–201 (2003).

9. Chesters, A. Modelling of coalescence processes in fluid-liquid dispersions: a review of current understanding.

10. Yang, H., Park, C. C., Hu, Y. T. & Leal, L. G. The coalescence of two equal-sized drops in a two-dimensional linear flow. *Phys. Fluids* **13**, 1087–1106 (2001).

11. Leal, L. G. Flow induced coalescence of drops in a viscous fluid. *Phys. Fluids* **16**, 1833–1851 (2004).

12. Singh, H. Aspects of milk-protein-stabilised emulsions. *Food Hydrocoll.* **25**, 1938–1944 (2011).

13. Poteau, S., Argillier, J.-F., Langevin, D., Pincet, F. & Perez, E. Influence of pH on Stability and Dynamic Properties of Asphaltenes and Other Amphiphilic Molecules at the Oil−Water Interface. *Energy Fuels* **19**, 1337–1341 (2005).

14. Kruglyakov, P. M. *Hydrophile-lipophile balance of surfactants and solid particles: physicochemical aspects and applications*. (Elsevier, 2000).

15. Ivanov, I. B., Danov, K. D. & Kralchevsky, P. A. Flocculation and coalescence of micron-size emulsion droplets. *Colloids Surf. Physicochem. Eng. Asp.* **152**, 161–182 (1999).

16. Pickering, S. U. CXCVI.—Emulsions. *J Chem Soc Trans* **91**, 2001–2021 (1907).

17. Binks, B. P. Particles as surfactants—similarities and differences. *Curr. Opin. Colloid Interface Sci.* **7**, 21–41 (2002).

18. Separation of solids in the surface-layers of solutions and 'suspensions' (observations on surface-membranes, bubbles, emulsions, and mechanical coagulation).—Preliminary account. *Proc. R. Soc. Lond.* **72**, 156–164 (1904).

19. Petkov, P. V., Danov, K. D. & Kralchevsky, P. A. Surface Pressure Isotherm for a Monolayer of Charged Colloidal Particles at a Water/Nonpolar-Fluid Interface: Experiment and Theoretical Model. *Langmuir* **30**, 2768–2778 (2014).

20. Vassileva, N. D., van den Ende, D., Mugele, F. & Mellema, J. Capillary Forces between Spherical Particles Floating at a Liquid−Liquid Interface. *Langmuir* **21**, 11190–11200 (2005).

21. Dalbe, M.-J., Cosic, D., Berhanu, M. & Kudrolli, A. Aggregation of frictional particles due to capillary attraction. *Phys. Rev. E* **83**, 051403 (2011).

22. Young, T. III. An essay on the cohesion of fluids. *Philos. Trans. R. Soc. Lond.* 65–87 (1805).

23. Tadros, T. F. Emulsion formation, stability, and rheology. *Emuls. Form. Stab.* **1**, 1–75 (2013).

24. Macy, R. Surface tension by the ring method. Applicability of the du Nouy apparatus. *J. Chem. Educ.* **12**, 573 (1935).

25. Allan, A. J. G. Wilhelmy's plate and Young's equation. *J. Colloid Sci.* **13**, 273–274 (1958).

26. Langmuir, I. The constitution and fundamental properties of solids and liquids. II. Liquids. *J. Am. Chem. Soc.* **39**, 1848–1906 (1917).

27. Hoorfar, M. & W. Neumann, A. Recent progress in Axisymmetric Drop Shape Analysis (ADSA). *Adv. Colloid Interface Sci.* **121**, 25–49 (2006).

28. Haendler, H. M. & McGuire, W. S. Surface tension by maximum bubble pressure. *J. Chem. Educ.* **14**, 591 (1937).

29. Mendoza, A. J. *et al.* Particle laden fluid interfaces: Dynamics and interfacial rheology. *Adv. Colloid Interface Sci.* **206**, 303–319 (2014).

30. Karbaschi, M. *et al.* Rheology of interfacial layers. *Curr. Opin. Colloid Interface Sci.* **19**, 514–519 (2014).

31. Worthington, A. M. II. On pendent drops. *Proc. R. Soc. Lond.* **32**, 362–377 (1881).

32. Worthington, A. M. IV. Note on a point in the theory of pendent drops. *Lond. Edinb. Dublin Philos. Mag. J. Sci.* **19**, 46–48 (1885).

33. Ferguson, A. Xxxviii. photographic measurements of pendent drops. *Lond. Edinb. Dublin Philos. Mag. J. Sci.* **23**, 417–430 (1912).

34. Bashforth, F. & Adams, J. C. *An attempt to test the theories of capillary action by comparing the theoretical and measured forms of drops of fluid*. (University Press, 1883).

35. Merrington, A. C. & Richardson, E. G. The break-up of liquid jets. *Proc. Phys. Soc. 1926-1948* **59**, 1 (1947).

36. Berry, J. D., Neeson, M. J., Dagastine, R. R., Chan, D. Y. C. & Tabor, R. F. Measurement of surface and interfacial tension using pendant drop tensiometry. *J. Colloid Interface Sci.* **454**, 226–237 (2015).

37. Mucic, N., Javadi, A., Kovalchuk, N. M., Aksenenko, E. V. & Miller, R. Dynamics of interfacial layers—Experimental feasibilities of adsorption kinetics and dilational rheology. *Adv. Colloid Interface Sci.* **168**, 167–178 (2011).

38. Leser, M. E., Acquistapace, S., Cagna, A., Makievski, A. V. & Miller, R. Limits of oscillation frequencies in drop and bubble shape tensiometry. *Colloids Surf. Physicochem. Eng. Asp.* **261**, 25–28 (2005).

39. Freer, E. M., Wong, H. & Radke, C. J. Oscillating drop/bubble tensiometry: effect of viscous forces on the measurement of interfacial tension. *J. Colloid Interface Sci.* **282**, 128–132 (2005).

40. Ravera, F., Loglio, G. & Kovalchuk, V. I. Interfacial dilational rheology by oscillating bubble/drop methods. *Curr. Opin. Colloid Interface Sci.* **15**, 217–228 (2010).

41. Dockx, G. *et al.* Designer liquid-liquid interfaces made from transient double emulsions. *Nat. Commun.* **9**, 1–8 (2018).

42. Pradilla, D., Barrera, A., Sætran, M. G., Sørland, G. & Alvarez, O. Mechanisms of physical stabilization of concentrated water-in-oil emulsions probed by pulse field gradient nuclear magnetic resonance and rheology through a multiscale approach. *Langmuir* **34**, 9489–9499 (2018).

43. Kamkar, M. *et al.* Polymeric-nanofluids stabilized emulsions: Interfacial versus bulk rheology. *J. Colloid Interface Sci.* **576**, 252–263 (2020).

44. Velandia, S. F. *et al.* Exploring the link between interfacial and bulk viscoelasticity in reverse Pickering emulsions. *Colloids Surf. Physicochem. Eng. Asp.* **624**, 126785 (2021).

45. Mason, T. G., Bibette, J. & Weitz, D. A. Elasticity of compressed emulsions. *Phys. Rev. Lett.* **75**, 2051 (1995).

Chapter III: Materials and Methods

The study used a model gel as a means to evaluate and deconvolute bulk contribution from interfacial viscoelasticity in oil/water (or water/oil) emulsions. The components of these systems and the methods used to characterize them are described in this chapter.

3.1. Bare Interface: Viscoelastic Moduli in a Weak Gel (chapter IV)

3.1.1. Gel preparation

The model gel used in this work is Kappa-carrageenan (KC) (sigma-aldrich, batch #BCBX5072), a sulfated plant polysaccharide extracted from seaweed, it was used as received. Aqueous solutions of KC were prepared by dissolving the appropriate mass of KC powder in ultrapure water (18MΩ.cm) under stirring for 2h at 80°C. The homogenous samples were allowed to rest one day in the fridge, then reheated at 60°C for 15min to completely liquify them for easier manipulation.

A density of KC vs temperature plot is drawn based on densitometer measurements (Mettler Toldo, France). Before loading the sample in the tube, the solution is degassed for 10 min to remove any dissolved air. The density is measured at the recurring 4 temperatures in this study: 30°C, 25°C. 20°C and 15°C, for Kc concentrations of 0.05, 0.5, 1 and 5 g/L (Table 1). Thus, the relationship between density and concentration is determined, from which the density of any other concentration is deduced.

[KC]	30°C	25°C	20°C	15°C
0	0.9956	0.9970	0.9982	0.9991
0.5	0.9959	0.9973	0.9985	0.9994
1	0.9962	0.9975	0.9987	0.9996
2	0.9967	0.9981	0.9992	1.0001
3	0.9972	0.9986	0.9997	1.0006
4	0.9977	0.9991	1.0002	1.0011
5	0.9980	0.9994	1.0005	1.0015
6	0.9987	1.0001	1.0012	1.0021
Indopol L-6	0.8160	0.8182	0.8208	0.8250
Indopol L-8	0.8263	0.8293	0.8323	0.8353

Table 1: Raw data of the density measurements for water and KC solutions at 0.05g/L, 0.5g/L, 1g/L and 5g/L

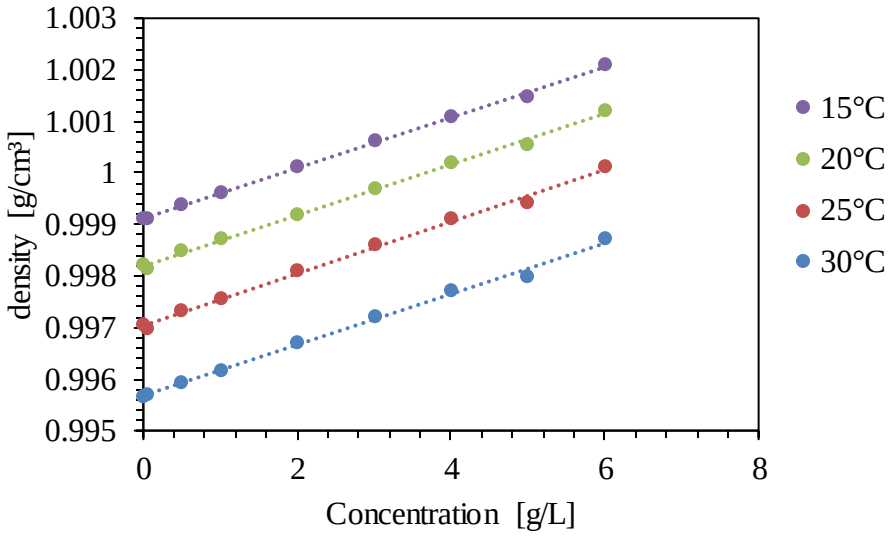

Figure 1: Density vs Concentration plot for KC solutions.

3.1.2. Oil

The oil chosen in this study is a low viscosity oil, Indopol® Polybutene (INEOUS) grade L-6, it has a viscosity of 0.01Pa.s measured by a shea flow test on a DHR3 rheometer. Density is given in the product brochure. Dodecane (signa-aldrich batch#MKBF7504V) was briefly used, but the interfacial tension with was found to decrease, most likely due to impurities[1].

3.1.3. Drop Profile Tensiometer

The drop tensiometer used in this project is a drop profile tensiometer (TRACKER; Teclis; Civrieux-d'Azergues, France). The machine was calibrated as follows: CCD Camera and image clarity were set using standard dark balls of known diameters (optical calibration), drop formation and motor injection speed were calibrated by following the injected volume per 1 motor turn at 10% of motor maximum speed (volumetric calibration), Lastly, a one image analysis is done on a drop by entering the densities of drop and bulk phases (in Kg/dm3). The bulk phase is placed in a glass cuvette of 6ml capacity.

Measurements were done on rising drops of oil in water or Kc at the tip of a curved "J" shaped needle of internal diameter Ø = 0.84mm and external diameter $Ø_e$ = 1.3mm). Before any experiment with Kc, the cuvette was preheated at 60°C to avoid thermal shock, the needle and syringe were also preheated using the circulation water bath. A thin layer of paraffin oil was spread on the top of the cuvette to avoid evaporation.

Kc solutions were prepared at 2, 3, 4, 5 and 6g/L as described in section 3.1.1. The reheated samples were transferred to the preheated cuvette, where a drop of Indopol L-6 was formed at the tip of the needle. Measurements were done at isotherms by allowing at least 10 minutes for the temperature to stabilize during a cooling-reheating cycle with isotherm steps at 30°C, 25°C, 20°C and 15°C, to make sure K^s' and K^s'' did not evolve with temperature.

The following parameters were applied during the interfacial oscillatory experiments: The frequency is varied between 0.05 and 1 Hz and the amplitude of oscillation is fixed at 10% of the initial drop volume 10 µL. We have ensured that these conditions are in the linear domain of the interfacial viscoelastic moduli of the samples (see chapter IV). Five volume oscillations are imposed followed by five blank cycles. This procedure is repeated until the steady state is reached; the moduli value. The viscoelastic moduli are extracted from the oscillations via a fourier transform and the surface tension from the static part of the protocol. The steady state is assumed if moduli values do not differ more than 10% between batches of oscillations, for higher frequencies the experiment lasted 10min while for lower frequencies only 5min were enough. Figure 2 shows typical measurement raw data and the calculation method. The specific algorithm

of the machine could not be found, but method of calculation is discussed in the bibliography part, basically $K^s \equiv d\ln\gamma/d\ln A$ with $K^{s'} = K^s*\cos(\theta)$ and $K^{s''} = K^s*\sin(\theta)$.

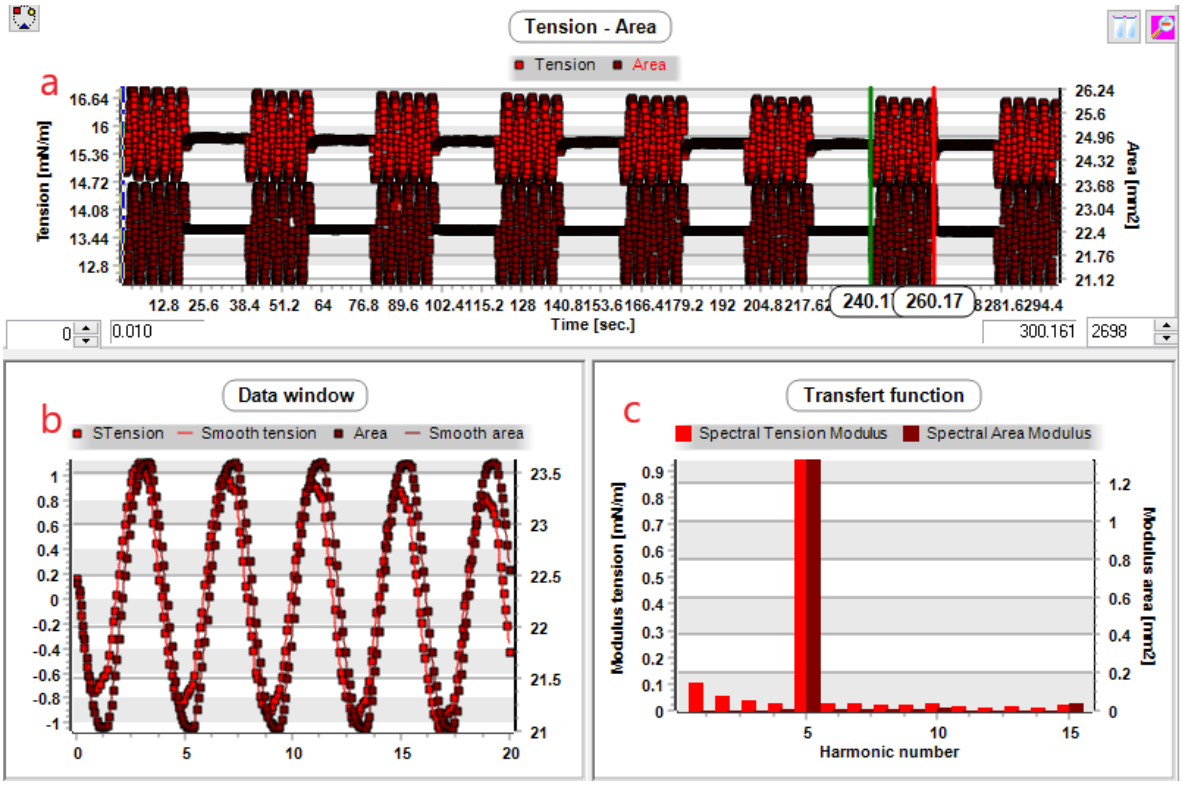

Figure #2: An example of a drop oscillation measurement raw data and treatment: a) volume/area variation and interfacial tension, b) Zoom on selected batch of data c) Fourier transform function harmonics

All measurements are repeated at least three times ensuring that the variability of the results is less than 10%.

3.1.4. Bulk Shear Rheology

Kc samples of the same concentrations (2 to 6g/L) were tested under shear. In an attempt to measure the yield stress of the weak gels, a low shear 40 (Contraves) viscometer was used, the shear rate was changed between 100 s-1 and as low as 6.10^{-4} s^{-1} and flow curves were obtained; however, the apparatus was found inadequate for the gelled state (see Chapter IV).

Dynamic Frequency sweeps were performed using a stress-controlled rheometer (DHR3; TA Instruments; Guyancour, France) equipped with the coaxial cylinders (Couette) geometry (rotor radius = 14 mm; stator radius = 15 mm; immersed height = 42 mm). Before any measurement, the geometry is preheated at 60°C to gently accommodate the freshly reheated KC sample. Temperature transition steps are imposed through time sweeps at 1Hz for 1000s to reach a steady state in the sample as we moved from one temperature isotherm to the next, thanks to this precaution, G' and G'' were found to not evolve as we proceeded with our frequency sweeps.

The frequency sweep is performed between 1 and 0.01 Hz at 10% strain which is in the linear regime for all samples and temperatures, as deduced from amplitude sweeps. Temperatures of 30, 25, 20, and 15°C were selected in a cooling-(re)heating cycle.

3.2. Surfactant-laden interface: Span® 80

3.2.1. Drop profile tensiometry

An oil-soluble surfactant is chosen for this part, the idea is to have a surfactant that does not interact with Kc. Sorbitan monooleate, or Span® 80 (Sigma-Aldrich), a liposoluble surfactant was mixed with indopol grade L-8 in the drop phase for interfacial tension measurements.

Adsorption kinetics were first studied by keeping the oil drop volume constant at 7-10µl at the tip of a curved needle with an internal diameter Ø = 0.84mm or 1.19mm in ultrapure water, Span 80 concentrations used were between 0.01% up to 0.1% w/w. Above 0.1%, IFT became too low and drop detachment rendered the measurement inaccurate, so 0.05% and 0.1% w/w concentrations of Span 80 were used in dynamic oscillatory tests.

Dynamic interfacial viscoelasticity was measured by applying a batch of five oscillations followed by 30s of rest, this step is repeated until a stable modulus is obtained for frequencies 0.05-1Hz, between 30°C and 15°C with Kc at 3, 4, 5g/L to have results with KC in both liquid and gel states.

3.2.2. Emulsion Characterization and stability

3.2.2.1. Emulsion preparation

Emulsions of indopol-water were prepared at various Water-Oil ratios (w/w%): 60-40 and 70-30, at various Span 80 concentrations (w/w%) in the oil phase: 0.5%, 2%. They were prepared by adding water drops to the oil+Span 80 phase then mixing with a vortex shaker. Emulsions with KC were prepared by adding preheated liquid KC 5g/L and allowed to cool then preheated before any measurements. Emulsions were prepared with Vortex shaker.

3.2.2.2. Confocal Microscopy

Emulsions, both Oil-W and Oil-KC are using a x25 and x63 magnification objectives on Zeiss confocal microscope. As there is no temperature control on the microscope, KC solutions could only be observed at room temperature or in gelled state. Dyes used were Rhodamine B (Sigma-Aldrich) and Fluoresceine salt FITC (sigma-aldrich), 5ppm in each phase.

3.2.2.3. Shear Rheology

The emulsions are loaded directly to the DHR3 rheometer with a 40mm plate-plate geometry with a 1mm gap. Amplitude sweeps are first done to find the linear viscoelastic region, then frequency sweeps are done at 0.6% between 1 and 0.01Hz. Emulsions containing KC 5g/L were studied in by loading them at 60°C temperature, then measuring at 30-25-20-15°C with a 1000s temperature equilibration step.

3.3. Oil/water interface stabilized by silica nanoparticles

3.3.1. Choice of Nanoparticle (NP) type

Interfacial viscoelasticity of a nanoparticle-laden interface was studied by spreading the NP on the interface from within the oil droplet to avoid interactions with the bulk phase, different types of hydrophobic silica NP were tested for this reason. To verify the interface adsorption of the

nanoparticles, dilatational oscillatory drop measurements were first used to evaluate interface viscoelasticity,

It was decided that Aerosil R816 (Evonik, Germany, batch #150042435) and Fumed silica NP (sigma-aldrich) should be used at 0.5%. The NP powder is first weighted, then Indopol L-8 or PDMSV20 is added as the oil phase. Isopropanol (Aldrich, 99% pure) was later introduced as a co-solvent, given the amphiphilicity of the NP and their tendency to aggregate. The NP+IPA+Indpol or PDMS mixture is then treated with ultrasounds at 25kHz and 22% amplitude for 1-3 minutes to break aggregates.

3.3.2. Drop Profile Tensiometry

First, the effect of IPA is observed; it lowers water/PDMS interfacial tension temporarily, so measurements are done once IFT is stable.

A drop of the NP+oil or NP+oil+IPA of 10ul is formed at the tip of a "J" shaped needle of Ø = 1.19mm and external diameter $Ø_e$ = 1.7mm, the adsorption kinetics and equilibrium interfacial tension were measured on a 10ul drop. An amplitude sweep is performed at 0.25Hz between 1% and 20% deformation to check for linear regime, an amplitude of 10% is found adequate.

Frequency dependence of the viscoelastic moduli is obtained through oscillatory measurements between 0.05 and 1Hz with 5 oscillations followed by 30s of rest, this was repeated until equilibrium was reached. The same protocol was applied with KC 5g/L as the bulk phase by cooling between 30°C and 15°C

References

1. Abdallah, W., Zhao, W., Gmira, A., Negara, A. & Buiting, J. Sensitivity Analysis of Interfacial Tension on Saturation and Relative Permeability Model Predictions. in *All Days* SPE-149038-MS (SPE, 2011). doi:10.2118/149038-MS.

Chapter IV: Viscoelastic Moduli in A Weak Gel

Submitted to the journal of Colloids and Interface Science

Doi: https://doi.org/10.1016/j.jcis.2022.04.047

Ahmad Jaber[1, 2], Thibault Roques-Carmes[2], Philippe Marchal[2], Tayssir Hamieh[3,4], Lazhar Benyahia[1,*]

1) Institut des Molécules et Matériaux du Mans (IMMM), UMR 6283 CNRS – Le Mans Université. 1, Avenue Olivier Messiaen, 72085 LE MANS cedex 9, France

2) Laboratoire Réactions et Génie des Procédés, UMR 7274 CNRS, Université de Lorraine, 1 rue Grandville, 54001 Nancy, France

3) Faculty of Science and Engineering, Maastricht University, P.O. Box 616, 6200 MD Maastricht, The Netherlands

4) Laboratory of Materials, Catalysis, Environment and Analytical Methods Laboratory (MCEMA), Faculty of Sciences, Lebanese University, Hadath, Lebanon.

Graphical Abstract

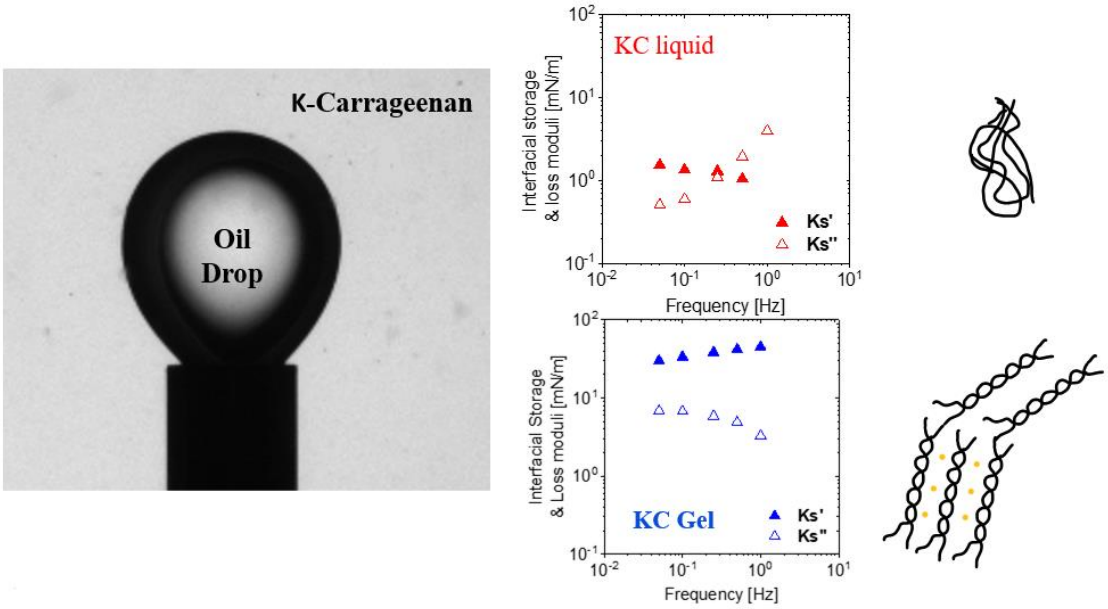

Abstract

Hypothesis

The measurement of interfacial viscoelastic moduli provides information on the ability of surface-active agents to texture the interface. However, the contribution of the bulk rheology cannot be ignored in particular when the continuous phase exhibits a gel-like behavior, even with low modulus.

Experiments

Between 2 and 6 g/L, κ-carrageenan aqueous solutions have no significant activities at interfaces. At low concentrations or high temperatures, they behave like Newtonian liquids. Upon heating or cooling, a reversible liquid/gel transition appears with a hysteresis where the rheological behavior can be easily modulated by adjusting κ-carrageenan concentration. The frequency dependence of bulk and interfacial viscoelastic moduli are determined using a conventional shear rheometer and a drop tensiometer with a polyisobutene oil, respectively.

Findings

The effect of concentration and temperature is analyzed and the frequency dependence of interfacial moduli is correlated with those of the bulk. In presence of a gelled κ-carrageenan

solution, an elastic behavior of the interface appears and strengthens as the elastic modulus of the suspended phase is high. It turns out that the oscillating pendant drop method could be a sensitive indicator of the presence of very weak gels, even hardly detected by a shear classical rheometry.

Keywords: Weak gel, Drop tensiometer, κ-carrageenan, interfacial viscoelasticity

4.1. Introduction

In emulsions and foams, all intra and intermolecular forces (Van der Waals, ionic, hydrogen. . .) contribute to the phase separation and the creation of an interface separating the two fluids. The minimization of this interface, favorable to the decrease of the global energy, is induced by a force, expressed per unit length, and called surface (air–liquid) or interfacial (liquid–liquid) tension[1]. The surface tension can provide an indication of the compatibility between the two phases. Indeed, high interfacial tension signifies a strong incompatibility between the liquids present and a less easy emulsification. This is usually overcome by using surface active agents such as surfactants, which, by their amphiphilicity, lower the interfacial tension between the two liquids, promote mixing, and at the same time prevent coalescence through steric or electro-steric effects[2–4].

The accumulation of surface-active agents at the interface, their organization and their dynamics inevitably induce static moduli indicated by the diminution of the surface tension. In addition, it induces also dynamic moduli, called viscoelastic, when probed by oscillatory measurements for example. In the latter case, the interfacial rheology is concerned. The measurement of surface tension[5] and dynamic interfacial rheology can be achieved through different techniques[6–9]. One of the most commonly used methods is the oscillating drop[10]. All these methods probe the interface itself in a quasi-static regime to limit bulk contribution[11,12] which is easily reached for low viscous fluid.

The determination of the interfacial tension is more critical for gels or yield stress fluids. This topic is only partially tackled in the literature and exclusively for strong gels and eventually for

static measurements to determine the surface tension as reported in ref.[13,14]. The authors proposed a method to measure the surface tension of yield stress fluids of highly elastic modulus, of about one order of magnitude the value of the yield stress, using capillary bridges.

For dynamic measurements, Freer[15] reported that viscous forces cannot be neglected in dynamic pendant drop analysis. Yeung and Zhang[16] showed, by simulation, the shear resistance of the interface at high frequency when developing the interfacial films in a pendant drop method.

This study aims at evaluating the impact of an extremely low threshold or a weak gel on the interfacial rheology of an oil/water interface. For this purpose, a weak model gel, consisting in aqueous solution of κ-carrageenan (KC), is chosen for its reversible gelation with temperature. κ-carrageenan is an anionic polysaccharide extracted from edible red algae[17]. It has many industrial applications such as cosmetics, food, health and pharmaceuticals[18]. κ-carrageenan is a sulfated polygalactan with an ester-sulfate content of between 15 and 40% and presents an average molar mass well over 100 kDa. It is formed by alternating units of D-galactose and 3,6-anhydro-galactose linked by a-1,3 and b-1,4-glycosidic bonds. At high temperatures the KC chains are in a random coil conformation and the solutions are rather Newtonian liquids.

By lowering the temperature below a critical temperature Tgel, the chains adopt a helix conformation. In the presence of salt, double helices can be formed and if the concentration is sufficient, they aggregate to form a 3D network conferring gel-like properties to the KC solution. By heating above Tsol > Tgel, the helices regain the random coil conformation and highlights the existence of a fully reversible hysteresis[19]. The two critical temperatures depend closely on KC concentration and the ionic strength but also on the chemical nature of the salt and justify the interest of this type of polysaccharide in various applications[20]. Thus, it happens that it becomes possible to have a liquid or a weak gel at the same temperature depending on the thermal history and the composition of KC solution. In this way, we propose to highlight the effect of bulk rheology, especially in the case of very weak gel, on the behavior of interfacial viscoelastic moduli.

4.2. Materials and Chemicals

4.2.1. Chemicals and solution preparation

A sulfated κ-carrageenan, extracted from seaweed, was supplied as a powder by Aldrich (batch #BCBX5072). It was used, without any supplementary modification or purification, to prepare aqueous solutions in pure MilliQ water (18 MΩ.cm). Aqueous solutions were prepared at 2, 3, 4, 5 and 6 g/L of KC. The appropriate mass of κ-carrageenan powder was dissolved in water under stirring at 80°C for 2 h. Then, the homogenous samples were stored in the fridge until the next day. The oil phase was a polyisobutylene oil purchased under the trademark Indopol from INEOS Oligomers. The selected grade was L-6 (>99% pure, batch #10 PB0250).

Before any experiment, the samples were preheated at 60°C during 15 min in a heating bath to bring them all to liquid state. Note that the aqueous κ-carrageenan solution was degassed 3 times using a vacuum desiccator in order to avoid air bubbles for all measurements. For interfacial rheology experiments, the density of the oil (Indopol) and aqueous (κ-carrageenan solutions) must be known for each studied temperature. For that purpose, the density of Indopol as a function of the temperature of this study, extracted from the product brochure, is summarized in Table S1 (SM). In addition, the density of the κ-carrageenan solutions is measured at different temperatures using a Mettler Toledo densitometer (Mettler Toldo, France). Samples were first degassed for 10 min to remove any dissolved air then density was measured at the 4 temperatures (30°C, 25°C. 20°C and 15°C) for the concentrations of 0.05, 0.5, 1 and 5 g/L. Thus, the dependence of the density with the concentration was determined at each temperate and allowed to deduce the density of any other concentration.

4.2.2. Bulk and interfacial rheology

κ-carrageenan solutions of concentrations from 2g/L to 6g/L were tested under shear. In an attempt to measure the yield stress of the weak gels, a low shear 40 (Contraves) viscometer with a bob-and-cup geometry (internal diameter R_i = 3mm, external R_a = 3.25mm, height = 9mm). The shear rate was changed between 100 s^{-1} and as low as 6.10^{-4} s^{-1} and flow curves were obtained at the temperature isotherms of 30°C, 25°C, 20°C and 15°C. The samples were given at least 1000s to reach equilibrium at each temperature step.

Bulk κ-carrageenan rheology was determined using a stress-controlled rheometer (DHR3; TA Instruments; Guyancourt, France). The lower limit of the torque was given as 0.5 nN/m in oscillatory mode and the sensitivity of about 0.05 nN/m. Consequently, the data were considered reliable only if the measured torque values were higher than or equal 50 nN/m. Before loading the sample, the coaxial cylinders (Couette) geometry (rotor radius = 14 mm; stator radius = 15 mm; immersed height = 42 mm) was preheated at 60°C. Isothermal measurement was performed after maintaining the sample at a given temperature for at least 1000 s to reach a steady state in the sample before any rheological measurement. The frequency sweep was performed between 1 and 0.01 Hz at 10% strain which was in the linear regime for all samples and temperatures. Temperatures of 30, 25, 20, and 15°C were selected in this study, unless specified.

All measurements were repeated at least three times ensuring that the variability of the results is less than 5%. Interfacial tension (static) and interfacial viscoelastic dilatational moduli (dynamic) of KC/oil interface were investigated via a drop-profile tensiometer (TRACKER; Teclis; Civrieux-d'Azergues, France). For the experiments, a rising drop of indopol was put into contact with the aqueous κ-carrageenan solution filling the transparent cell. The temperatures were fixed to 30, 25, 20 and 15°C and held up at least 10 min to get a thermal steady state. To avoid any evaporation of the sample, a layer of paraffin oil was deposited on the top of the aqueous solution. The frequency was varied between 0.05 and 1 Hz and the amplitude of oscillation was fixed at 10% of the initial drop volume chosen equal to 10µL. We have ensured that these conditions were in the linear domain of the interfacial viscoelastic moduli of the samples (see A1 in Annexes). Five oscillations of volume were imposed followed by five blank cycles. This

procedure was repeated until the steady state was reached. Then, the interfacial viscoelastic moduli were averaged on the last five oscillations. The viscoelastic moduli were extracted from the oscillations and the surface tension from the static part of the protocol. All measurements were repeated at least three times ensuring that the variability of the results was less than 10%. In particular, for static measurement, the determination of the surface tension was found accurate at ±0.5 mN/m. Note that a thorough discussion about the reproducibility is given in the Discussion part.

4.3. Results

4.3.1 Bulk rheology

4.3.1.1. Yield Stress Measurement

Viscosity measurements for all κ-carrageenan samples between 30°C and 15°C are shown in fig. 1. During cooling, all sample exhibit a Newtonian behavior with a viscosity plateau independent of shear rate at 17-20mPa.s at 30°C, the samples are liquid and flow in response to shear.

As the temperature is lowered, the viscosity of the samples increases. At 25°C, 2g/L and 3g/L show a plateau again at 20mPa.s, 4g/L and 5g/L show a plateau at 30mPa.s but it increases noticeably near extremely low shear rates, while the viscosity of the 6g/L sample increases exponentially as the slope becomes negative with decreasing shear as soon as $25s^{-1}$, which is the signature of a gel. At 20°C, 2g/L and 3g/L remain Newtonian at 20mPa.s, 4-6g/L exhibit a negative trend with decreasing shear rate that is more evident as the concentration increases, the samples are in a gelled state. Lastly, at 15°C, 2g/L and 3g/L behave as low viscosity liquids, and although 3g/L shows a slightly negative slope with shear rate both samples are still liqide-like, 4-6g/L are all in a gel state with negative trends.

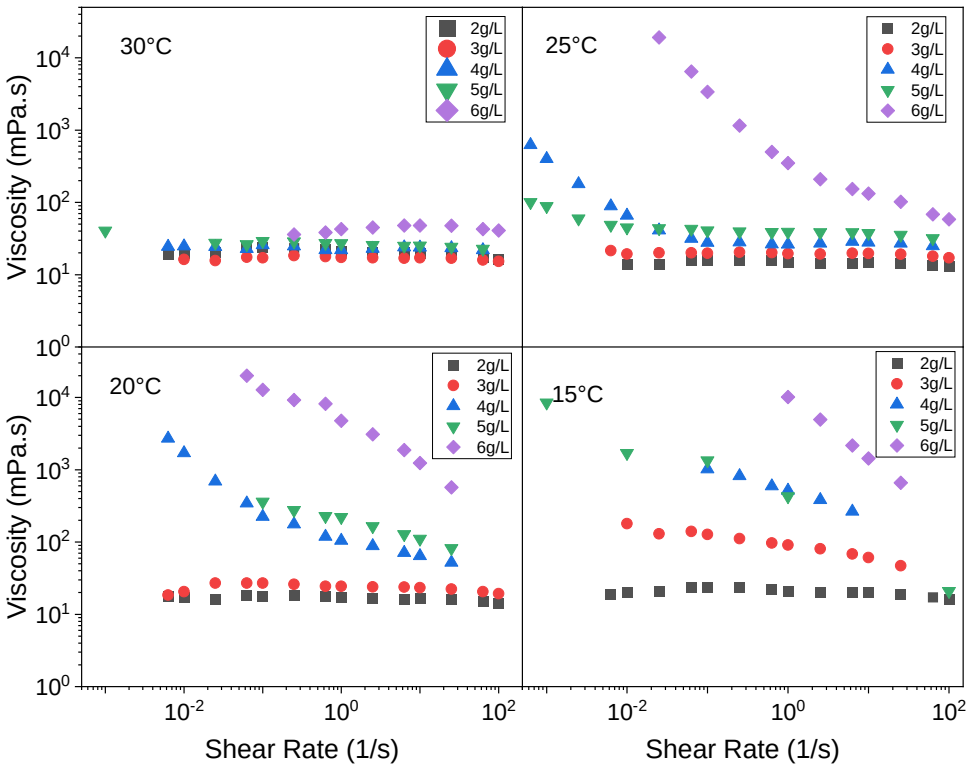

Figure 1. Flow curves of KC (viscosity vs Shear rate) solutions at 2-6g/L during cooling between 30°C and 15°C in a cooling procedure.

It is worth mentioning that the low shear sensitivity is due to a torsion string that transmits its force to a receptor and then to the instrument. An elastic gel can be deformed indefinitely under constant shear as it pulls on the string, the torsion does not reach a finite point for an accurate measurement, therefore these measurements provide an approximation of the yield stress of such weak gels, which is less than 1Pa for the gels considered in this study.

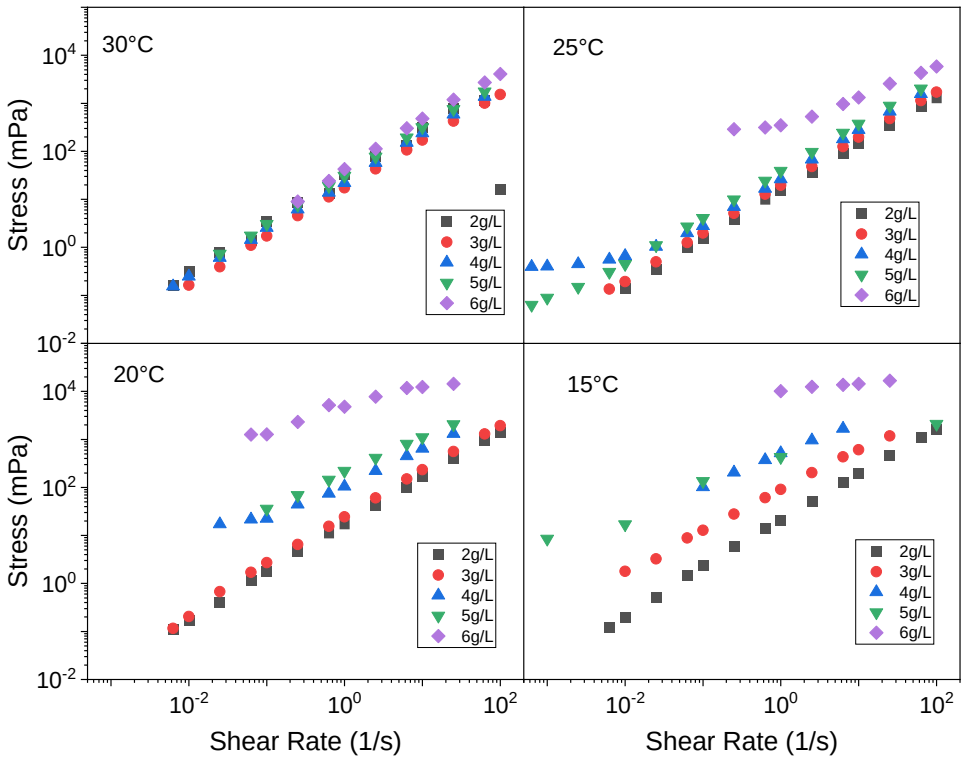

Figure 2. Flow curves of KC (Stress vs Shear rate) solutions at 2-6g/L during cooling between 30°C and 15°C in a cooling procedure.

4.3.1.1. Thermo-rheological behavior of κ-carrageenan solutions

Fig. 3 shows G' and G'', the elastic and viscous moduli respectively at 0.01 Hz, after cooling or heating stage of κ-carrageenan solution at 6 g/L. At each temperature, to reach a steady state, the sample is maintained at least during 1000s before to perform the rheological measurement. As the temperature decreases, the two moduli follow a strong increase, whereas G' becomes higher than G'' at 15°C testifying for a sol–gel transition. The elastic modulus of the 6 g/L of KC solution taken at 0.01 Hz, increases from 0.0001 Pa at 30°C to 0.39 Pa at 15°C. However, it's important to mention that the moduli below 0.001 Pa are to be considered with caution even the measured torque is in the acceptable range of the device. In fact, other artefacts such as inertia may affect the measures. So, the data below 0.001 Pa are given as a guide for eyes. When increasing the temperature, G' and G'' both decrease but G' remains larger than G'' revealing a hysteresis of the sol–gel transition of κ-carrageenan solution. If the temperature is increased

further, a liquid state is obtained at higher temperature, namely up to 50°C for this sample (not shown).

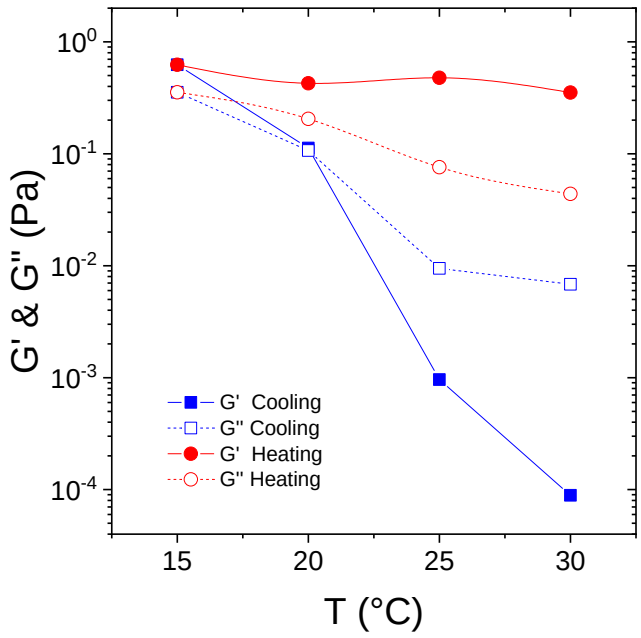

Figure 3. Viscoelastic moduli G' (●) and G'' (○) at 0.01Hz of κ-carrageenan solution at 6 g/L during cooling (blue) and heating (red) stage.

Indeed, the chemical structure of κ-carrageenan is fundamental in determining the sol–gel transition. This molecular understanding is well documented[21,22] but is briefly mentioned here. Aqueous solutions containing κ-carrageenan at low concentrations and high temperatures are Newtonian liquids as the polysaccharide chains are under the form of loose coils. In presence of specific counterion, as the concentration rises and the temperature decreases, a coil to helix conformation transition occurs. Above a critical concentration C*, interconnection of the double helices happens and a gel can be formed. The transition temperatures during heating or cooling depend on the ionic strength, the nature of ions, and the concentration of polymer[17-18]. In the present study, the sulfated κ-carrageenan is used and thus the charges of the macromolecules are screened with potassium ions. The product is used as received without any further purification or adjustment of the ionic strength. The interesting feature of this hysteresis is to obtain a liquid or a

gel behavior for the same solution at the same temperature depending on the thermal history. Thus, it becomes possible to evaluate the effect of the bulk viscoelastic properties on the interfacial tension and the viscoelastic moduli of the oil/water interface independently of the surface activity of the polymer. It is worth mentioning that different heating and cooling cycles do not affect the reversibility of the hysteresis loop.

4.3.1.2. Frequency dependence of the viscoelastic moduli of κ-carrageenan solutions at various temperatures

Frequency dependence of G' (elastic modulus) and G'' (viscous modulus) of κ-carrageenan solution is studied as a function of concentration and temperature. Fig. 4 presents the isothermal frequency dependence of G' and G'' at different temperatures after cooling or heating for 6 g/L of KC. The same data for the other concentrations of κ-carrageenan are given in Fig. 5 and Figs. 6-8.

During cooling from 60°C, it appears that at 30°C, G' is almost undetectable while the G'' versus the frequency exhibits a slope of 0.99 ± 0.00 in a log–log scale, close to 1 as it was expected from a pure viscous liquid were investigated. Reducing the temperature to 25°C, the G'' increases slightly while its slope = 0.92 ± 0.001 remains close to 1. G' becomes detectable but one order of magnitude lower than G''. The behavior of the κ-carrageenan solution remains liquid-like although the slope of G' has not reached 2 in the range of the explored frequencies indicating a large distribution of the relaxation time of these κ-carrageenan solutions[24]. At 20°C, G' shows a remarkable increase and becomes almost equal to G'' at lower frequencies. In addition, G' seems to tend towards a plateau of about 0.1 Pa. Both G' and G'' present a power law dependence with the frequency with an exponent of about 0.62 ± 0.007 (i.e. a slope of 0.62 ± 0.007 in a log–log scale). Clearly, the system undergoes a solid-gel behavior between 25 and 20°C.

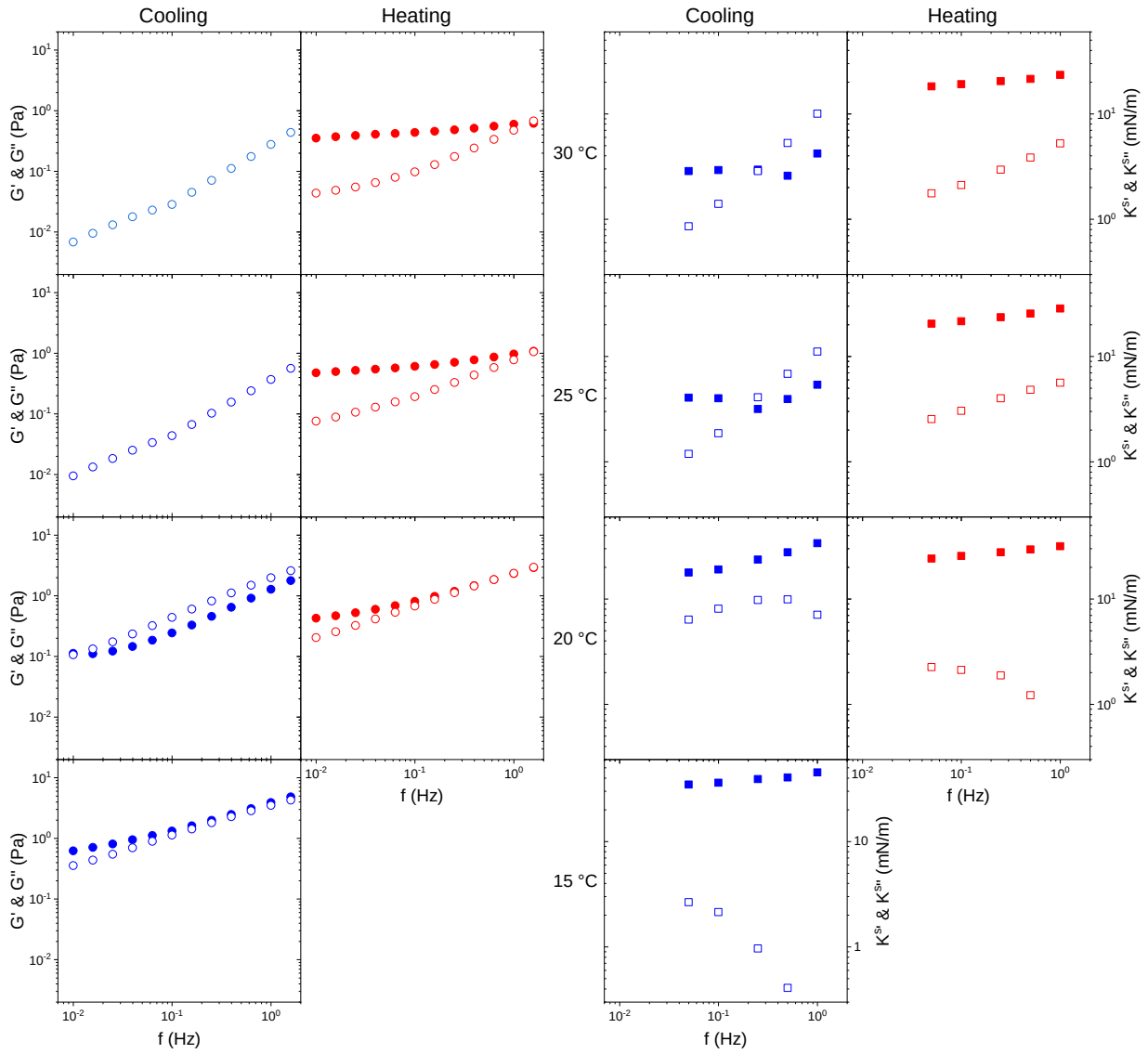

Figure 4. Isothermal frequency dependence of G' (●), G" (○), Kˢ' (■) and Kˢ" (□) for 6 g/L of k-carrageenan at different temperatures during cooling or heating, as indicated in the figure.

The gel behavior appears more pronounced when the temperature decreases to 15°C. In fact, the two moduli increase with G' being superior for most of the frequency while the exponent of the power law decreases to 0.430 ± 0.008. During the heating ramp, the gel behavior is more evident. At 20°C, the elastic modulus continues to increase and surpasses G'', especially at low frequencies showing a plateau of about 0.7 Pa, which is a signature of a weak gel. Reheating to 25°C and 30°C, this signature becomes clearer for almost the entire range of frequency, i.e. the G' plateau persists while G'' slope increases slightly, in stark contrast with the cooling phase.

These results confirm and refine the previous finding obtained in the previous section. It points out that a liquid or a gel can be obtained at the same temperature based on the thermal history of the κ-carrageenan solutions.

Under heating, G' increases and becomes larger than G'' with a well-marked plateau, even at 30°C where the κ-carrageenan solution was a liquid after cooling from 60°C. So, for the same temperature, 25 and 30°C namely, the κ-carrageenan solution is a gel or a liquid-like depending if it is heated or cooled, respectively. The samples containing 5 g/L of κ-carrageenan (Fig. 5) shows a similar behavior than 6 g/L except that the moduli are lower compared to 6 g/L. Different behaviors are encountered with lower concentrations of KC. At 4 g/L, the elastic modulus appears at 20 and 15°C during cooling and then persists during heating (Fig. 6).

However, G' remains mainly lower than G'' even if the two moduli become close at 25 and 30°C and at lower frequencies. Clearly G' appears tends towards a plateau at low frequencies where its value would likely be higher than G'' and confirm the weak gel character of the 4 g/L KC solution. At 2 g/L, G' is hardly detectable and G'' presents a slope of about 1.04 ± 0.004 versus frequency regardless of the temperature, even for heating or cooling (Fig. 8). No sol–gel transition and no hysteresis of the rheological behavior are observed between 60 and 15°C. Thus, for the same temperature, the same viscosity of the sample is measured either after cooling or heating. At 3 g/L, the rheological behavior is quasi-similar to that obtained at 2 g/L, except at 15°C (Fig. 7). For this latter temperature, G' increases significantly with the frequency but does not surpass G''. However, when heating the G' disappears rapidly.

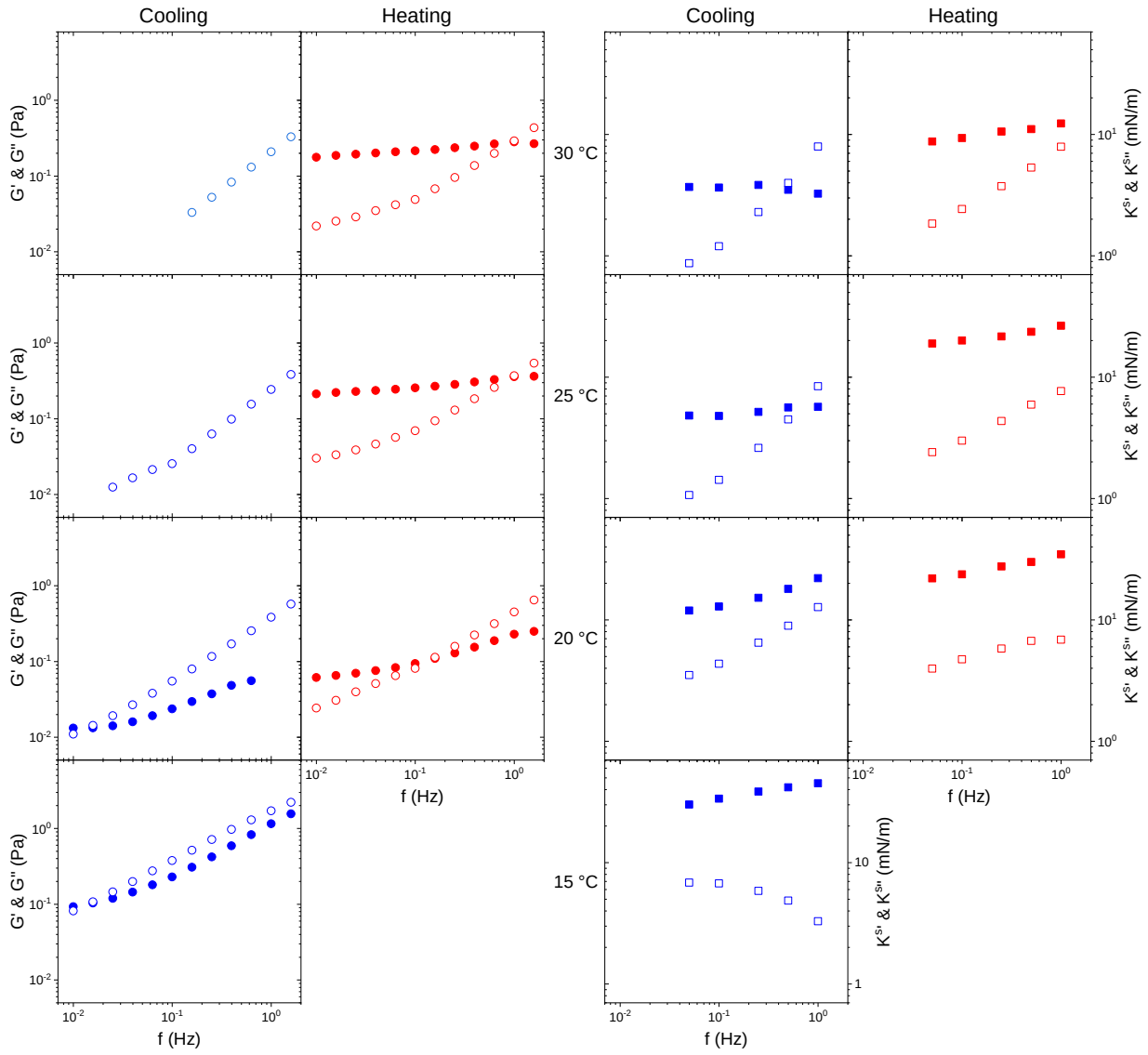

Figure 5. Isothermal frequency dependence of G' (●), G" (○), Kˢ' (■) and Kˢ" (□) for 5 g/L of k-carrageenan at different temperatures during cooling or heating, as indicated in the figure.

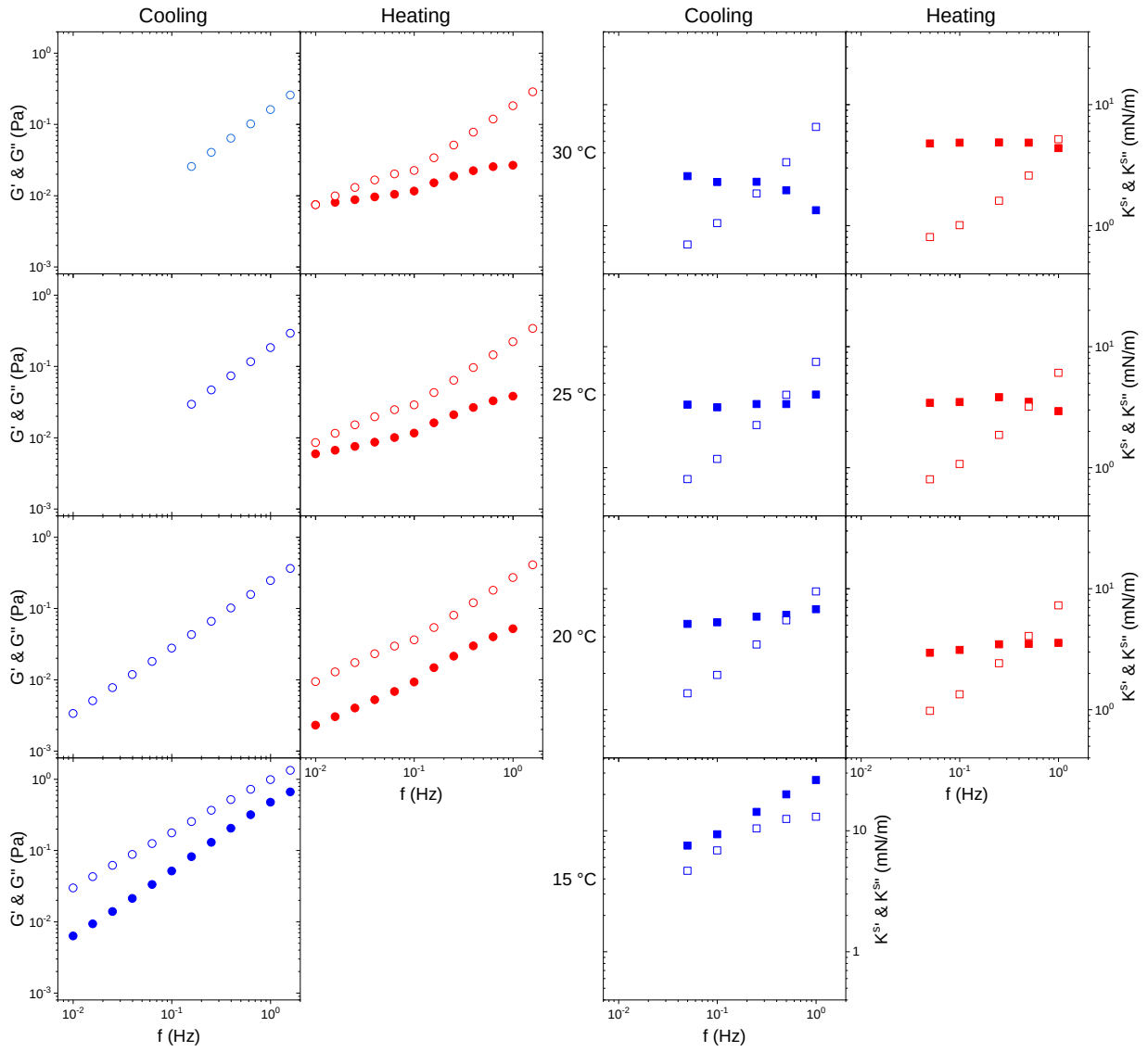

Figure 6. Isothermal frequency dependence of G' (●), G" (○), Kˢ' (■) and Kˢ" (□) for 4 g/L of k-carrageenan at different temperatures during cooling or heating, as indicated in the figure.

As general trends, for lower κ-carrageenan concentrations (2 and 3 g/L), the liquid behavior dominates during cooling or heating stage. For 5 and 6 g/L of KC, the gel behavior appears at 20°C during cooling and remains even after heating up to 30°C. The 4 g/L shows an intermediate behavior (Fig. 6). It remains liquid during the whole cooling phase but changes to a gel-like behavior at 25 and 30°C. Indeed, although G'' remains higher than G' over the whole frequency window explored, G' clearly tends towards a plateau at low frequencies of the order of 0.01 Pa, denoting a very weak gel character. An attempt was made to determine the flow yield stress of κ-

carrageenan solutions through steady state flows. However, it was not possible to determine this value reliably due to the sensitivity limit of our rheometer and suggest that the yield stress would be lower than 1 mPa. Note also that the data demonstrate the absence of strong moduli. Indeed, in the latter case, the elastic modulus G' would be one order of magnitude higher than G''. More particularly, the elastic modulus would remain constant with the frequency and the phase-shift angle very low. This configuration is never obtained in the present study since we deal with weak gels.

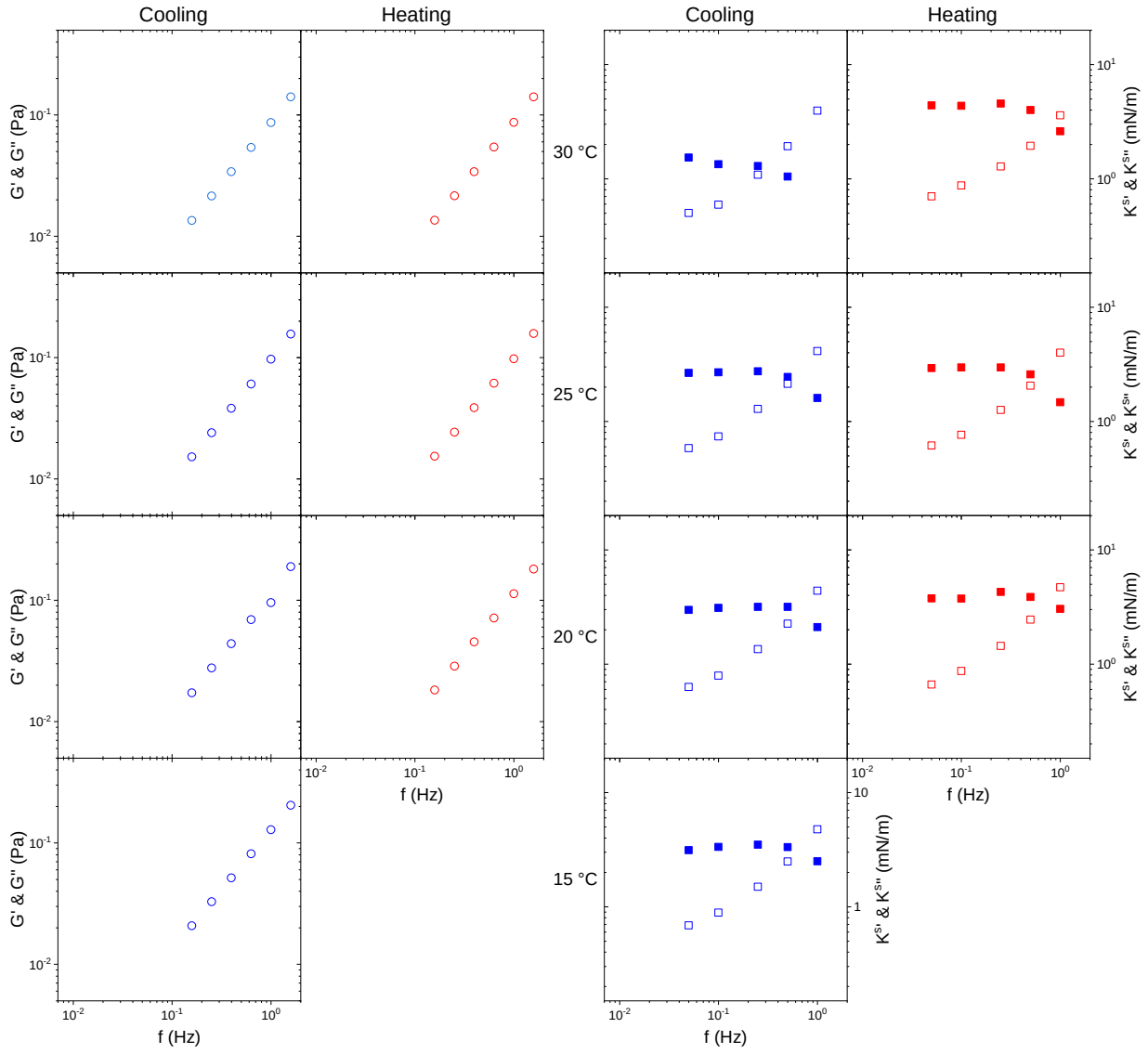

Figure 7. Isothermal frequency dependence of G' (●), G" (○), Kˢ' (■) and Kˢ" (□) for 3 g/L of k-carrageenan at different temperatures during cooling or heating, as indicated in the figure.

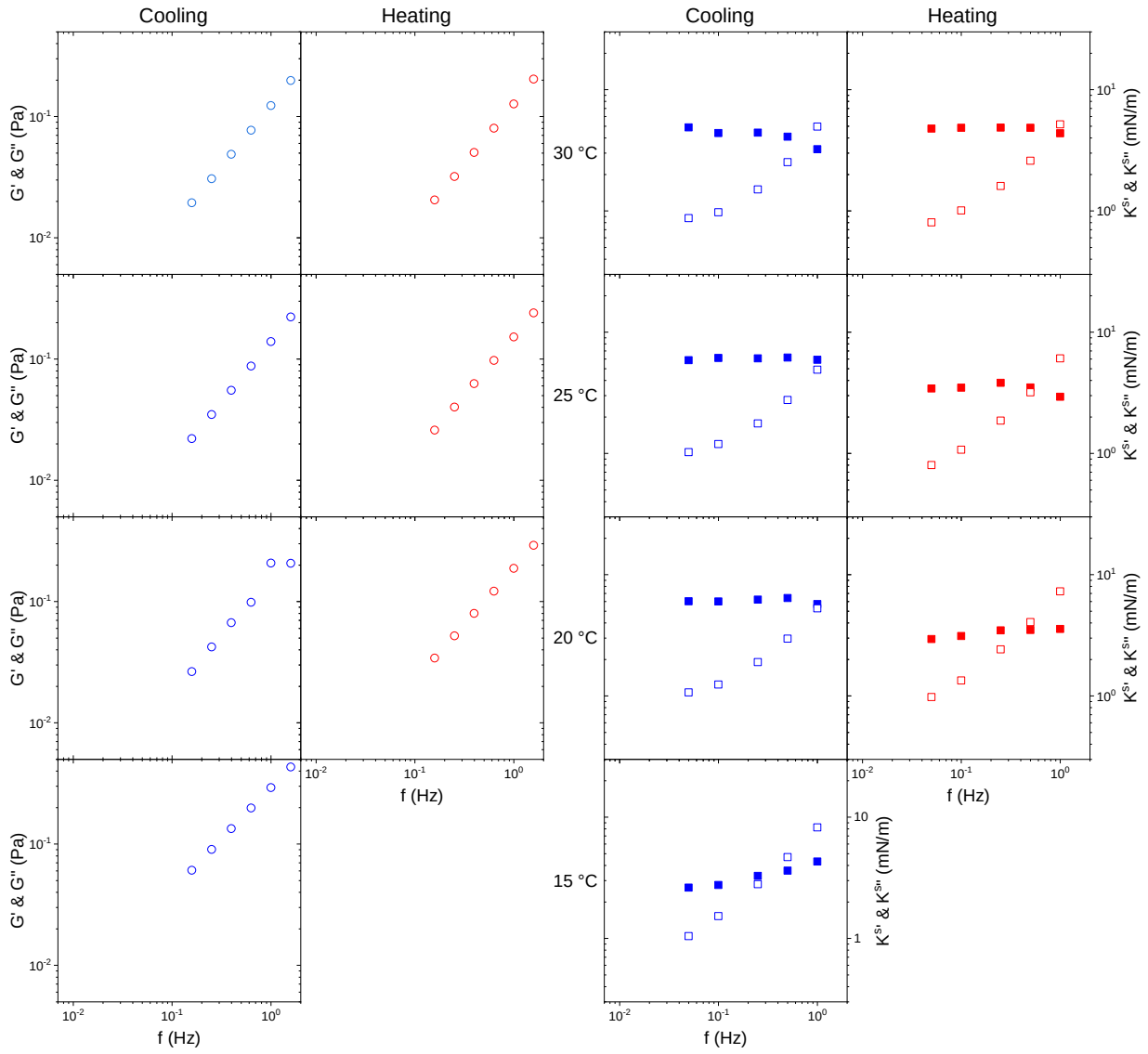

Figure 8. Isothermal frequency dependence of G' (●), G" (○), Kˢ' (■) and Kˢ" □) for 2 g/L of k-carrageenan at different temperatures during cooling or heating, as indicated in the figure.

4.3.2. Interfacial phenomenon

4.3.2.1. Static interfacial tension

The interfacial tension of indopol/water interface is given in Fig. 9 for all κ-carrageenan concentrations and temperatures. The interfacial tension is quasi-independent of κ-carrageenan concentration and temperature. It varies only between 14 and 16.5 mN/m which is slightly lower than indopol/water net interface, found between 17 and 18 mN/m. This result confirms that κ-carrageenan has no interfacial activity and only slightly modifies the water/Indopol interfacial tension, see discussion for more details.

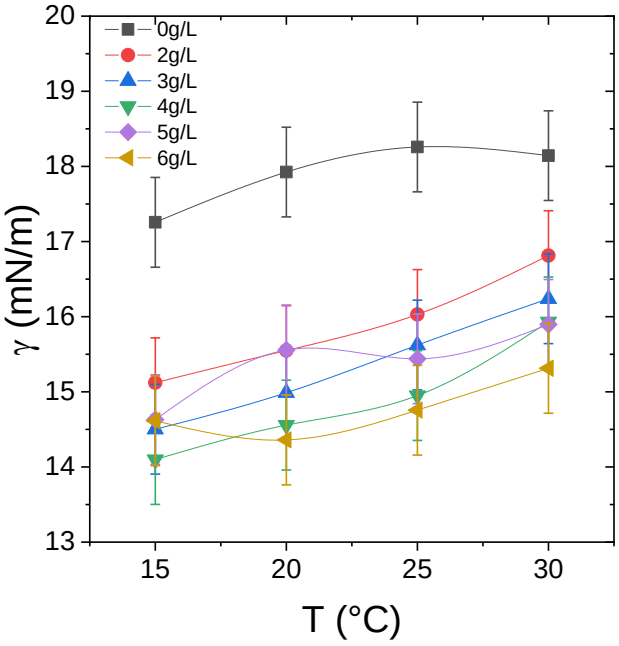

Figure 9. Interfacial tension between indopol and -carrageenan solution at different concentrations and different temperatures. The lines are drawn to guide the eyes.

4.3.2.2. Interfacial rheology

Fig. 4 shows the frequency dependence of the interfacial dilatational viscoelastic moduli, $K^{s'}$ (elastic) and $K^{s''}$ (viscous), for κ-carrageenan solution at 6g/L between 30 and 15°C during a cooling and heating cycle. At 30°C during cooling, the value of $K^{s'}$ is low and constant of about 3.64 mN/m. It is higher than that measured for Indopol/water net interface which is about 0.46 mN/m. Meanwhile, $K^{s''}$ shows a power law dependence versus frequency.

The same trend is observed at 25°C with slightly higher value of $K^{s'}$ of about 4.68 mN/m. At 20°C, both moduli increase. However, $K^{s'}$ increases remarkably with frequency between 11.92 and 22mN/m and surpasses $K^{s''}$ (3.5–12.7 mN/m) on the entire frequency range. At 15°C, a different behavior can be emphasized notably for the frequency behavior of $K^{s''}$. The gap between $K^{s'}$ and $K^{s''}$ widens as the former reaches 30–45 mN/m, whereas the latter exhibits a negative trend with the frequency. On reheating, $K^{s'}$ remains higher than $K^{s''}$ for all the frequencies and temperatures. In addition, both moduli increase with the frequency. At 20 and 25°C, there is almost no significant difference between the frequency dependence of the moduli. At 30°C, the changes of $K^{s''}$ are not significant whereas $K^{s'}$ shows a lower value but with the same frequency dependence trend at lower reheating temperatures.

The comparison between heating and cooling shows an important difference between $K^{s'}$ and $K^{s''}$ for the same temperature depending on the thermal history of the sample, as it was observed for the viscoelastic moduli of the bulk. Similar trends of the interfacial viscoelastic moduli are observed for the other concentrations. The evolution of the interfacial viscoelastic moduli with the frequency during cooling and heating for a κ-carrageenan concentration of 6 g/L is similar to that observed with 5 g/L (Fig. 5). In short, during cooling at 30 and 25°C, $K^{s'}$ does not vary significantly with the frequency while $K^{s''}$ increases with the frequency.

At 20°C and, mostly at 15°C, no crossover between K^{s}' and K^{s}'' occurs. More interestingly, K^{s}'' decreases with the frequency at 15°C. On the heating part, K^{s}' remains larger than K^{s}'' for all the frequencies and temperatures. At 15 and 20°C, the frequency behavior of the interfacial moduli are similar during heating and cooling. However, they display different frequency dependence at higher temperatures. At 4g/L, a great change in the absolute value and the frequency dependence of K^{s}' happens (Fig. 6). Under cooling and heating, the moduli follow the same frequency dependence. In fact, K^{s}' remains constant with the frequency while K^{s}'' increases with the frequency. The cross-over between the two curves is affected by both the temperature and the κ-carrageenan concentration. A slightly different behavior can be seen at 4 g/L of κ-carrageenan at 15°C. Similar behavior are reported for the κ-carrageenan concentrations lower than or equal to 4 g/L (Figs. 7-8).

To summarize, the transition temperature where K^{s}' surpasses K^{s}'' increases with the concentration. Moreover, the modulus K^{s}', is higher for the higher concentrations as it can be seen particularly at 15°C. Indeed, a great change in the absolute value and the frequency dependence of K^{s}' happens at 4 g/L. In parallel, K^{s}'' shows a maximum versus the frequency. If the concentration continues to increase, K^{s}' reaches a higher plateau and remains almost independent of the frequency whereas K^{s}'' drops with the frequency.

4.4. Discussion

First, it appears interesting to discuss the accuracy and reproducibility of the data. Fig. 4 displays the overall data obtained for different concentrations at 15°C. The figure includes the different repetitions for each sample through the error bars. In spite of the difference between the values for the same system, the difference is significant when the conditions are varied (different concentrations of κ-carrageenan). This highlights that the difference between the data obtained for each concentration and temperatures are significant. This also emphasizes that the difference is not due to low signal to noise ratio. Regarding the interfacial dilatational viscoelastic moduli,

$K^{s'}$ and $K^{s''}$ vary with the concentration and temperature. Specifically, $K^{s'}$ increases and becomes higher than $K^{s''}$ over the entire range of frequencies when the solution goes through a sol–gel transition, either by increasing concentration or by a thermal history. $K^{s''}$ also increases with the concentration and temperature in the liquid state but it goes through an increase to a decrease with the frequency when the κ-carrageenan solution becomes a gel. Since the interface rheology can be influenced by adsorption of surface-active agent at the liquid/liquid interface [25,26], the surface-activity of κ-carrageenan need to be discussed in detail. Firstly, in our knowledge, no article from the literature claims a possible interfacial activity of κ-carrageenan. On the other hand, the available data in the literature dealing with the surface and interfacial tension at liquid/liquid interfaces in the presence of κ-carrageenan confirm that this polysaccharide is not a surface-active molecule[23,24]. As an example, Huang et al.[27] used the Du Nouy ring method to characterize O/W surface tension of about 14 polysaccharides. They concluded unambiguously that κ-carrageenan has no surface activity at O/W interfaces. Nakajima et al.[28] reported similar findings using the pendant drop method for the water/air surface. Secondly, our measurements with κ-carrageenan confirm the previous finding since the O/W interfacial tension remains almost unchanged regardless of concentration and temperature, as showed in SI. The interfacial tension is found close but slightly lower than the Indopol/water net interface, of about 16 mN/m even the solution of κ-carrageenan is a gel or a liquid. In particular, the data are not ordered while the interfacial tension is expected to decrease regularly with κ-carrageenan concentration in the case of an eventual adsorption of κ-carrageenan at the liquid/liquid interface.

Finally, it is interesting to notice that our measurements reveal a slightly lower interfacial tension in presence of κ-carrageenan compared to the indopol/water pure interface. Two explanations are possible. The most plausible in our opinion would be the consequence of an averaging effect of the dielectric constant of the solution. Actually, when κ-carrageenan is added to the water, it modifies the dielectric susceptibility of the mixture (water + κ-carrageenan, compared to pure water) which impacts the Hamaker constant that is related to energy of cohesion arising from dispersion forces[29,30]. So, the interfacial tension is affected by the dielectric constant of the two media. This aspect is clearly visible when ethanol is added to water which leads to a significant

drop of the water surface tension even at very low ethanol amounts[31] and we know that ethanol is not a surface-active molecule. The same reason induces the increase of the surface tension of water when adding salts[32]. Thus, we believe that the slight reduction of the interfacial tension in our case can be reasonably attributed to the change of the dielectric susceptibility of the water in the presence of the κ-carrageenan.

Nevertheless, the second hypothesis could be a concentration gradient at the interface taking the form of depletion or concentration excess of polymer at the molecular scale. This phenomenon is manly induced by surface segregation effect as it was reported for a film of a normal (hydrogenated) polystyrene film when blended with deuterated[33]. To prove this assumption, molecular scale measurement, like neutron scattering are necessary, which is out of the scope of this paper.

So, the changes in the interfacial viscoelastic moduli with the frequency, concentration and the temperature cannot be attributed to an evident surface activity of κ-carrageenan. Furthermore, at similar temperature and constant κ-carrageenan content, different interfacial activity signals in terms of elasticity are recorded while, if real, the adsorption of κ-carrageenan must remain similar. Consequently, the variation of observed interfacial elasticity is due to the sol–gel hysteresis behavior of the continuous phase since the aqueous solution of κ-carrageenan can be at gel state or liquid at the same temperature and concentration depending on the thermal history of the sample. Thus, we believe that it is not the κ-carrageenan interfacial layer but the viscoelasticity of the continuous phase which affects the recorded interfacial signal. The bulk rheology reflects the thermal sensitivity of κ-carrageenan solutions. At low temperature, the change from coil to helix conformation explains the increase in the elastic part of the complex modulus. The plateau of G' at low frequencies denotes a gel behavior of the solution at higher concentrations (6 and 5 g/L of KC) and lower temperatures (15°C and in certain cases 20°C).

Comparing the behavior of K^{s}' and K^{s}'' on one hand, and G' and G'' on the other hand, one can see the evidence of the bulk rheology contribution on the interfacial viscoelastic moduli. The difference between the sol–gel mechanism in bulk becomes observable at 15°C and is impacted by the κ-carrageenan concentration. For this purpose, we focus on the evolution of K^{s}' and K^{s}''

as a function of frequency at 15°C for the different concentrations. The results are presented in Fig. 4. The frequency dependence of both moduli depends on the concentration of κ-carrageenan and the sol or gel behavior of the continuous phase. However, the effect is more singular on K^s''. On the one hand, K^s' increases with concentration and with frequency except for 2 g/L. The freezing behavior of the continuous phase seems to affect only the value of the modulus. The two highest values are recorded when the κ-carrageenan solutions form a gel at 5 and 6 g/L. On the other hand, a different behavior can be highlighted with the modulus K^s''. At 2 and 3 g/L, the solutions show an unambiguous liquid behavior. The viscous interfacial modulus increases with frequency. At 4 g/L, an intermediate state between liquid and gel has been evoked. Conversely, at 5 and 6 g/L when the continuous phase is a weak gel, a totally different evolution is highlighted. In this concentration range, a decrease of K^s'' with the frequency occurs. This appears as a clear signature of the weak gel of the continuous phase surrounding the indopol drop. To confirm these trends, data at other temperatures can be used. Samples at 4, 3 and 2 g/L are representative of a liquid state of the continuous phase. For all samples, without exception, K^s' and K^s'' increase with frequency. Moreover, a similar evolution is encountered at 30, 25 and 20°C for 5 and 6 g/L under cooling since the aqueous phase is in the liquid state at these high temperatures. It thus appears that the thermal history of the sample affects the response of the interfacial viscoelastic moduli measurements. This work suggests that the measurement of an apparent signature of interfacial viscoelastic properties, especially with the pendant oscillating drop, does not necessarily mean the consequence of an interfacial adsorption/desorption activity of a molecule or macromolecule at the interface. In fact, the principle of measuring the viscoelasticity of the Tracker is based on the instantaneous determination of the contact angle between the needle and the drop during expansion/compression. Then, through the Laplace equation, a viscoelastic modulus of the interface is determined.

Currently, in the case of a volume phase of very low viscosity, the procedure is considered valid if the Bond number is very low. In the case of viscoelastic mediums, the dynamic behavior of the drop oscillations is due to a subtle equilibrium between the stress and strain tensors of the continuous media, in the drop and the surrounding liquid, and if appropriate, of the interface. The latter is quite simple in the absence of surface-active species and only reflects the effect of interfacial tension. For surfactant-based films, the surface stress tensor is most likely solely an

isotropic stress[10]. Thus, the extraction of the dilatational viscoelastic moduli from the drop shape oscillations, using Laplace equation, could be applied without too much error. For strong gels, the presence of extra or deviatoric stresses does not allow to overcome their influence, as it was reported for gel-like protein layers on air/water interface in the Langmuir-Blodgett experiment present[34], of even with a very viscous oscillating drop[16]. The rigorous consideration of the stress tensors of the two liquids is essential to extract unambiguously the rheological properties of the interface. While this has already been addressed for static tests[35–37] the consideration of the rheology of the medium surrounding the oscillating drop has not yet been described.

To summarize, we show that the viscoelastic properties at the interface can be correlated to the bulk rheology derived from the sol–gel mechanism. We discuss the relationship between the elastic and viscous evolution with the frequency for various κ-carrageenan concentrations and temperatures taking into account the liquid or gel behavior of the continuous phase. However, the complete consideration of the rheology of the surrounding medium in the determination of the viscoelastic dilatational properties of an interface will require a more complete and probably more complex modeling and numerical simulations in order to quantitatively separate the contribution of the volume and the interface.

4.5. Conclusion

In this study, the impact of an extremely weak gel on the interfacial rheology of an oil/water interface is addressed. In the case of a solution with no interfacial activity, we have shown that interfacial viscoelasticity measurements still display rheological signatures that would suggest, incorrectly, the presence of an elastic interface. Indeed, the viscoelastic signature of the interface seems to be clearly correlated with the rheology of the volume. The reported results provide useful guidelines for efficiently estimating interfacial viscoelastic properties at liquid/liquid interfaces in the presence of a weak gel. A weak model gel, based on aqueous solution of κ-carrageenan (KC), is selected thanks to its reversible gelation with temperature and its non-interfacial activity. It can go through a sol–gel or gel-sol transition under cooling or heating, respectively. At low κ-carrageenan concentrations (2–4 g/L) or high temperatures (25–30°C), the

κ-carrageenan solutions behave like Newtonian fluids as the polysaccharide chains are under the form of loose coils. At lower temperatures (15–20°C), they go through a liquid-gel transition for sufficiently high κ-carrageenan contents (mainly 5 and 6g/L and in certain cases 4 g/L) since coils are joined into double-helices which produce the aggregation into the firm 3D network of a hydrogel if the concentration is above C*. The two transitions happen at different temperatures depending on κ-carrageenan concentration revealing an interesting hysteresis feature. A liquid or a weak gel can be reached at the same temperature depending on the thermal history. The interfacial viscoelastic moduli are probed by indopol drop volume oscillations in aqueous solutions containing κ-carrageenan at various concentrations and temperatures. On the one hand, K^s' increases with frequency regardless of the liquid or gel behavior of the continuous phase. The presence of the gel affects only the value of the modulus which is enhanced as the strength of the gel increases. On the other hand, a more singular behavior is emphasized with the viscous modulus K^s''. When the continuous phase is liquid, K^s'' increases with frequency. In the presence of an intermediate state between liquid and gel (κ-carrageenan 4 g/L) K^s'' does not vary with the frequency. In the presence of a weak gel in the continuous phase (5 and 6 g/L) a diminution of K^s'' with the frequency occurs. This appears as a clear signature of the weak gel of the continuous phase surrounding the indopol drop. While previous works have addressed the effect of a viscous phase on the interfacial properties measured with an oscillating pendant drop experiment, only few works have reported on the impact of a gel rheology on this type of measurements. To our knowledge, the effect has only been reported for highly elastic gels. In the case of weak gels, which do not even resist their weight if they are tilted, the question remains: how to extract the contribution of the bulk rheology from that of the interface? Modification or numerical simulations are still needed to properly account for the complex rheology of the bulk on the interface response during viscoelastic measurements by an oscillating pendent drop method.

List of Figures

References

(1) Joos, P.; Fainerman, V. B.; Loglio, G.; Lucassen-Reynders, E. H.; Miller, R.; Petrov, P. *Dynamic Surface Phenomena*; VSP: Utrecht, 1999.

(2) Deshmukh, O. S.; van den Ende, D.; Stuart, M. C.; Mugele, F.; Duits, M. H. G. Hard and Soft Colloids at Fluid Interfaces: Adsorption, Interactions, Assembly & Rheology. *Adv. Colloid Interface Sci.* **2015**, *222*, 215–227. https://doi.org/10.1016/j.cis.2014.09.003.

(3) Eggers, J. Nonlinear Dynamics and Breakup of Free-Surface Flows. *Rev. Mod. Phys.* **1997**, *69* (3), 865–930. https://doi.org/10.1103/RevModPhys.69.865.

(4) Leal-Calderon, F.; Bibette, J.; Schmitt, V. *Emulsion Science: Basic Principles*; Springer : Springer e-books: New York, NY, 2007.

(5) Drelich, J.; Fang, C.; White, C. L. MEASUREMENT OF INTERFACIAL TENSION IN FLUID-FLUID SYSTEMS. 15.

(6) Brooks, C. F.; Fuller, G. G.; Frank, C. W.; Robertson, C. R. An Interfacial Stress Rheometer To Study Rheological Transitions in Monolayers at the Air−Water Interface. *Langmuir* **1999**, *15* (7), 2450–2459. https://doi.org/10.1021/la980465r.

(7) Miller, R.; Ferri, J. K.; Javadi, A.; Krägel, J.; Mucic, N.; Wüstneck, R. Rheology of Interfacial Layers. *Colloid Polym. Sci.* **2010**, *288* (9), 937–950. https://doi.org/10.1007/s00396-010-2227-5.

(8) Jaensson, N.; Vermant, J. Tensiometry and Rheology of Complex Interfaces. *Curr. Opin. Colloid Interface Sci.* **2018**, *37*, 136–150. https://doi.org/10.1016/j.cocis.2018.09.005.

(9) Mendoza, A. J.; Guzmán, E.; Martínez-Pedrero, F.; Ritacco, H.; Rubio, R. G.; Ortega, F.; Starov, V. M.; Miller, R. Particle Laden Fluid Interfaces: Dynamics and Interfacial Rheology. *Adv. Colloid Interface Sci.* **2014**, *206*, 303–319. https://doi.org/10.1016/j.cis.2013.10.010.

(10) Lucassen, J.; Van Den Tempel, M. Dynamic Measurements of Dilational Properties of a Liquid Interface. *Chem. Eng. Sci.* **1972**, *27* (6), 1283–1291. https://doi.org/10.1016/0009-2509(72)80104-0.

(11) Leser, M. E.; Acquistapace, S.; Cagna, A.; Makievski, A. V.; Miller, R. Limits of Oscillation Frequencies in Drop and Bubble Shape Tensiometry. *Colloids Surf. Physicochem. Eng. Asp.* **2005**, *261* (1–3), 25–28. https://doi.org/10.1016/j.colsurfa.2004.11.043.

(12) Renggli, D.; Alicke, A.; Ewoldt, R. H.; Vermant, J. Operating Windows for Oscillatory Interfacial Shear Rheology. *J. Rheol.* **2020**, *64* (1), 141–160. https://doi.org/10.1122/1.5130620.

(13) Boujlel, J.; Coussot, P. Measuring the Surface Tension of Yield Stress Fluids. *Soft Matter* **2013**, *9* (25), 5898. https://doi.org/10.1039/c3sm50551k.

(14) Jørgensen, L.; Le Merrer, M.; Delanoë-Ayari, H.; Barentin, C. Yield Stress and Elasticity Influence on Surface Tension Measurements. *Soft Matter* **2015**, *11* (25), 5111–5121. https://doi.org/10.1039/C5SM00569H.

(15) Freer, E. M.; Wong, H.; Radke, C. J. Oscillating Drop/Bubble Tensiometry: Effect of Viscous Forces on the Measurement of Interfacial Tension. *J. Colloid Interface Sci.* **2005**, *282* (1), 128–132. https://doi.org/10.1016/j.jcis.2004.08.058.

(16) Yeung, A.; Zhang, L. Shear Effects in Interfacial Rheology and Their Implications on Oscillating Pendant Drop Experiments. *Langmuir* **2006**, *22* (2), 693–701. https://doi.org/10.1021/la051795w.

(17) Necas, J.; Bartosikova, L. Carrageenan: A Review. *Vet. Med. (Praha)* **2013**, *58* (6).

(18) Piculell, L. Gelling Carrageenans. *Food Polysacch. Their Appl.* **2006**, *239*.

(19) Viebke, C.; Piculell, L.; Nilsson, S. On the Mechanism of Gelation of Helix-Forming Biopolymers. *Macromolecules* **1994**, *27* (15), 4160–4166.

(20) Rochas, C.; Rinaudo, M. Activity Coefficients of Counterions and Conformation in Kappa-carrageenan Systems. *Biopolym. Orig. Res. Biomol.* **1980**, *19* (9), 1675–1687.

(21) Nguyen, P. N. Influence de composés perfluoroalkylés sur des films minces de phospholipides à une interface gaz/eau. 132.

(22) Meunier, V.; Nicolai, T.; Durand, D. Structure and Kinetics of Aggregating κ-Carrageenan Studied by Light Scattering. *Macromolecules* **2000**, *33* (7), 2497–2504.

(23) Ferry, J. D. *Viscoelastic Properties of Polymers*; John Wiley & Sons, 1980.

(24) Larson, R. G. *Foams, Emulsions, and Blends, The Structure and Rheology of Complex Fluids*; Oxford University Press, New York, 1999.

(25) Mucic, N.; Javadi, A.; Kovalchuk, N. M.; Aksenenko, E. V.; Miller, R. Dynamics of Interfacial Layers—Experimental Feasibilities of Adsorption Kinetics and Dilational Rheology. *Adv. Colloid Interface Sci.* **2011**, *168* (1–2), 167–178. https://doi.org/10.1016/j.cis.2011.06.001.

(26) Ravera, F.; Loglio, G.; Kovalchuk, V. I. Interfacial Dilational Rheology by Oscillating Bubble/Drop Methods. *Curr. Opin. Colloid Interface Sci.* **2010**, *15* (4), 217–228. https://doi.org/10.1016/j.cocis.2010.04.001.

(27) Huang, X.; Kakuda, Y.; Cui, W. Hydrocolloids in Emulsions: Particle Size Distribution and Interfacial Activity. *Food Hydrocoll.* **2001**, *15* (4–6), 533–542. https://doi.org/10.1016/S0268-005X(01)00091-1.

(28) NAKAJIMA, S.; MATSUMOTO, T.; AKIYAMA, A.; MASUDA, M.; SAKIYA, N.; WATANABE, Y.; UEDA, Y. Effect of Food-Grade Polysaccharide Gelling Agents on High-Oil-Containing Gels and Their Physical Properties. *J. Home Econ. Jpn.* **2019**, *70* (8), 522–534.

(29) Israelachvili, J. N. *Intermolecular and Surface Forces*; Academic press, 2011.

(30) Chaudhury, M. K. The Hamaker Constant and the Dispersion Force Component of the Surface Tension of Liquid Mercury. *J. Colloid Interface Sci.* **1987**, *119* (1), 174–180.

(31) Khattab, I. S.; Bandarkar, F.; Fakhree, M. A. A.; Jouyban, A. Density, Viscosity, and Surface Tension of Water+ Ethanol Mixtures from 293 to 323K. *Korean J. Chem. Eng.* **2012**, *29* (6), 812–817.

(32) Jungwirth, P.; Tobias, D. J. Specific Ion Effects at the Air/Water Interface. *Chem. Rev.* **2006**, *106* (4), 1259–1281.

(33) Geoghegan, M.; Nicolai, T.; Penfold, J.; Jones, R. A. L. Kinetics of Surface Segregation and the Approach to Wetting in an Isotopic Polymer Blend. *Macromolecules* **1997**, *30* (14), 4220–4227.

(34) Petkov, J. T.; Gurkov, T. D.; Campbell, B. E.; Borwankar, R. P. Dilatational and Shear Elasticity of Gel-like Protein Layers on Air/Water Interface. *Langmuir* **2000**, *16* (8), 3703–3711. https://doi.org/10.1021/la991287k.

(35) Hegemann, J.; Knoche, S.; Egger, S.; Kott, M.; Demand, S.; Unverfehrt, A.; Rehage, H.; Kierfeld, J. Pendant Capsule Elastometry. *J. Colloid Interface Sci.* **2018**, *513*, 549–565. https://doi.org/10.1016/j.jcis.2017.11.048.

(36) Nagel, M.; Tervoort, T. A.; Vermant, J. From Drop-Shape Analysis to Stress-Fitting Elastometry. *Adv. Colloid Interface Sci.* **2017**, *247*, 33–51. https://doi.org/10.1016/j.cis.2017.07.008.

(37) Pepicelli, M.; Verwijlen, T.; Tervoort, T. A.; Vermant, J. Characterization and Modelling of Langmuir Interfaces with Finite Elasticity. *Soft Matter* **2017**, *13* (35), 5977–5990. https://doi.org/10.1039/C7SM01100H.

Annexes

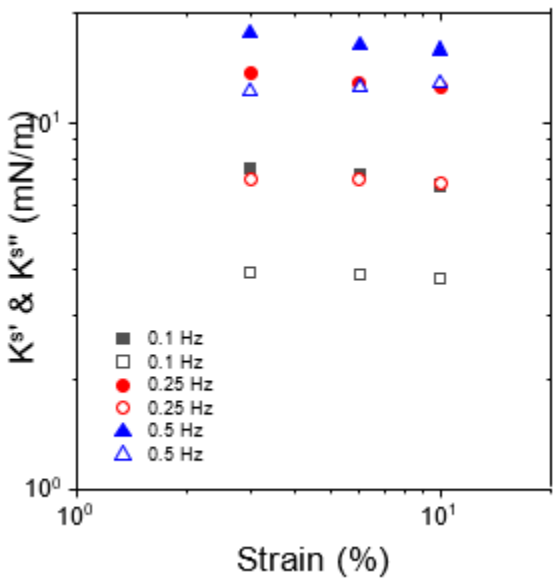

Annex A1: Strain dependence of K^s***' (close symbols) and*** K^s***" (open symbols) at 0.1 Hz (squares), 0.24 Hz (circles), and 0.5 Hz (triangles). The temperature and volume of the rising drop of indopol in 5 g/L of*** κ-carrageenan ***solution are fixed at 15°C and 10 µL, respectively.***

Chapter V: Viscoelastic Moduli of Surfactant-laden interface in A Weak Gel

5.1. Introduction

In the previous chapter, the influence of the continuous phase, mainly under the form of a weak gel, on the elastic and viscous interfacial moduli was highlighted, the work was conducted with a bare liquid/liquid interface of indopol/water in the absence of surface activity of the κ-carrageenan (KC). In this chapter, a surfactant is introduced into the system in order to probe the interface and the rheological behavior in the presence of a layer of surfactant adsorbed at the interface which should ensure a viscoelastic behavior of the liquid/liquid interface[1–3]. In this chapter, we investigate the effect of the bulk, under the form of liquid or weak gel, on the interfacial properties and the viscoelastic moduli of an oscillating drop in the presence of surfactant.

First, the choice of the surfactant can be briefly discussed. In our system, a rising drop of indopol is formed surrounded by an aqueous phase containing κ-carrageenan (KC). The surfactant must not be introduced in the continuous aqueous phase in order to avoid interactions with κ-carrageenan. Consequently, the surfactant has to be initially present in the indopol organic phase (in the drop), thus it becomes necessary to use a surfactant displaying better affinity for the oil than for the aqueous phase, as such the surfactant may have a Hydrophilic-Lipophilic Balance (HLB) lower than 10. Sorbitan monoleate surfactants, commercially denoted as Span, appear as good candidates. Span 80 has been selected in this study.

In a second step, emulsions are prepared with these formulations. In order to highlight the interfacial phenomenon, concentrated emulsions with dispersed fractions larger than or equal to 60% have to be prepared. However, the presence of Span leads to W/O emulsions meaning that the κ-carrageenan gel phase is in the water droplets instead of being in the continuous phase. Despite all these constraints, a tentative of exploration of the relationships between bulk and interfacial rheological properties is conducted.

The κ-carrageenan concentration and temperature are varied in order to modulate the liquid and gel behavior as well as the gel properties. Two Span concentrations are used in order to tune the coverage of the liquid/liquid interface.

5.2. Materials and Methods

5.2.1. Chemicals

Sorbitan monooleate, Span® 80 (Sigma-Aldrich batch #BCBZ8539), was used as a surfactant. It was bought in its pure liquid form. Its concentration was presented as a w/w%. The oil phase was Polybutène under the name of Indopol® grade L-8 (INEOS Oligomers), the aqueous phase ultrapure MilliQ® water (18 MΩ.cm). κ-carrageenan (KC) solutions from 3 to 5 g/L were prepared as described in the materials and methods chapter.

A highly concentrated Indopol+Span 80 emulsion was prepared using a vortex, the initial solution was at 20w/w%, from this solution diluted solution were prepared by adding the necessary amount of Indopol before mixing. Air bubbles remaining in the solutions were removed using a vacuum desiccator.

5.2.2. Drop profile tensiometry

Interfacial tension (static) and interfacial viscoelastic dilatational moduli (dynamic) of water/oil interface were investigated via a drop-profile tensiometer (TRACKER; Teclis; Civrieux-d'Azergues, France). For the experiments, a rising drop of indopol was put into contact with the aqueous KC-carrageenan solution filling the transparent cell. Span 80-Indopol L8 mixtures were prepared to be used as the drop phase, Span 80 being a liposoluble surfactant prevented interactions with KC.

Interfacial tension (static), i.e. temporal evolution of the interfacial tension at constant drop volume, were first studied by keeping the oil drop volume constant at 7-10 µL at the tip of a curved needle with an internal diameter Ø = 0.84 mm or 1.19 mm in ultrapure water. Span 80 concentrations used were between 0.01 up to 0.1 w/w%. Above 0.1 w/w%, IFT became too low

and drop detachment rendered the measurement inaccurate. Consequently, 0.05 and 0.1 w/w% concentrations of Span 80 were used in dynamic oscillatory tests.

Dynamic interfacial viscoelasticity measurements were first carried out on the water/oil interface. To this aim, drop volume variation was set at 10% of the initial drop volume. Batches of five oscillations were applied followed by 30 s of absence of oscillations. Oscillation frequency was varied between 0.05 and 1 Hz. Amplitude tests showed that the linear domain was respected. For KC solutions, the samples and equipment were preheated and the same oscillation protocol was applied, by applying a batch of five oscillations at 10% volume variation then followed by 30 s of rest. This step was repeated until a steady state of modulus was obtained for each frequency. The same protocol was applied to KC solutions at 3-6 g/L, the samples were first pre-heated then tests were performed at 30 °C and 15 °C to compare gel and liquid bulk phase contributions, depending on the concentration.

5.2.3. Emulsion preparation and characterization

5.2.3.1. Emulsion preparation

Emulsions of indopol-water were prepared at various Water-Oil ratios (w/w%) of 60-40%, 70-30, at various Span 80 concentrations (w/w%) in the oil phase: 0.05%, 0.1%, 1%, 2%. They were prepared by adding water on top of the oil+Span 80 phase then mixing with a vortex shaker. Emulsions with Kc were prepared by adding preheated KC at 60°C KC 5g/L, mixed with a vortex shaker allowed to cool. Emulsions were prepared with a vortex shaker in wt%, the final weight of the emulsion was 4g.

5.2.3.2. Confocal Microscopy

Emulsions, both O/W and O/W-Kc were observed once at equilibrium using a x25 and x63 magnification water immersion objectives. Drop radius and packing were then reported. As there was no temperature control on the microscope, KC solutions could only be observed at room temperature or in gelled state. Dyes used were Rhodamine B (Sigma-Aldrich) and Fluoresceine salt FITC (sigma-aldrich) 5 ppm in each phase, FITC is readily soluble in water while

Rhodamine is dissolved in indopol with acetone as a co-solvent that is given ample time to evaporate.

5.2.3.3. Shear Rheology

W/O emulsions were loaded directly to the DHR3 rheometer with a 40 mm plate-plate geometry with a 1 mm gap. Amplitude sweeps at 1Hz were first done to find the linear viscoelastic region. Then, frequency sweeps were carried out at fixed strain = 0.6% between 1 and 0.01 Hz. Emulsions are reheated to 50-60°C in a water bath for easier loading on the peltier plate that is preheated at 60°C and they are given 1000s to reach equilibrium before conducting the frequency sweeps, then the sample temperature is brought down to room temperature 20°C and given 1000s to reach thermodynamic equilibrium before launching the sweeps.

5.3. Results and Discussion

5.3.1. Interfacial tension

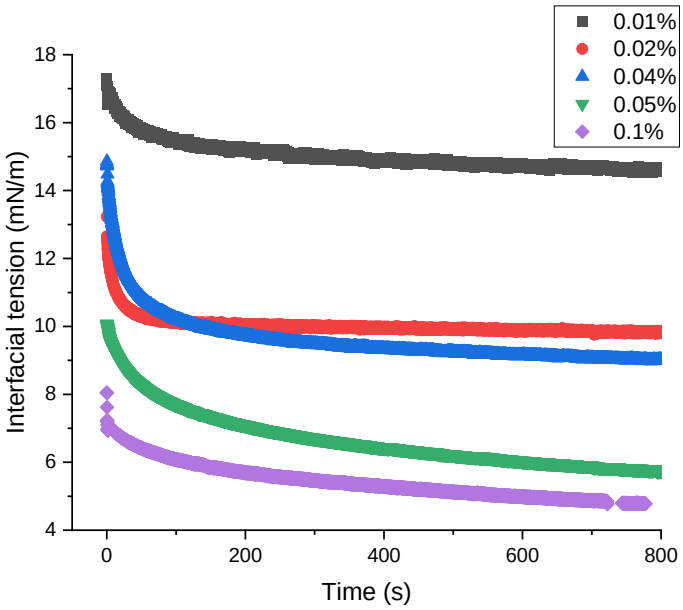

Figure 1: Variation of the indopol/water interfacial tension with time in the presence of Span 80 at different concentrations.

Figure 1 represents the temporal evolution of the indopol/water interfacial tension at different Span concentrations.

Interfacial tension of the pure Indopol/water interface is 18 mN/m. In the presence of Span, all the curves show the same trend. For a given span concentration, initially and for a short time, the interfacial tension decreases sharply. As time passes, the slope of the curve decreases and tends towards a plateau. This curve can give access to the kinetic of adsorption and the diffusion of the surfactant. In the framework of this study, we focus only on the values of the interfacial tension once stabilized i.e. at the plateau. In absence of Span, the interfacial tension of the Indopol/water interface is 18 mN/m and it decreases in the presence of Span. This confirms the adsorption of the surfactant at the interface. The interfacial tension decreases gradually with the Span content up to a value of 4.78 mN/m reached at 0.1% w/w Span 80. At this concentration the oil drop starts to detach and IFT is very low, preventing further reliable measurements.

To proceed, it is important to verify whether a monolayer of surfactant is present or not at the interface. Thus, we propose to use the Gibbs equation of surface equation as means to fit the data and assess the surface coverage:

$$\Gamma = -\frac{1}{RT}\frac{d\gamma}{d\ln C}$$

Where Γ is the surface coverage, γ is the interfacial tension, C is the concentration of the surfactant, T is the temperature and R is the constant of perfect gas law. Table 1 shows the extracted equilibrium value of the interfacial tension for each concentration.

Concentration (w/w%)	Equilibrium IFT
0.01	14.27
0.02	9.75
0.04	2.19
0.05	4.9
0.1	4.78

Table 1: Indopol/Water Interfacial Tension (Equilibrium IFT) measured at equilibrium for different surfactant concentrations.

Figure 2 gives the slope of γ vs lnC ($\frac{d\gamma}{d\ln C}$). The surface per molecule is $S = 1/N_A * \Gamma$, where is N_A is Avogadro's constant.

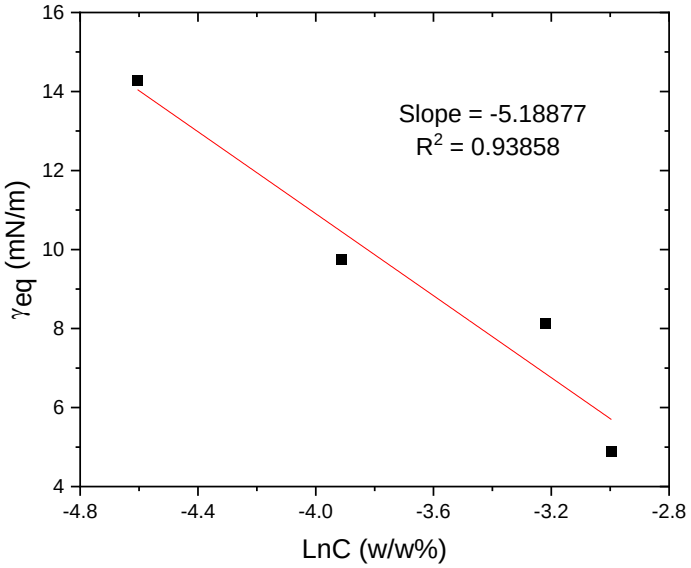

Figure 2: Interfacial tension as a function of the natural logarithm of the concentration of Span. The red line is a linear fit through the data points.

A surface excess of $\Gamma = 2.13.10^{-6}$ mol/m^2 is obtained while the area per molecule A is equal to 0.779 nm^2/mol. While those values are not close enough to those reported in literature for a Span 80 monolayer[4], it shows that a considerable amount of surfactant molecules are present on the interface. The mechanism of adsorption of a surfactant from the bulk to the drop interface has been studied in literature[5,6]. It starts with depletion of Span 80 from the drop to the interface. Then, the viscoelasticity appears as a result of reorganization of molecules during dilatation/compression (reorientation model) or mass transfer between the two phases (Frumkin model), albeit neither cases could be verified during our work.

In the following, span concentrations of 0.05 and 0.1 % will be used since they lead to fairly close values of interfacial tensions and amounts of span adsorbed. With these concentrations, we can avoid detachment while having a considerable amount of surfactant on the interface.

5.3.2. Interfacial rheology

Figure 3 displays the evolution of the viscoelastic moduli of the indopol/water interface in the presence of 0.05% of Span in indopol and 5 g/L of KC in water for temperatures ranging between 30 and 15 °C.

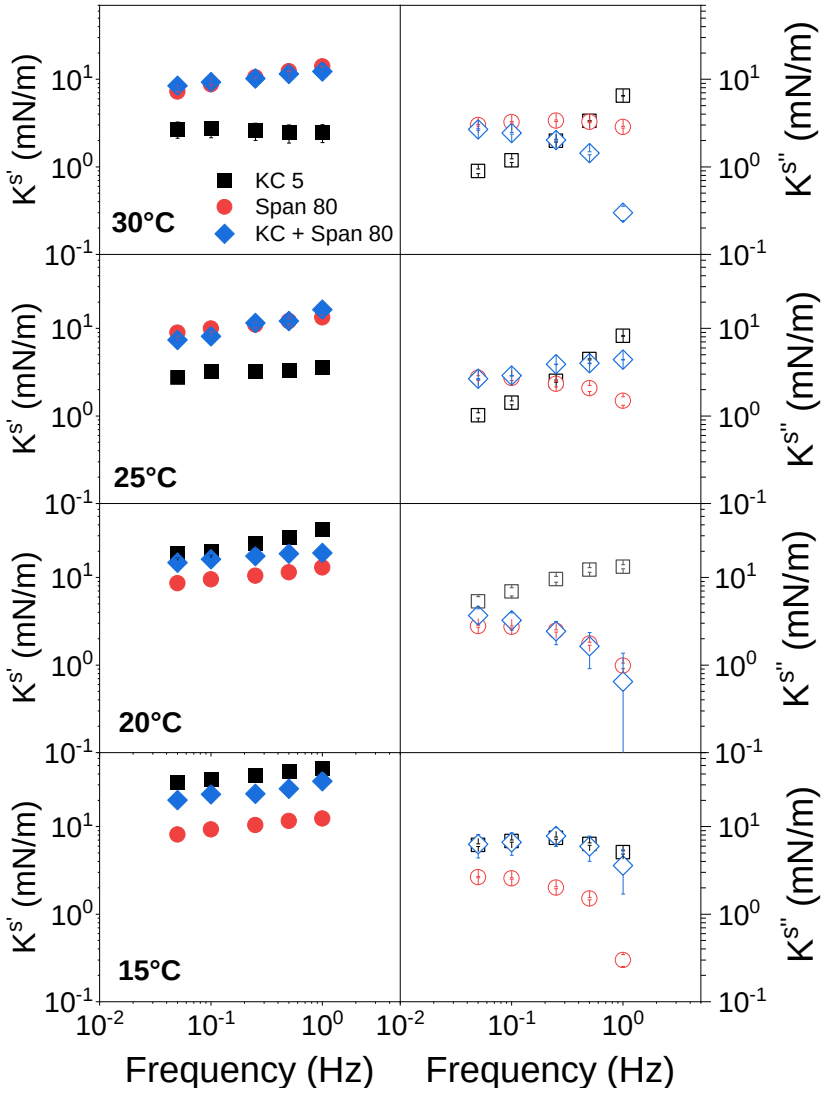

Figure 3: Isothermal frequency dependence of K^s' (filled symbols) and K^s'' (empty symbols) in presence of KC 5g/L in the bulk phase without Span ("KC 5" ■,□), or Span 80 at 0.05%w/w adsorbed at the interface in water without KC ("Span 80" ●,○), and a combination of the two, i.e. KC 5g/L in the bulk phase and 0.05%w/w Span 80 in indopol ("KC + Span 80" ◆,◇).

For the indopol/water interface in the presence of Span but in absence of KC ("Span 80"), the data reveal a weakly elastic interface caused by the adsorption of Span 80 molecules to the oil/water interface. K^s' is about 10-12mN/m and K^s'' 1 mN/m. An elastic interface is detected and the evolution of the moduli with the frequency as well as the values correspond to the order of magnitude of those classically encountered with surfactant at the liquid/liquid interfaces[6–9].

It appears interesting to compare the curves of Indopol-Span 80/water ("Span 80" without KC) with those of Indopol/KC-water ("KC 5" without Span). At 30 °C and 25 °C, when the aqueous phase is under liquid form, the presence of Span enhances the elasticity of the interface since K^s' shifts from 1 mN/m to 10 mN/m thanks to the surfactant adsorption at the interface. Conversely, at lower temperatures (20℃ and 15 °C), when the KC takes the form of a weak gel, the elasticity becomes larger in absence of Span. This emphasizes that the effect of the continuous phase under the form of the gel has a major impact on the viscoelasticity of the system compared to the adsorption of the surfactant. This confirms that this effect cannot be neglected as reported in the previous chapter.

The most interesting feature appears when the system containing Span 80 in oil and KC in water is addressed ("KC + Span 80"). On the one hand, when the KC is liquid (T = 30-25°C), the elasticity curves collapse perfectly with those with Span but without KC ("Span 80"). In other words, we find that K^s'(Indopol+Span/water) = K^s'(Indopol+Span/water+KC) for all the frequencies. This indicates that the Span layer plays the major role in the elasticity of the interface, i.e. the elasticity of the interface comes from the Span adsorbed layer. This result is very interesting because it confirms the absence of surface activity of KC. On the other hand, when the KC becomes a gel, the sol-gel transition occurs for temperatures lower than or equal to 20°C, a strange behavior takes place. The elasticity K^s' (Indopol/water-KC) without Span ("KC 5") is larger than the elasticity K^s' (Indopol-Span/water-KC) of the system with Span and KC ("KC + Span 80"). In other words, the elasticity measured is lower in the presence of Span when the continuous phase is a weak gel. This behavior takes place for all the frequencies at 15 and 20°C. The difference seems to increase with the strength of the gel since the variation between the curves is larger at 15 °C than at 20 °C. The strength of the gel is greater at 15°C than at 20°C. Another interesting feature is that the elasticity vs frequency curve for Span 80/KC ("KC + Span 80") falls between KC alone ("KC 5") and Span alone ("Span 80") curves.

Additional experiments are performed at different span concentrations, KC contents and temperatures to confirm these behaviors. By playing with KC contents and temperatures, it becomes possible to tune the strength of the gel while the use of various span concentrations is necessary to test different surface coverages of the interface. In the following, the liquid and gel states of the KC are treated separately.

Figure 4 displays the viscoelastic properties of the interfaces in the presence of Span for systems containing 3 g/L of KC at 15°C, 4 g/L of KC at 20°C, and 5 g/L of KC at 30°C, respectively. The span concentrations used are 0.05% and 0.1%, as indicated in the figures. For all these systems, the KC is in a liquid state. The data in absence of Span are also added in the figure. All the curves show the same trend as above (Figure 3 with KC 5 g/L and T = 30-25°C, 0.05% of Span). Liquid KC shows a viscous signature where K^s'' is a power law and K^s' is low and independent of frequency, with the addition of Span 80 we can see an increase of K^s' to around 10 mN/m and K^s'' showed little dependence of frequency.

When the Span concentration is reduced to 0.05%, the curves still follow the same evolutions regardless of the KC concentration at 30 °C (Figure 5). At 30°C, K^s' and K^s" both follow a power law, the former being higher indicating an elastic interface. The signature is similar to the oil/water + Span interface, but the exponent of the power law of K^s" increases with concentration from 0.16 at 3 g/L to 0.27 at 6 g/L, a gentler slope than the Indopol/KC interface in chapter IV (0.65). All the data confirm the signal when the KC is liquid and confirms that the elasticity of the interface is due to the adsorbed layer of Span.

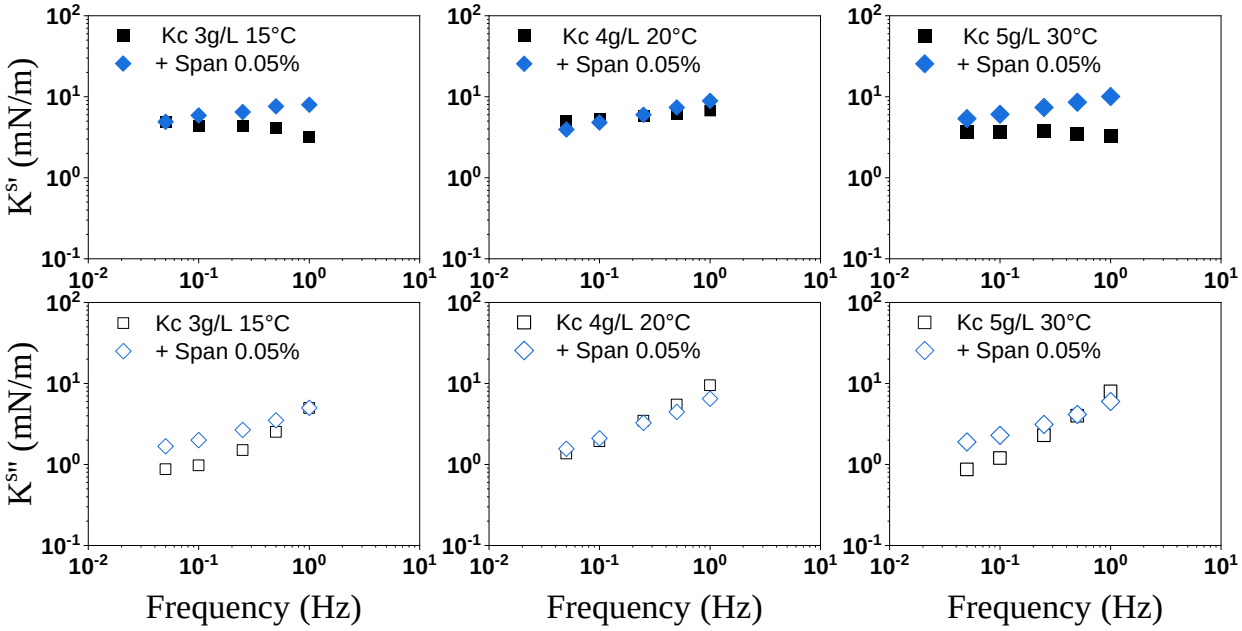

Figure 4: The viscoelastic properties of the interfaces (K^{s}' (filled symbols) and K^{s}" (open symbols) in the presence of Span for systems containing 3 g/L of KC at 15 °C, 4 g/L of KC at 20 °C, and 5 g/L of KC at 30 °C, respectively. In the legend, the squares ■, □ correspond to the system without Span while the diamonds refer to the system with Span ◆,◇. As an example, "Kc 3g/L 15°C" indicates the system without Span while "+ Span" corresponds to the same system but in the presence of Span. The Span concentration is fixed at 0.05%.

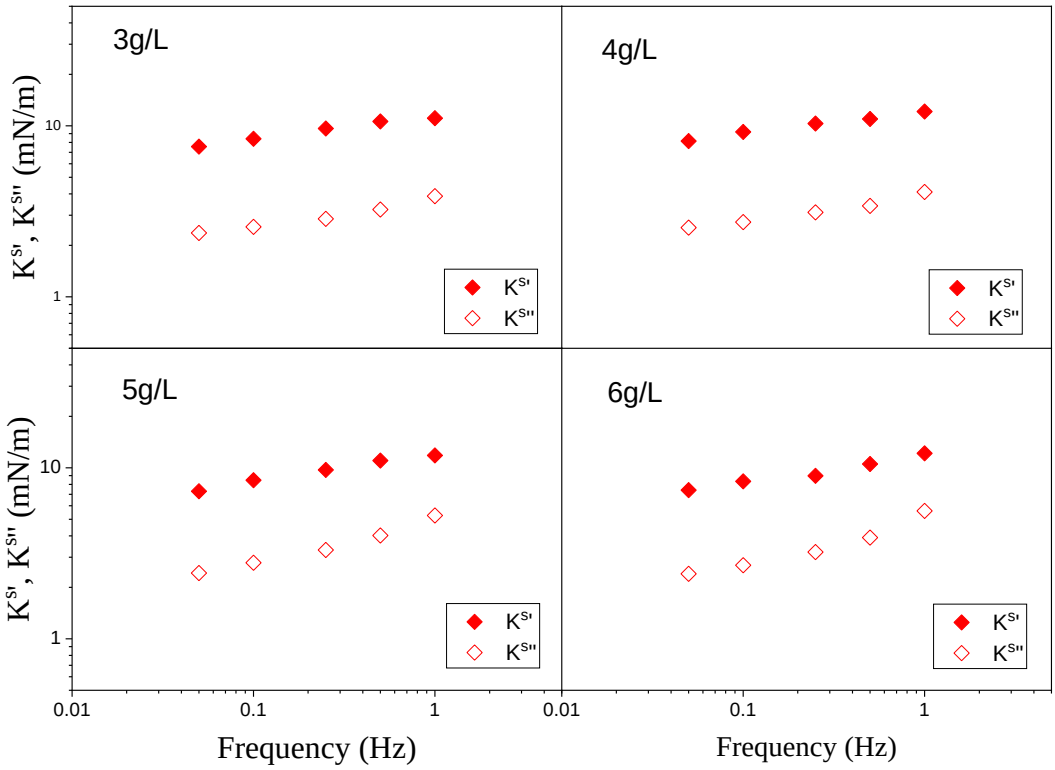

Figure 5: Interfacial moduli of an indopol droplet mixed with 0.05% Span 80, in KC solutions 3-6 g/L at **30°C**. Kˢ': Filled symbols ◆, Kˢ'': Open symbols ◇

For the gel state, Figures 6 and 7 are used. In Figure 6, the interfacial elasticity and viscous moduli at a KC concentration of 5 g/L at 15 and 20°C for Span concentrations of 0.05 and 0.1% are reported as a function of the frequency. In the gel state, KC is elastic with K^{S}' rising and reaching 30-40 mN/m at 15°C, while Kˢ'' follows a negative trend vs frequency. It should be mentioned that these KC gels in these conditions is a metastable system during the solution-gel (sol-gel) transition as cross-linking occurs as we can see at 5 g/L at 20°C, both Kˢ' and Kˢ'' exhibit a power law trend vs frequency. One curious observation is the noticeable decrease of the viscoelastic moduli with the addition of Span 80, which reoccurred in further tests. These results confirm the previous observations which indicate a reduction of the apparent interfacial elasticity in the presence of Span. Similar trends occur with 0.05% of Span 80 at 15 °C in the presence of 4, 5 and 6 g/L of KC (Figure 7). At 15°C, the samples exhibit a noticeable increase in Kˢ' to 28-30 mN/m, while Kˢ'' reaches an inflexion point at 4 g/L and follows a negative trend with

frequency at higher concentrations. The behavior is dominantly elastic, and the shift in relaxation caused by the aggregation of KC chains can be seen. However, the noticeable decrease in the elastic modulus, in comparison with the bare interface (K^s' reached 40 mN/m) is still highlighted.

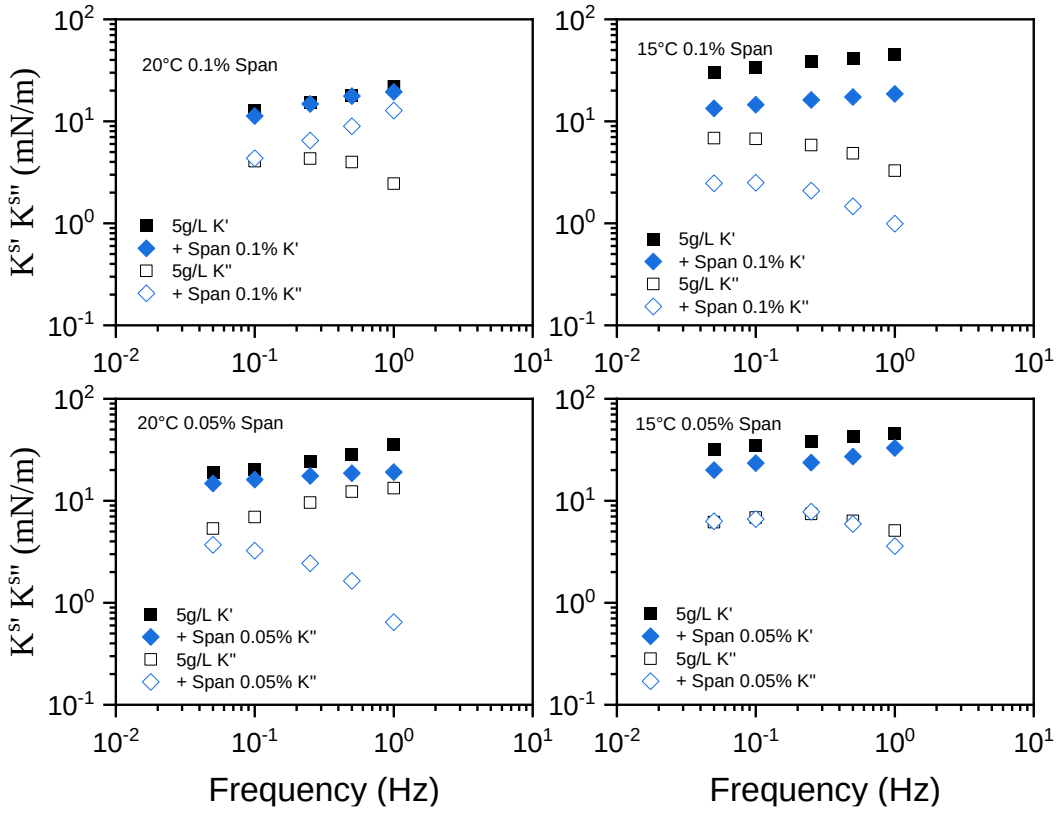

Figure 6: The viscoelastic properties of the interfaces K^s' (filled symbols) and K^s" (open symbols) in the presence of Span 0.05% and 0.1% for systems containing 5 g/L of KC at 15 °C and 20 °C. In the legend, the squares ■,□ correspond to the system without Span while the diamonds ◆, ◇ refer to the system with Span. As an example, "5g/L K^s' " indicates the system without Span while "+ Span 0.1% K" corresponds to the same system but in the presence of Span.

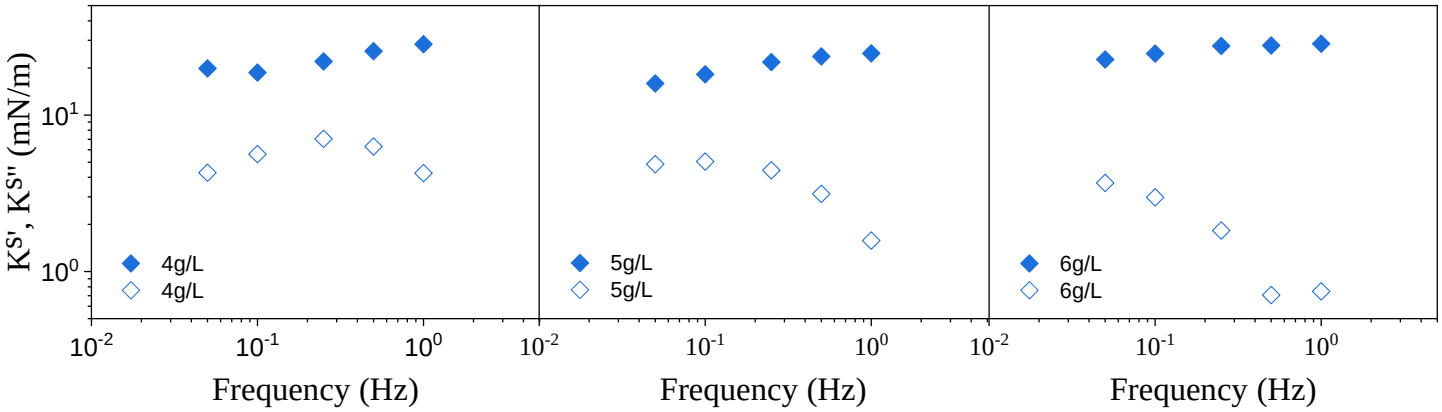

Figure 7: Interfacial moduli of an indopol droplet mixed with 0.05% Span 80 in KC solutions 4-6g/L at 15 °C. K^s': Filled symbols, K^s'': Open symbols

All these data highlight that the drop of elasticity in the presence of Span when KC is under the form of a weak gel is a real trend and a signature of the combination of KC gel in the continuous phase and Span at the liquid/liquid interface.

To our knowledge, this is the first time this phenomenon has been observed. The origin of the weakened viscoelasticity in the presence of Span is an interesting challenge. A tentative to understand this feature starts from considering the nature of the adsorbed surfactant layer which is not rigid but rather soft. The final elasticity would depend on the interaction between the soft layer of surfactant at the interface and the hard gel of the continuous phase. The gel in the continuous phase appears fragilized in the presence of Span, one possible interpretation is slippage between the surfactant layer and the hydrogel which leads to shear-like banding: when the drop oscillates, shear-like bands are created and the hard gel shears the interface. Consequently, the drop deforms more easily. The span layer act as a lubricant of the interface between the drop and the bulk. The system deforms where it is easier, then at the interface. It is reported in literature that yield stress fluids exhibit such behavior in interfacial rheology experiments[10,11]. It is possible that the dilatation of the interface is opposed by the elastic deformation of the continuous phase, weakening the combined effect of the surfactant layer and the surrounding gel. Numerical simulations would be needed to evaluate such a scenario and it

could be an interesting perspective in the future, as to our knowledge, no model or work in literature has treated this case.

5.3.3. Water-in-Oil emulsions

Interfacial tension and viscoelasticity play an important role in emulsion stability and overall rheological behavior[12] thus we prepared emulsions with span 80 and KC to see how the gel and the interface impact the overall bulk rheology. Concentrated emulsions with dispersed fractions larger than or equal to 60% have to be prepared. However, the presence of Span leads to W/O emulsions meaning that the gel phase due to κ-carrageenan is in the water droplets rather than in the phase.

5.3.3.1. Visual aspect and Confocal microscopy

Water-oil emulsions were prepared by first mixing oil and span, and then adding water droplets for Water/Oil ratios 60/40 and 70/30 w/w%. Emulsification process is mainly carried out with a vortex shaker. Note that these are preliminary experiments on the visual aspect and microscopy, the aqueous phase does not contain KC. Figures 8 and 9 show the macroscopic aspect of 60/40 Water/Oil emulsions containing 0.05% and 2% w/w of span 80, respectively, the result is a weak gel fluid that flows when the vial is tilted. Other emulsions prepared at 70/30 water/oil ratio show excess water at the bottom of the vial, the volume fraction of the emulsified water is around 40% yet the position of the turbid emulsion was quite intriguing, so the nature of the emulsion – O/W or W/O – could not be determined visually.

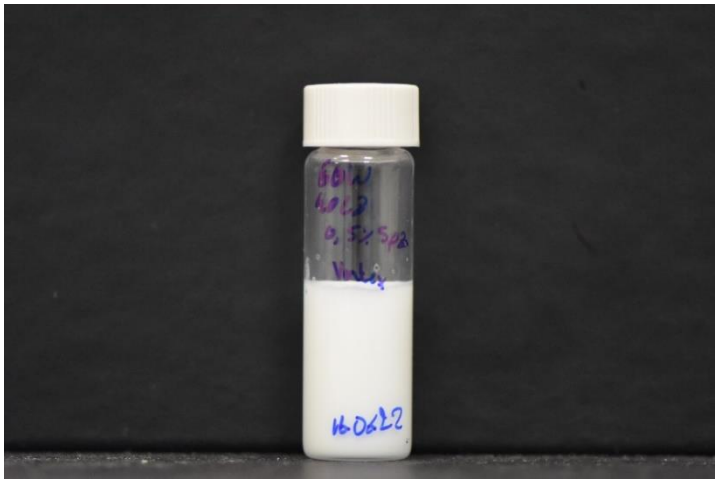

Figure 8: Image of an emulsion 60W/40L8 Span 80 0.5% w/w%.

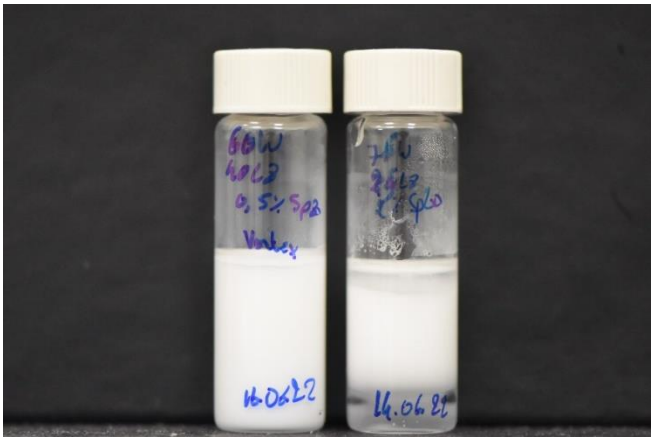

Figure 9: Image of a 60W/40L8 Span 80 0.5% emulsion and another at 70W/30L8 2% Span 80.

To better understand the structure of the emulsion, Rhodamine B was added to tag the water phase. As shown in Figure 10, neither the bulk phase nor the dispersed phase could be distinguished as Rhodamine B seemed to adhere to the interface of the droplets. We believe this is due to the higher affinity between Rhodamine and Span 80 molecules which allows the surfactant molecules to capture the dye.

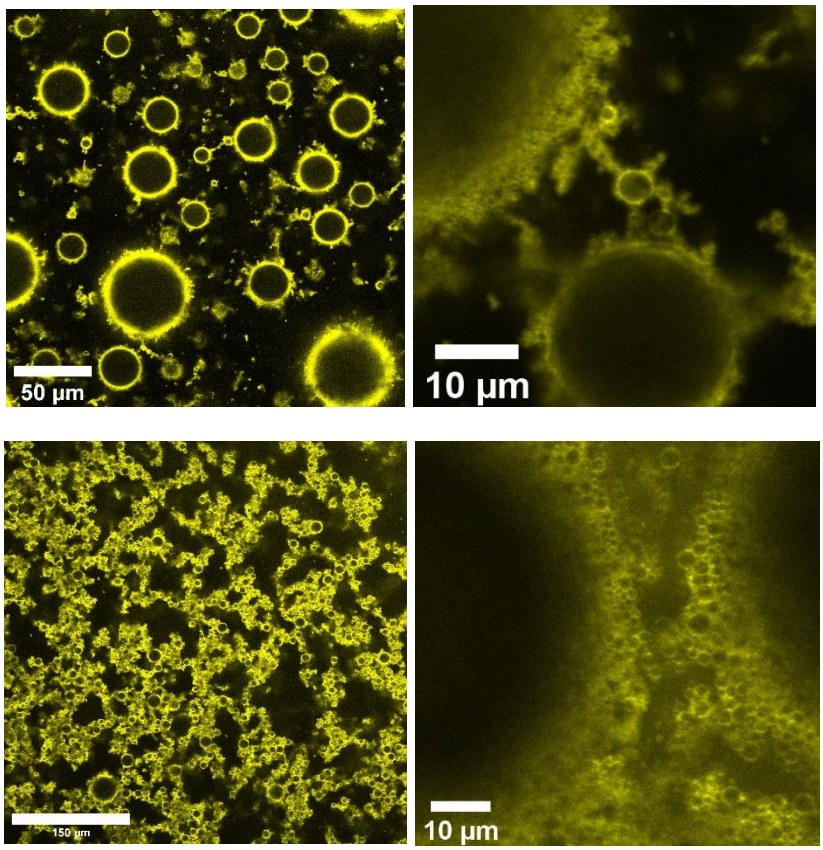

Figure 10: CLSM Images of water/Indopol emulsions with Span 80. Rhodamine B (5 ppm) as the fluorescent dye (yellow) under radiation of 541 nm LASER, observed using a x25 zoom lens (right side) and x63 zoom on left side.

By replacing Rhodamine B with Fluoresceine (FITC) and using the 488 nm high intensity laser, a completely different image can be obtained (Figure 11). The FITC tags the water. The picture shows densely packed water droplets dispersed in a tiny fraction of the oil phase, which seems more in line with the macroscopic aspect of the emulsion and the gel-like flow behavior inside the vial. These experiments highlight the importance of the nature of the fluorescent probes in the visualizations by confocal microscopy. Indeed, their interactions with the system are essential to reach unequivocal conclusions.

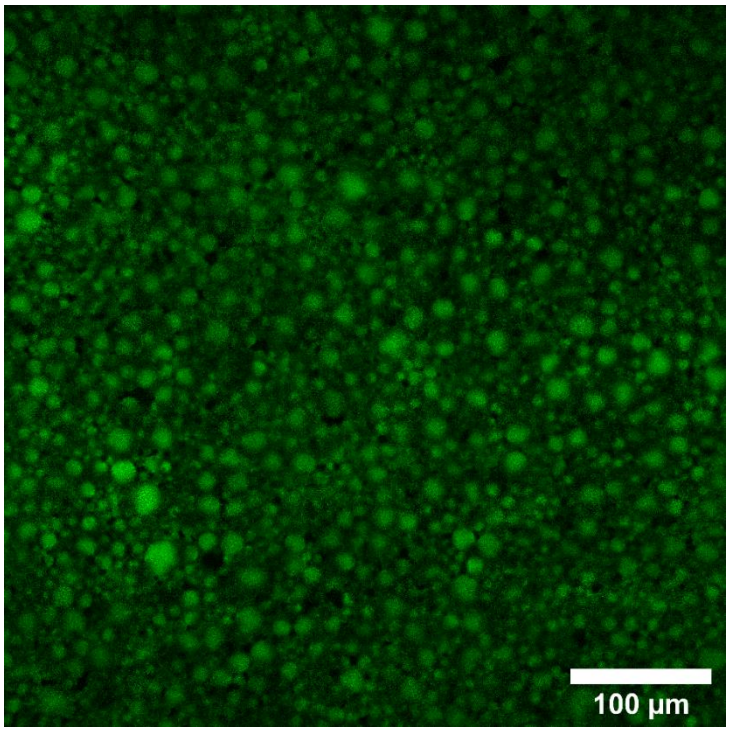

Figure 11: Confocal Image of a 60W/40L8 0.5% Span 80 taken with x25 zoom lens, water droplets were marked with Fluorescine (FITC) at 5 ppm. Black spots represent the oil phase.

5.3.3.2. Shear rheology

First, the emulsions prepared without KC are discussed (Figure 12). Shear rheology measurements reveal that G' is larger than G'' in the whole frequency domain leading to a mean elastic modulus of 10Pa for the 60W/40L8 emulsions with 0.5% w/w Span 80. The yield stress is attributed to the dense packing of the droplets and the elasticity of the interfaces providing resistance against shear. Densely packed emulsions were studied in several papers[13–17]. It was found that a relationship exists between G', the volume fraction of the dispersed phase ϕ, the surface tension σ, and the radius of the monodisperse droplets r. The rise of the viscous modulus G'' reflects the relaxations of the fluid phase. Higher concentrations of surfactant (2% w/w Span 80) lead only to a higher modulus but the shape of the curve remained the same.

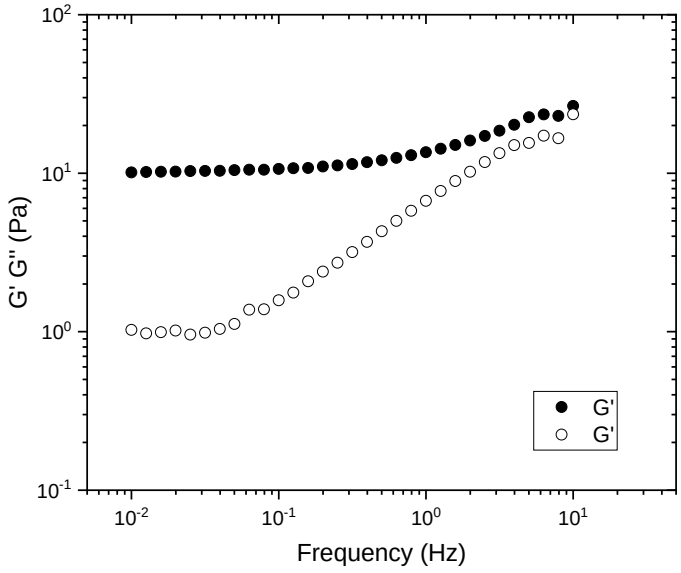

Figure 12: 60W/40L8 0.5% Span 80 frequency sweep using a 1mm gap Plate/Plate geometry. G' filled symbols, G'' open symbols.

The addition of a weak gel (Kappa-Carrageenan at 5g/L) does not change the overall behavior (Figure 13). A slight but regular increase of G' is observed when the temperature is decreased from 30°C to 15°C. This indicates that G' is enhanced when the dispersed phase is shifted from a liquid to a gel. In other words, the addition of 5g/L of KC gel induces a very small rise in the G' plateau as we lowered the temperature of the sample. However, it is not significant compared to the interfacial contribution of the surfactant films around the water droplets.

It Is unclear if a correlation between the interfacial rheology measurements and the emulsion shear measurements could be made given the different situation where in the former, the gel was in the continuous phase, while in the latter, the gel is within the droplets, which is a more complex setup given concentration restraints on KC solution; higher concentrations mean a more viscous aqueous phase which in turn affects emulsion reproducibility and hinders rising drop formation and maintaining a Gaussian shape. Studying the rheology of gelled droplets surrounded by an elastic film could be an interesting prospect but is not in the scope of our study.

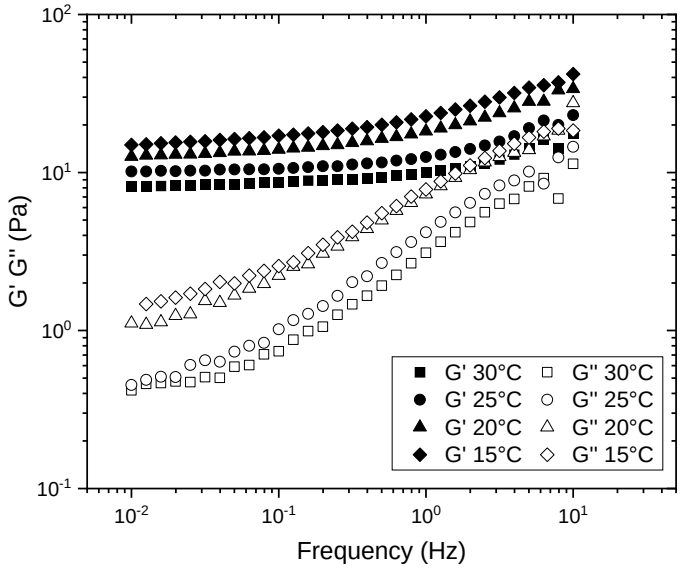

Figure 13: 60KC/40L8 0.5% Span 80 at 30°C, 25, 20 and 15°C. 1mm gap Plate/Plate geometry. G' filled symbols, G'' open symbols.

5.6. Conclusion

The present work aimed to study how the effect of the bulk, under the form of liquid or weak gel, impacts the interfacial properties of the viscoelastic moduli of an oscillating drop in the presence of a surfactant (Span 80). The second objective was to try to decouple interfacial rheology and bulk rheology of an emulsion stabilized by a surfactant and a tunable hydrogel, by combining drop tensiometry and three-dimensional shear rheology. The idea was to correlate the rheology with the structure of the emulsion. The κ-carrageenan concentrations and temperatures were varied to modulate the liquid and gel behavior as well as the gel properties and two Span concentrations were used to ensure a large coverage of the liquid/liquid interface.

Interfacial rheology revealed that the effect of the surfactant layer depended significantly on the state of the aqueous continuous phase containing KC. The first case is when the aqueous phase was in liquid form, the presence of Span enhanced the elasticity of the interface**.** The Span layer played the major role in the elasticity of the interface, i.e. the elasticity of the interface came

from the Span adsorbed layer. The second case is when the KC became a gel, a remarkable increase of the elasticity provided was observed with or without Span. This emphasized that the effect of the continuous phase under the form of the gel had a major impact on the viscoelasticity of the system compared to the adsorption of the surfactant. This confirmed that this effect cannot be neglected as we already reported in the previous chapter. Unexpectedly however, the elasticity measured was lower in the presence of Span when the continuous phase was a weak gel. The origin of the weakened viscoelasticity in the presence of Span remains unclear. The gel in the continuous phase seemed fragilized at the interface with Span. One possible interpretation was slippage between the surfactant layer and the hydrogel which lead to shear banding. The span layer acted as a lubricant of the interface between the drop and the bulk. Numerical simulations would be needed to evaluate such a scenario and it could be an interesting perspective in the future, as to my knowledge, no model or work in literature has treated this scenario.

In a second step, emulsions were prepared with these formulations. In order to highlight the interfacial phenomenon, concentrated emulsions with dispersed fractions larger than or equal to 60% were prepared. However, the presence of Span 80 lead to W/O emulsions indicating that the gel phase formed by κ-carrageenan was in the water droplets and indopol as the continuous phase. Nevertheless, we attempt here an exploration of the relationships between bulk and interfacial rheological properties. Volume shear rheology measurements revealed that, in absence of KC, G' is larger than G'' in the whole frequency domain. The addition of a weak gel (Kappa-Carrageenan at 5g/L) did not change the overall behavior. A slight but regular increase of G' was observed when the temperature was decreased from 30°C to 15°C. This indicated that G' increased when the dispersed phase was shifted from a liquid to gel. However, it was not significant compared to the interfacial contribution of the surfactant films around the water droplets. It is unclear if a correlation between the interfacial rheology measurements and the emulsion shear measurements could be made given the different situation where in the former, the gel was in the continuous phase, while in the latter, the gel is within the droplets, a potential solution is the usage of another non-ionic surfactant like Brij[18].

References

(1) Möbius, D.; Miller, R.; Fainerman, V. B. *Surfactants: Chemistry, Interfacial Properties, Applications*; Elsevier, 2001.

(2) Fainerman, V. B.; Lylyk, S. V.; Aksenenko, E. V.; Petkov, J. T.; Yorke, J.; Miller, R. Surface Tension Isotherms, Adsorption Dynamics and Dilational Visco-Elasticity of Sodium Dodecyl Sulphate Solutions. *Colloids Surf. Physicochem. Eng. Asp.* **2010**, *354* (1–3), 8–15. https://doi.org/10.1016/j.colsurfa.2009.02.022.

(3) Mucic, N.; Javadi, A.; Kovalchuk, N. M.; Aksenenko, E. V.; Miller, R. Dynamics of Interfacial Layers—Experimental Feasibilities of Adsorption Kinetics and Dilational Rheology. *Adv. Colloid Interface Sci.* **2011**, *168* (1–2), 167–178. https://doi.org/10.1016/j.cis.2011.06.001.

(4) Santini, E.; Liggieri, L.; Sacca, L.; Clausse, D.; Ravera, F. Interfacial Rheology of Span 80 Adsorbed Layers at Paraffin Oil–Water Interface and Correlation with the Corresponding Emulsion Properties. **2007**, 10.

(5) Fainerman, V. B.; Kovalchuk, V. I.; Aksenenko, E. V.; Miller, R. Dilational Viscoelasticity of Adsorption Layers Measured by Drop and Bubble Profile Analysis: Reason for Different Results. *Langmuir* **2016**, *32* (22), 5500–5509. https://doi.org/10.1021/acs.langmuir.6b01134.

(6) Aksenenko, E. V.; Kairaliyeva, T.; Makievski, A. V.; Fainerman, V. B.; Miller, R. Adsorption and Surface Dilational Visco-Elasticity of C n EO m Solutions as Studied by Drop Profile Analysis Tensiometry. *Colloids Surf. Physicochem. Eng. Asp.* **2018**, *547*, 95–101. https://doi.org/10.1016/j.colsurfa.2018.03.029.

(7) Santini, E.; Liggieri, L.; Sacca, L.; Clausse, D.; Ravera, F. Interfacial Rheology of Span 80 Adsorbed Layers at Paraffin Oil–Water Interface and Correlation with the Corresponding Emulsion Properties. *Colloids Surf. Physicochem. Eng. Asp.* **2007**, *309* (1–3), 270–279. https://doi.org/10.1016/j.colsurfa.2006.11.041.

(8) Ravera, F.; Loglio, G.; Pandolfini, P.; Santini, E.; Liggieri, L. Determination of the Dilational Viscoelasticity by the Oscillating Drop/Bubble Method in a Capillary Pressure Tensiometer. *Colloids Surf. Physicochem. Eng. Asp.* **2010**, *365* (1–3), 2–13. https://doi.org/10.1016/j.colsurfa.2010.01.040.

(9) Mucic, N.; Kovalchuk, N. M.; Pradines, V.; Javadi, A.; Aksenenko, E. V.; Krägel, J.; Miller, R. Dynamic Properties of CnTAB Adsorption Layers at the Water/Oil Interface. *Colloids Surf. Physicochem. Eng. Asp.* **2014**, *441*, 825–830. https://doi.org/10.1016/j.colsurfa.2012.08.071.

(10) Majumdar, S.; Krishnaswamy, R.; Sood, A. K. Shear Banding in a Yield Stress Bearing Langmuir Monolayer. *Soft Matter* **2011**, *7* (17), 7805–7812.

(11) Martin, J. D.; Hu, Y. T. Transient and Steady-State Shear Banding in Aging Soft Glassy Materials. *Soft Matter* **2012**, *8* (26), 6940–6949.

(12) Velandia, S. F.; Ramos, D.; Lebrun, M.; Marchal, P.; Lemaitre, C.; Sadtler, V.; Roques-Carmes, T. Exploring the Link between Interfacial and Bulk Viscoelasticity in Reverse Pickering Emulsions. *Colloids Surf. Physicochem. Eng. Asp.* **2021**, *624*, 126785.

(13) Mason, T. G.; Bibette, J.; Weitz, D. A. Elasticity of Compressed Emulsions. *Phys. Rev. Lett.* **1995**, *75* (10), 2051.

(14) Princen, H. M. Rheology of Foams and Highly Concentrated Emulsions: I. Elastic Properties and Yield Stress of a Cylindrical Model System. *J. Colloid Interface Sci.* **1983**, *91* (1), 160–175.

(15) Princen, H. M.; Kiss, A. D. Rheology of Foams and Highly Concentrated Emulsions: III. Static Shear Modulus. *J. Colloid Interface Sci.* **1986**, *112* (2), 427–437.

(16) Dimitrova, T. D.; Leal-Calderon, F. Rheological Properties of Highly Concentrated Protein-Stabilized Emulsions. *Adv. Colloid Interface Sci.* **2004**, *108*, 49–61.

(17) Dimitrova, T. D.; Leal-Calderon, F.; Gurkov, T. D.; Campbell, B. Surface Forces in Model Oil-in-Water Emulsions Stabilized by Proteins. *Adv. Colloid Interface Sci.* **2004**, *108*, 73–86.

(18) Depraetere, P.; Florence, A. T.; Puisieux, F.; Seiller, M. Some Properties of Oil-in-Water Emulsions Stabilized with Mixed Non-Ionic Surfactants (Brij 92 and Brij 96). *Int. J. Pharm.* **1980**, *5* (4), 291–304.

Chapter VI: Interfacial viscoelastic moduli of nanoparticle-laden interface in a weak gel

6.1. Introduction

In this chapter, we studied the effect of nanoparticles on the interfacial rheological properties of indopol oil droplets oscillating in aqueous solution of KC under the form of a gel or a liquid. The approach is similar to that of the previous chapter, but the surfactant adsorbed layer is replaced by a layer of nanoparticles at the interface. Much like the sensitivity issue with interfacial shear rheology[1], dilatational interfacial rheology with oscillating droplets in the presence of nanoparticles is not an easy task and remains challenging. For instance, previous attempts in our lab (Thesis Frederico, not published) lead to unsuccessful trials because the silica particles have formed crusts and wrinkles at the liquid/liquid interface. Other results with particles and oscillating droplets remain rarely reported in the scientific literature. We feel that the choice of particles and/or the position of the particles in the continuous phase or in the droplet might play a non-neglectable role.

We first go through the selection of the particles conducted with the objective to find the silica particles which adsorb at the indopol/water interface. In this study, we selected hydrophobized silica particles to be dispersed in indopol in order to have only KC in the aqueous phase.

We focus mainly on the interfacial rheology with oscillating drop in the presence of silica and absence of KC in water with the objective to obtain a detectable value of the elastic modulus which attests the adsorption of the particles at the liquid/liquid interface. To form a layer at the interface, the particles have to diffuse from the indopol subphase into the interface and adsorb on the interface. Isopropanol (IPA) is added as a co-solvent in indopol leading to better adsorption of silica particles onto the oil/water interface.

Then, interfacial rheology experiments are conducted with indopol-isopropanol droplets containing silica nanoparticles (oscillating in water medium containing KC at a concentration of

5g/L. The silica concentration in oil is fixed to 0.5%. During the experiments, the temperature was varied from 30°C to 15°C.

Finally, the results obtained with span and silica in the presence of KC are compared and discussed, the span+KC combination showed a lower elastic modulus than the gel while the NP+KC seemed to strengthen the elasticity.

6.2. Materials & Methods

	Particle Type			
Properties	FS	Aerosil R816	Aerosil R202	IPA-ST
Particle Size (nm)	7	12	14	10-15
BET surface area (m^2/g)	395±25	190±20	100±20	300 ±20
Surface Group	-	hexadecyl	Dimethylsiloxane	-

Table 1: The properties of the silica nanoparticles used in this study. Aerosil® are hydrophobically modified fumed silica NP, whereas IPA-ST are amorpheous silica nanoparticles in Isopropanol (IPA) 30% wt%

We used different types of nanoparticles in our study. Fumed silica "FS" are smaller with no surface modifications. Aerosil R816. R202 and R974 are treated to have surface groups as shown in table 1. IPA-ST are amorphous silica NP dispersed in Isopropanol. Two different types of low viscosity oils were used: Polybutenes "Indopol" grade L-6 and L-8, and PDMS47V20. The aqueous phase was MilliQ ultrapure water, while k-carrageenan (KC) was bought as powder from sigma-aldrich.

Curved "J" needles were used in these tests, mainly a G16 (internal diameter Ø = 1.19mm external diameter $Ø_e$ = 1.7mm, teflon coated). Drop volume is set at 10µl and deformation at 10% of the initial drop volume, unless stated otherwise.

The aim of this work is to study interfacial viscoelasticity using a rising drop of oil in an adjustable bulk phase i.e., the KC hydrogel. To separate the interface and bulk responses, the NP

must not have direct interactions with KC, thus we chose the Aerosil fumed silica nanoparticles that are synthetized to be hydrophobic so they can be dispersed in the oil phase and have the affinity and to adsorb to the interface and form a layer with a significant viscoelastic modulus, this can be verified with the oscillating drop method.

The NP at our disposal are Aerosil fumed silica nanoparticles. A previous study focused on the effect of their varying degrees of hydrophobicity on oil/water emulsions[2].

6.3. Pure indopol

In this part, the selection of the particles is conducted. Hydrophobic silica are mainly considered. The particles are dispersed in indopol in order to have only KC in the aqueous continuous phase. The objective is to find the silica particles which adsorb at the indopol/water interface. We focus mainly on the interfacial rheology with oscillating drop in the presence of silica with the objective to obtain a detectable value of the elastic modulus which attests the adsorption of the particles at the liquid/liquid interface. To form a layer at the interface, the particles have to diffuse from the indopol bulk into the interface and adsorb on the interface. Note that for these tests the aqueous continuous phase does not contain KC.

6.3.1. Aerosil R816

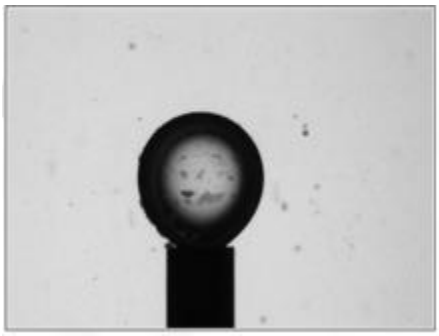

Figure 3: A rising oil drop in water, the black fragments within the drop are fumed silica nanoparticle aggregates. The indopol+NP mixture was treated with ultrasound waves.

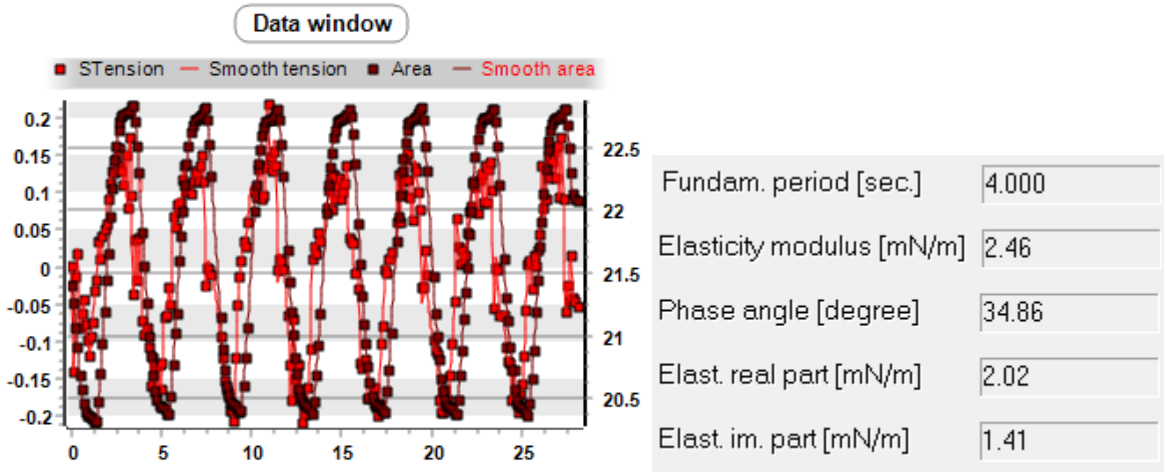

Figure 4: Analysis of interfacial tension signal after a dynamic drop test. The right hand side shows the extracted elastic (real) and viscous parts (imaginary) of the interfacial viscoelastic modulus.

Figure 3 and 4 show the results of the rising drop experiments. We can see aggregates in the drop and a low interfacial viscoelastic modulus, it can be deduced from these results that aggregation has limited particle diffusion and adsorption to the interface.

6.3.2. Aerosil R202

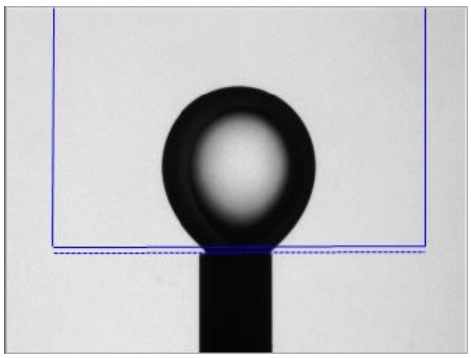

Figure 5: Drop profile of a drop of indopol + R202 Aerosil particles 0.5% w/w%

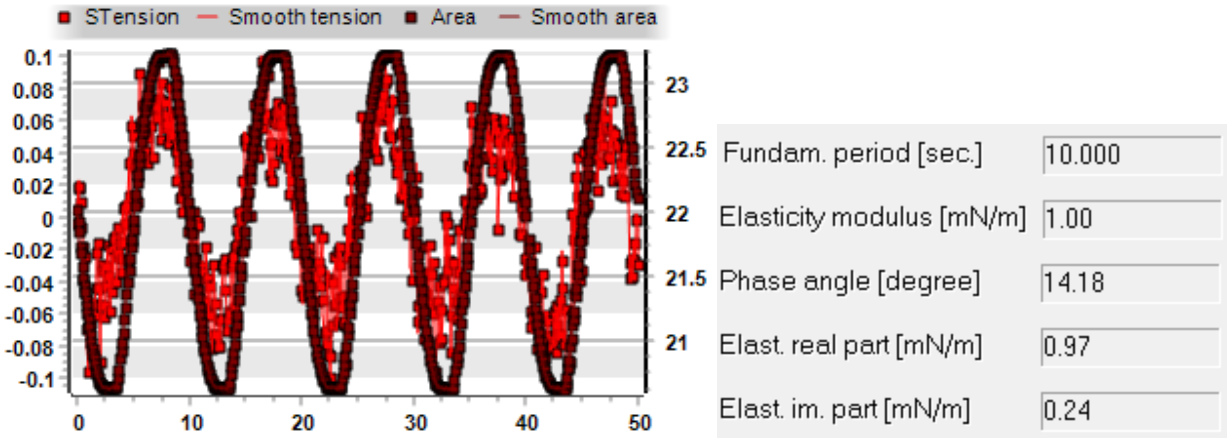

Figure 6: Analysis of the IFT signal after the oscillation of a drop profile of a drop of indopol + R202 Aerosil particles 0.25% w/w%.

R202 nanoparticles did not adsorb to the interface either in our tests, we did not see aggregates as much as with R816. Thus, from the interfacial modulus and the IFT measurement (figure 4 and 6), we can assume the nanoparticles did not have enough affinity to the interface.

It can appear strange to see an absence of interfacial elasticity in interfacial rheology while emulsions with water/indopol and silica have already been obtained[2–4]. Confocal microscopy images in Barros et al.[2] have confirmed the adsorption of silica at the liquid/liquid interface after emulsification using an ultrasound mixer. This seems to establish that the adhesion of the particles at the liquid/liquid interface can be different between the emulsion and the system used in interfacial rheology because the mixing process is fundamental in the adsorption of the particles to the liquid/liquid interface. Indeed, during the emulsification, the migration and adsorption of the particles to the liquid/liquid interface are favored by the flow produced by the stirrer device. Consequently, it is relatively easy to place and fix the particles at the interface. Conversely, with the oscillating drops, the particles can migrate to the interface based only on the diffusion mechanism. This process follows a power law of the form $t \propto R^3$ where t is the time necessary for the diffusion of the particles and R the particles radius[5]. Larger particles lead to longer diffusion times. In addition, the particles have to cross an activation energy in order to go and attach to the interface. Mechanical energy is necessary to cross this barrier. At the same time, the particle which is wetted by the continuous phase has to be dewetted by the second liquid to go to the interface. For all these reasons, it can be concluded that it is easier to put the particles at the interface during emulsification process as compared to interfacial rheology because the diffusion and the passing of the activation energy barrier are favored by the shearing and mechanical energy produced by the stirrer device.

6.4. Modifying the medium: Indopol-isopropanol

Mixtures of indopol and nanoparticles have not resulted in an elastic layer, the aggregation of the particles limits the diffusion and adsorption towards the interface, therefore, we opted to change the wetting properties of the medium by introducing isopropanol (IPA) as a co-solvent. The samples are treated with ultrasound for 3 minutes. This option was first tested with organosilicasol nanoparticles.

6.4.1. Effect of IPA

Isopropanol was found to lower the oil/water interfacial tension temporarily as seen in figure 7. The effect of adding ethanol on water/air was previously discussed in chapter 3, we believe here is a similar case where IPA is a volatile and hydrophilic molecule so it briefly lowers the interfacial tension before equilibrium is reached. When we added nanoparticles, the surface-active IPA seemed to act first and lower the interfacial tension for around 30s before it starts rising until it stabilizes around a value slightly lower than the value of the indopol/water interface (18mN/m).

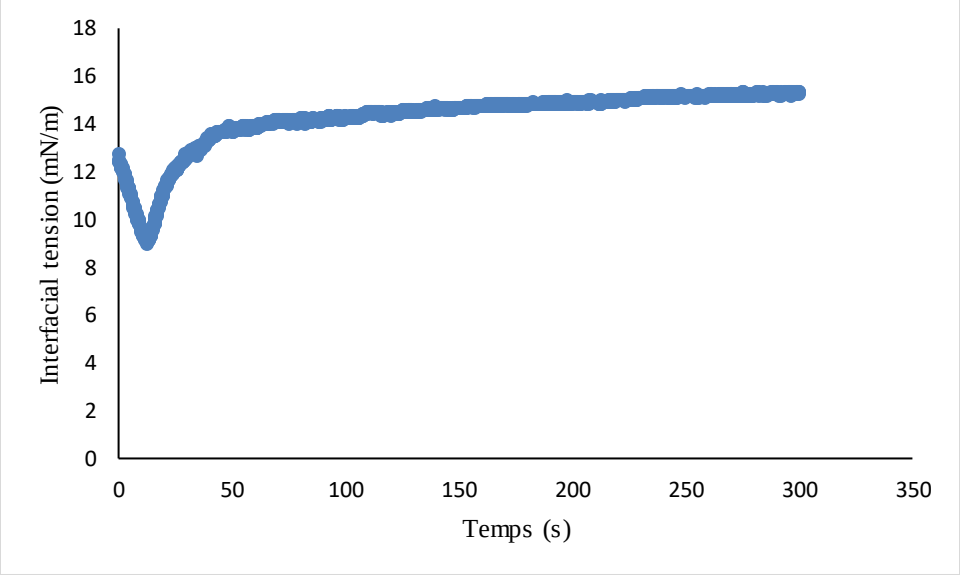

Figure 7: Isotherme IFT of the indopol L-8/water interface with the addition of 10% wt% of Isopropanol.

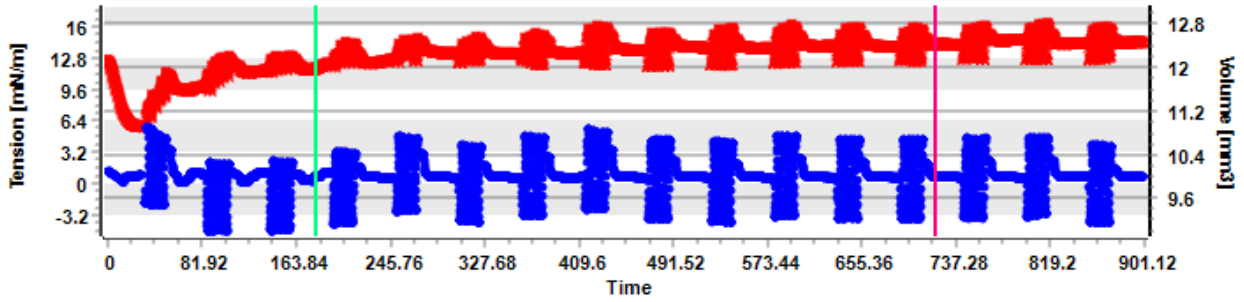

Figure 8: Oscillatory measurement of an indopol-L8 drop with 0.5% wt% R816 nanoparticles and 10% wt% Isopropanol.

6.4.2. Organoslicasol Nanoparticles (IPA)

To overcome the aggregation, we introduced a new type of nanoparticles: IPA-ST organosilicasol particles. They are amorphous silica NP dispersed in isopropanol (IPA), the introduction of isopropanol as a co-solvent changes the electro-steric interactions within the oil phase, giving the NP freedom to move. Moreover, IPA is a volatile hydrophilic molecule, much like in water-ethanol mixtures, it lowers the interfacial tension of water, but it quickly evaporates. In our setup, IPA lowers the oil/water interfacial tension and promotes NP adsorption and diffusion to the interface before it evaporates. Figure 5 shows the first test with IPA-ST.

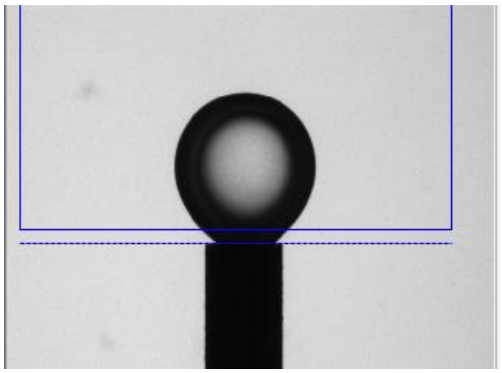

Figure 9: Aspect of a rising drop of IPA-ST + indopol mixture

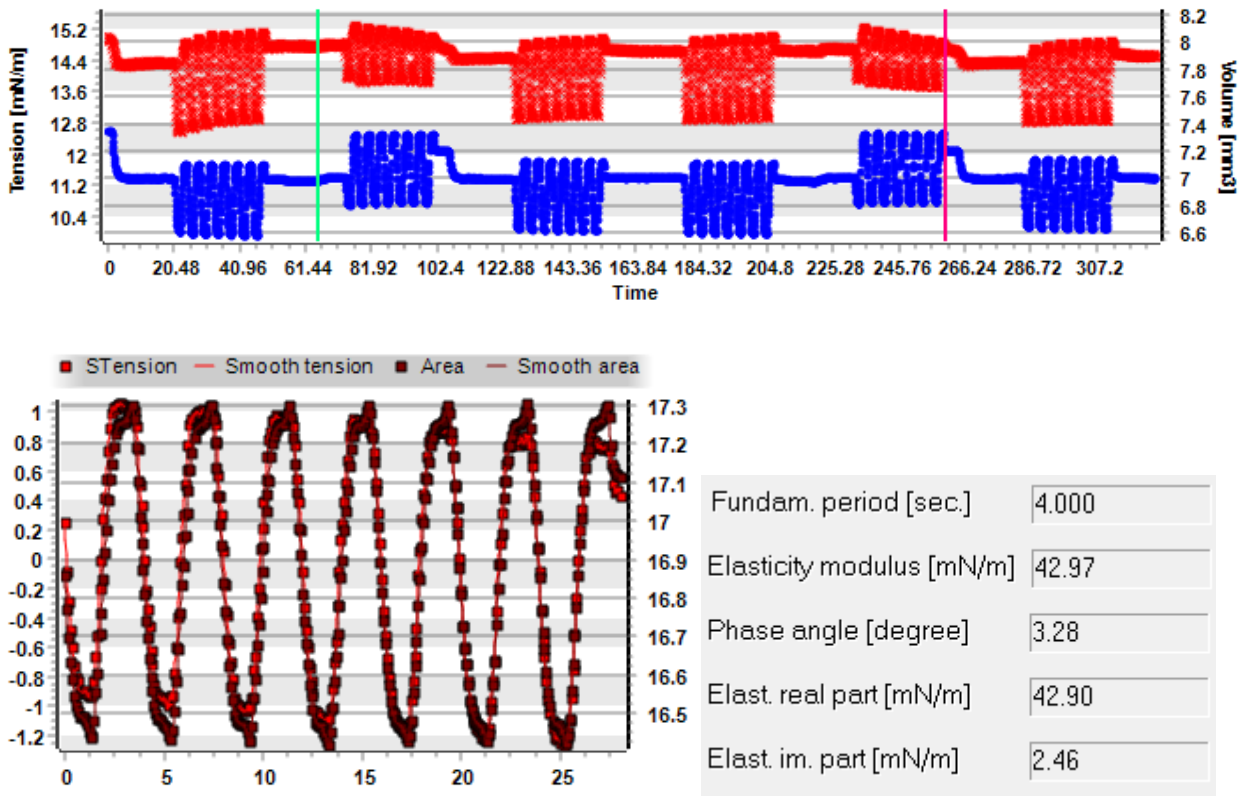

Figure 10: Analysis of the IFT signal after the oscillation of a drop profile of a drop of indopol + IPA 10% w/w% + organosilicasol IPA-ST nanoparticles 0.5% w/w%.

The resulting viscoelastic modulus is much higher this time (figure 10) and we do not see any visible aggregates in the droplet. We believe the IPA lowered the interfacial tension between the nanoparticles and the oil phase, improving the wetting conditions and allowing better mobility near the interface for an elastic layer to form. After 30s the interfacial tension stabilized at a slightly lower value than the pure water/oil IFT.

6.4.3. IPA-Aerosil mixtures

We moved to make our own mixtures using Aerosil NP with the same ratio of IPA (10w/w%) and NP (0.5%), below the results with Aerosil **R816** and fumed silica "**FS**" particles.

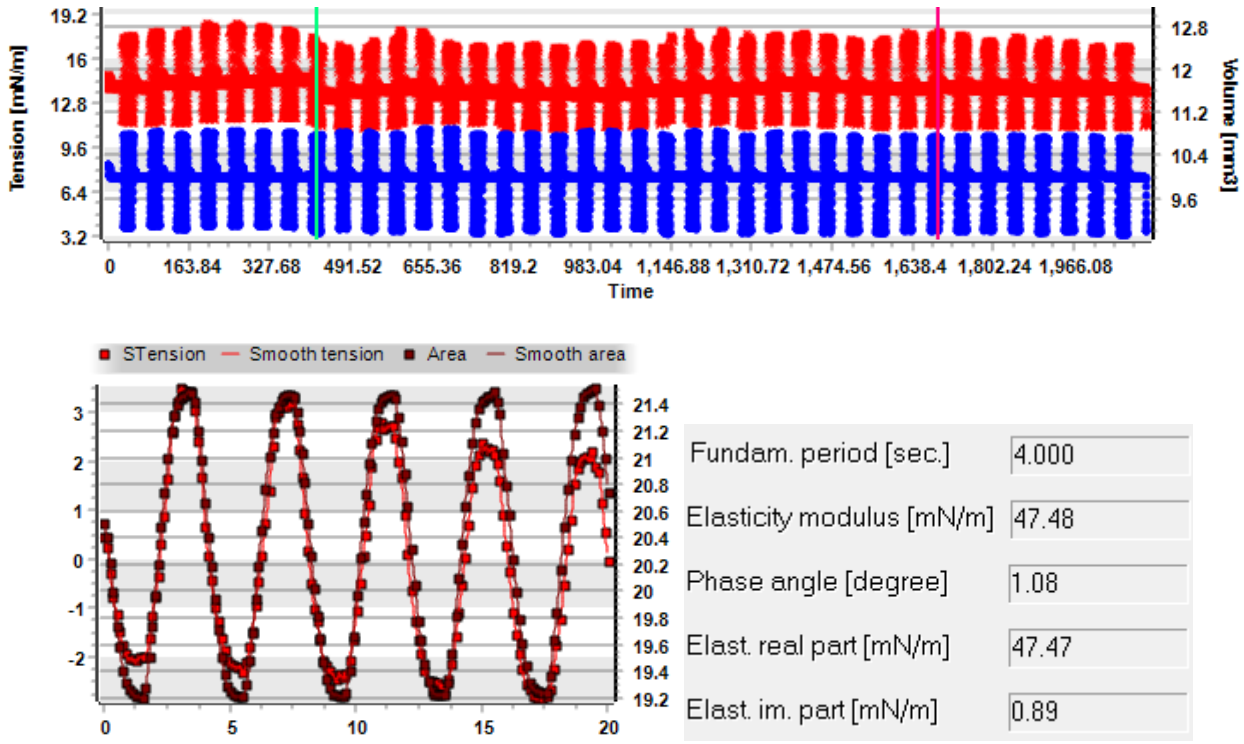

Figure 11: Analysis of the IFT signal after the oscillation of a drop profile of a drop of indopol + IPA 10% w/w% + R816 nanoparticles 0.5% w/w%.

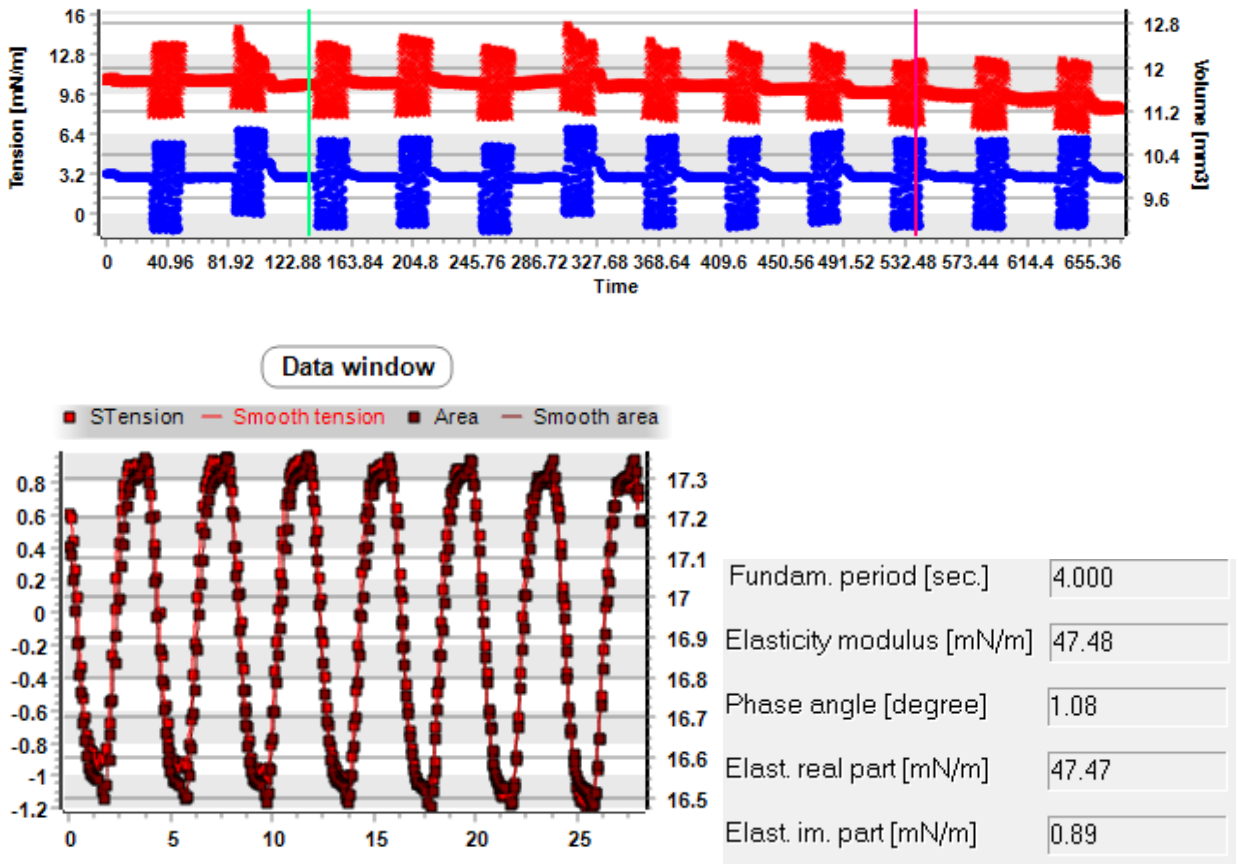

Figure 12: Analysis of the IFT signal after the oscillation of a drop profile of a drop of indopol L8 + IPA 10% w/w% + **FS** nanoparticles 0.5% w/w%.

6.5. PDMS with IPA

The last parameter we changed was the oil type from Polybutenes to polydimethylsiloxane (PDMS47V20). We found the initial IFT between water-PDMS to be 20mN/m. In an attempt to replicate the past experiments with PDMS at the same ratios of IPA (10%) and NP (0.5%), we noticed a significant drop of the IFT to 4mN/m before it stabilizes at 6mN/m, and for the FS and R816 we obtained a K^s' of 18mN/m and 15mN/m respectively (figure 13-14). In figure 15, the concentration of R816 was changed to 0.1% wt%, the first results were rather impressive with K^s' consistently at ±30mN/m in subsequent measurements.

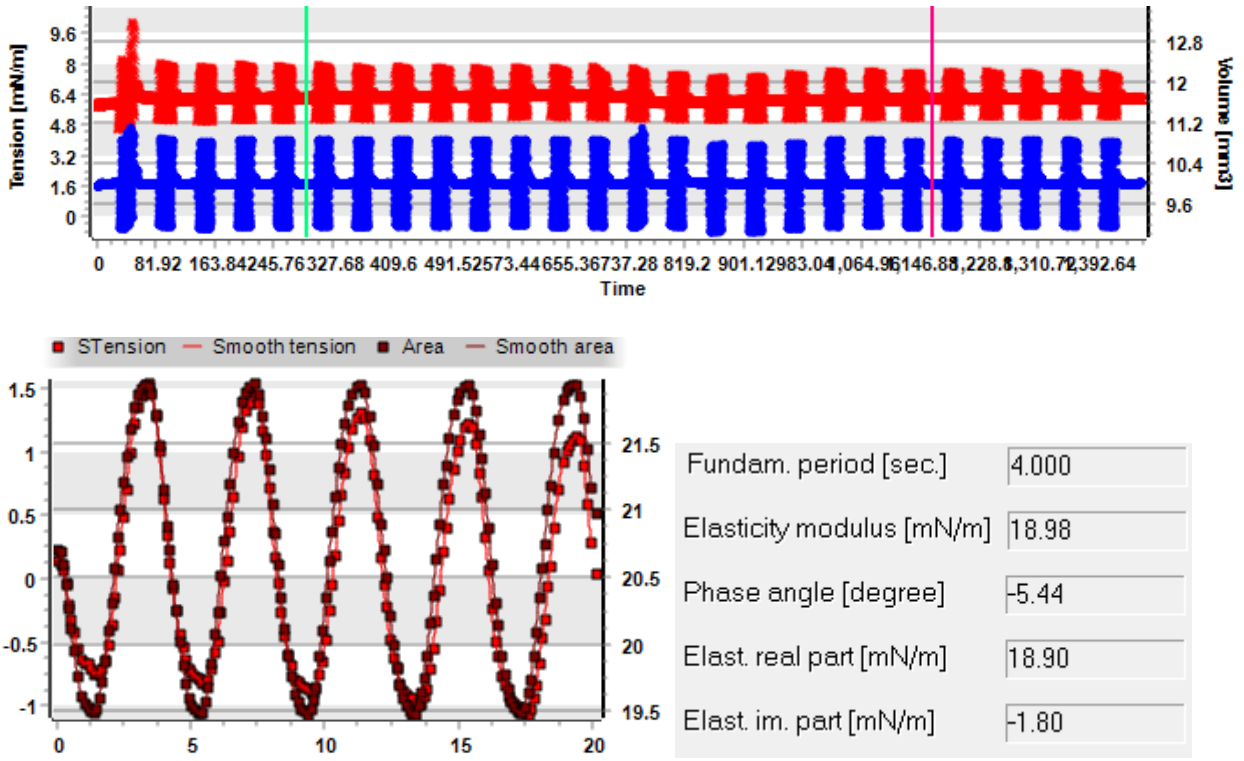

Figure 13: Analysis of the IFT signal after the oscillation of a drop profile of a drop of PDMS + IPA 10% w/w% + **FS** nanoparticles 0.5% w/w%.

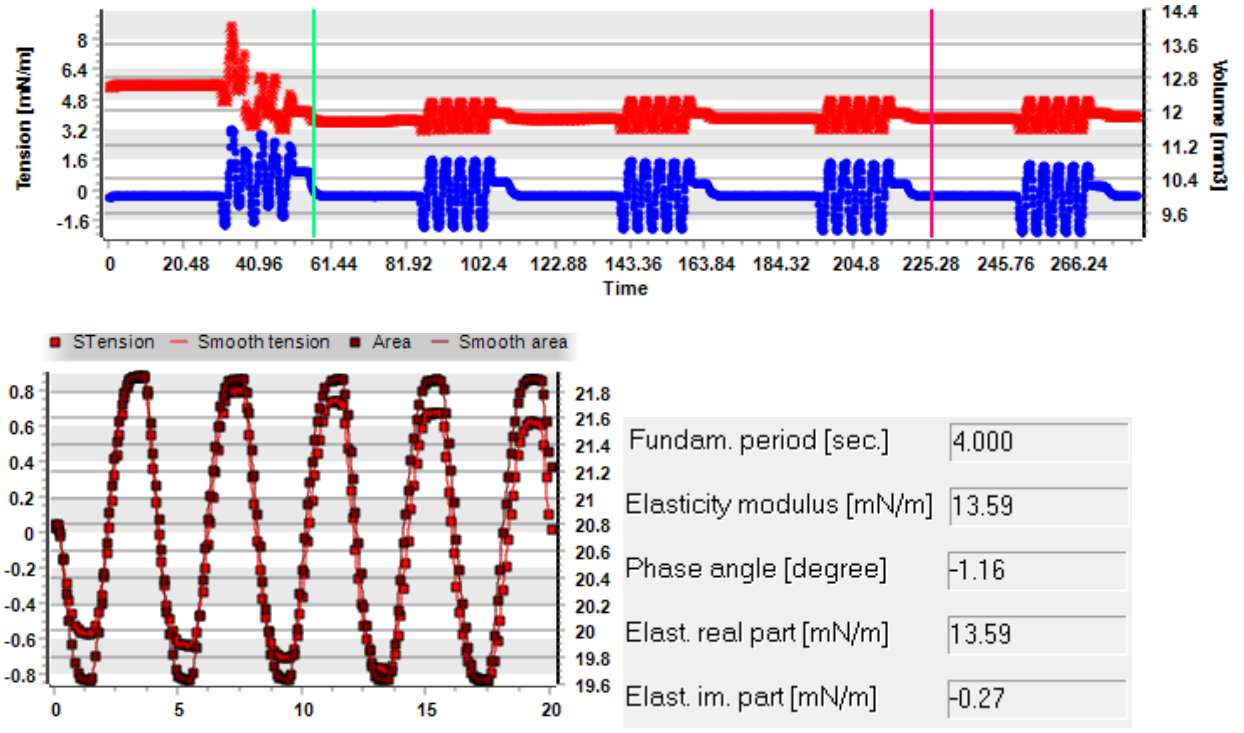

Figure 14: Analysis of the IFT signal after the oscillation of a drop profile of a drop of PDMS + IPA 10% w/w% + **R816** nanoparticles **0.5%** wt%.

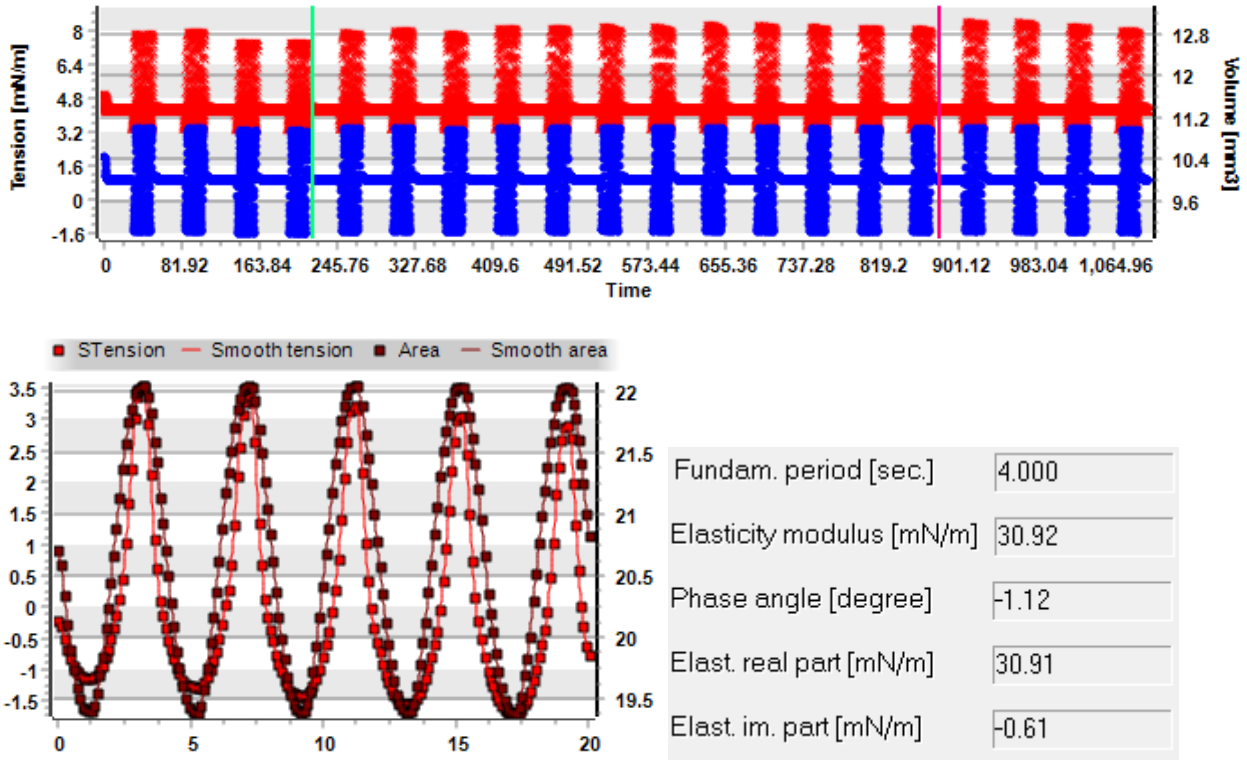

Figure 15: Analysis of the IFT signal after the oscillation of a drop profile of a drop of PDMS + IPA 10% w/w% + **R816** nanoparticles **0.1%** wt%.

R816 nanoparticles could adsorb to the water/PDMS interface whether at 0.5% or 0.1 wt%, and fumed silica "FS" have also shown capability to adsorb and provide interfacial elasticity (fig 13-15), these measurements with PDMS+IPA have yielded an elastic modulus in the range of 21-35mN/m in our experiments.

Indopol L-8 + IPA mixtures have yielded higher elastic moduli overall but in the same order of magnitude. This serves to validate our proof of concept where nanoparticles could adsorb by diffusion alone from within the drop, the role of IPA in this step could be understood if we consider the adsorption/desorption[6,7]:

$$E = \pi R^2 \gamma_{ow}^2 (1 \pm \cos\theta)$$

IPA lowers the interfacial tension between oil/water (fig. 7), decreasing momentarily the energy barrier for adsorption/desorption of nanoparticles, and once it is diffused, the adsorbed NP remain and the activation energy rises, "trapping" the particles at the interface.

On this note, we notice an interesting feature concerning the IFT: With indopol as the drop phase, the IFT at equilibrium is 12-14mN/m (lower than 18mN/m for the raw Indopol/water interface), and we record slightly higher K^s' values of 45mN/m and 37mN/m. With PDMS as the oil phase, the IFT decreases to 4-6mN/m and we record K^s' at 18-30mN/m for the same nanoparticles. A lower absolute value of IFT is not an indicator of a more efficient adsorption and interfacial viscoelasticity, as we can see the elastic modulus is higher in indopol+IPA mixtures than in PDMS+IPA.

The viscoelasticity of particle-laden interfaces comes from strong dipole-dipole interactions that arise from the charge distribution between the two phases, nanoparticle rearrange themselves.

6.6. Interfacial rheology in presence of KC

In this part, interfacial rheology experiments are conducted with indopol-isopropanol droplets (10% IPA) containing IPA-ST silica oscillating in water medium containing KC at a concentration of 5g/L. The silica concentration in oil is fixed to 0.5%. During the experiments, the temperature is varied from 30°C to 15°C. The results are displayed in figure 16 (right column). For the sake of comparison, the data with the same system but without particles are reported in the same figure (column of the left). Recall that the KC is liquid at 30 and 25°C while it becomes a gel at 15°C.

At temperatures of 30, 25 and 20°C, when the continuous medium is liquid, the elastic and viscous moduli and their evolution with the frequency depend on the presence or absence of particles. In the presence of silica particles, the interfacial elastic modulus is larger than the viscous modulus. In terms of frequency dependence, K^s' does not vary substantially with the frequency while K^s'' slightly increases. In addition, the trend and the values of K^s' and K^s'' are identical at 30, 25, and 20°C. Based on what we see, the trend of evolution of the elastic interfacial modulus versus frequency is not substantially affected but the value of the interfacial elastic modulus is significantly larger in the presence of silica at the interface. The difference is around one order of magnitude. This highlights the effect of the enhancement of the interfacial elasticity in the presence of adsorbed particles. This aspect has been already reported in several instances[8]. Conversely, the frequency evolution of the viscous modulus is not similar in the

presence and the absence of SiO_2. In the absence of silica particles, the viscous modulus increases sharply with the frequency. The presence of particles adsorbed reduces the slope of the K^s'' vs frequency curves and K^s'' increases only slightly with the frequency. It appears also that the viscous modulus is higher in the presence of silica in the whole range of frequency. At the largest frequency of 1 Hz, the two moduli reach approximately the same value.

At 15°C, the KC forms a gel in the aqueous continuous phase. As expected, the shapes of the K^s' vs frequency and K^s'' vs frequency curves are affected by the switch from a liquid state to a gel state: K^s' increases linearly with the frequency at 15 °C while it remains constant at 30-20 °C. The viscous modulus tends to decrease at high frequency when KC is a gel while it slightly increases under liquid state of the continuous phase. Additionally, the elastic interfacial modulus reaches higher values at 15°C compared to those obtained at larger temperatures. The same conclusions apply for the viscous interfacial modulus.

It is also relevant to compare the impact of the particles on the K^s' and K^s'' interfacial moduli. To this aim, we discuss the data obtained at 15°C in the presence and in the absence of particles. The presence of silica does not modify the shape of the curves (K^s' vs frequency and K^s'' vs frequency). This indicates that the frequency trend of the modulus are driven by the gel continuous phase rather than the layer of particles when the continuous phase is under the form of a gel. Moreover, the presence of the adsorbed layer of particles enhances the elastic character of the interface since the K^s' values with silica are larger than those in the absence of particles. This emphasizes that the interfacial layer of particles improves the elasticity of the interface and the system. It can be considered that the elastic modulus in the presence of silica and gel of KC is the sum of the contribution of the elastic modulus of the particles at the interface and the contribution of the gel continuous phase. The interaction between a hard silica interface layer and a hard gel in the continuous phase strengthens the elasticity of the system. The same conclusions can be drawn also with the viscous modulus.

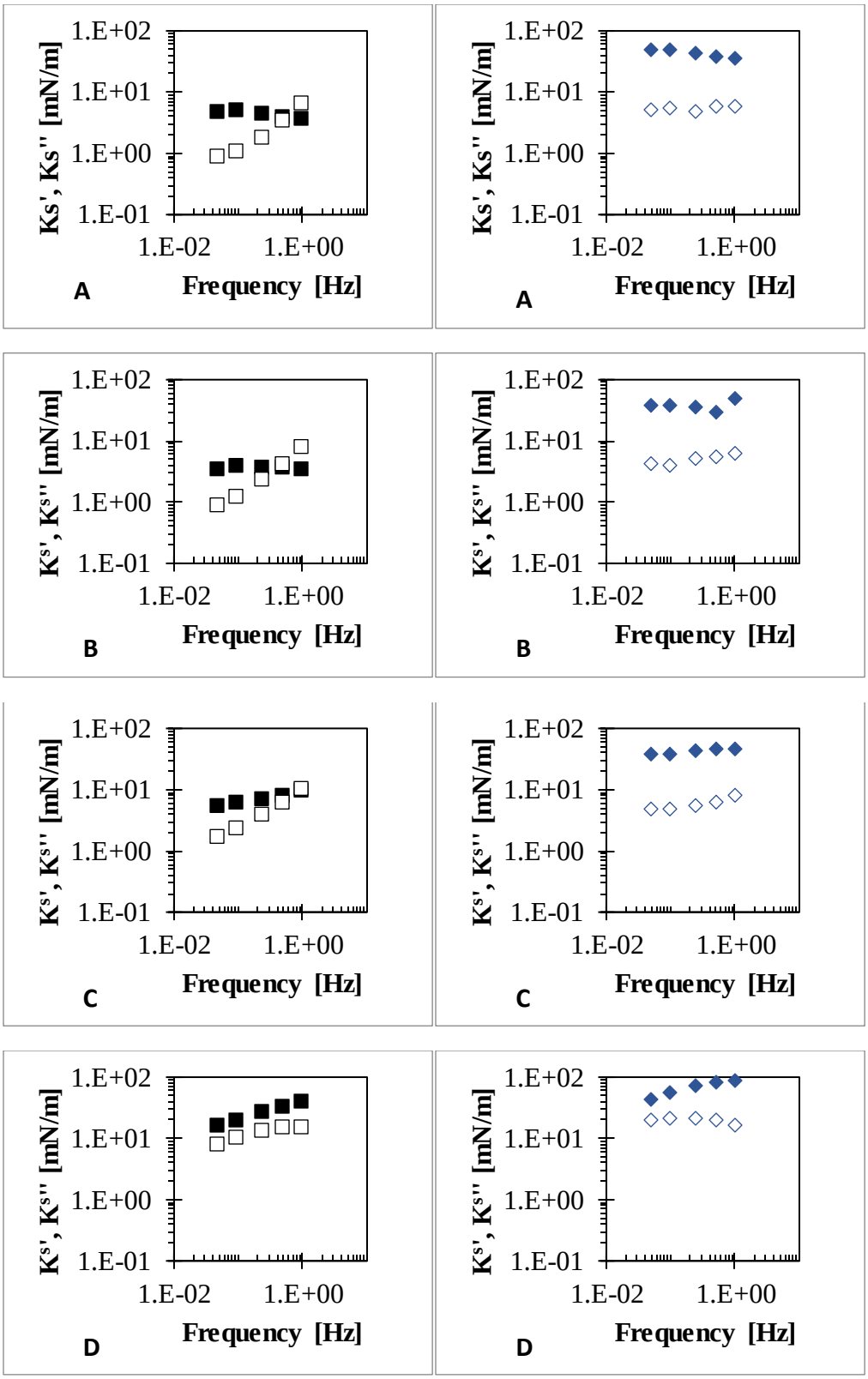
1.E+02
1.E+01
1.E+00
1.E-01
1.E-02
1.E+00
Ks', Ks'' [mN/m]
Frequency [Hz]
A
A
B
B
C
C
D
D

Figure 16: Isothermal frequency dependence of K^s' and K^s" in presence of KC 5g/L in the bulk phase without silica particles (right-hand column) and with 0.5% of R816 silica particles layer adsorbed at the interface (left-hand column). In all the cases, the KC concentration is equal to 5 g/L and the isopropanol concentration reads as 10% in the indopol/isopropanol/silica drop phase. A: 30°C, B: 25°C, C:20°C, D: 15°C

6.7. Comparison of particles and surfactants laden interfaces

In the framework of this thesis, surfactant and particles were addressed and put into contact with a continuous phase containing KC under the form of a gel or a liquid state. It seems pertinent to compare the results obtained with span and silica in the presence of KC. The two systems adsorb at the interface and create hard solid interfacial layer for silica and soft interfacial layer with span, respectively. The results were already presented in this thesis in this chapter for the particles (Figure 16) and in the previous chapter for the surfactant (Figure 3 from chapter 4). In both situations, KC of 5g/L was employed for temperatures between 30 and 15°C. Consequently, we decided not to redraw the figures and only discuss the results and the main conclusions. The situations for which the KC is liquid and solid gel are treated separately.

When the KC is liquid, the presence of span and particles at the liquid/liquid interface increases the elastic modulus of the interface. Both soft (span) and hard (mineral particles) layers at the interface enhance the elastic modulus of the interface. However, the value of K^s' with particles is substantially larger than that with span meaning that the hard interfacial layer leads to higher interfacial elasticity than with soft interfacial layer. This kind of conclusion was already observed[9]. However, only one silica content was used. Moreover, this conclusion remains valid for two span concentrations and various KC contents. The conclusions presented in this chapter concern hard particles and surfactants but the question arises also with soft particles or macromolecules such as proteins. The scientific literature[10–13] seems to show that there could be a relatively continuous evolution when we go from hard particles to polymers through soft particles up to surfactants. The general trend shows that all improves when the particles go from rigid (hard particles) to molecular (macromolecules, proteins or surfactants).

When the KC becomes a gel, the interfacial elastic modulus remains the highest with the silica layer. More interestingly, when compared with the bare interface (without silica and surfactant), two trends can be extracted. When the interface is covered with hard silica particles, the presence of silica enhances the elasticity of the interface (K^s' (silica/KC) >> K^s' (KC)). Conversely, in the case where the interface is covered with a layer of soft surfactant, the presence of span weakened the elasticity of the interface. In other words, K^s' (span/KC) << K^s' (KC). As already discussed, the presence of the gel in the continuous phase affects the elasticity of the interface. It appears also that the hardness of the adsorbed species at the liquid/liquid interface creating a soft or hard interfacial layer impacts the final elasticity measured. The interaction between the interface and the continuous phase plays a major role in the final elasticity. When the solid continuous gel is put into contact with soft surfactant interfacial layer, a hard/soft interaction occurs. This produces a reduction of the interfacial modulus due to shear-like banding. The apparent interfacial modulus K^s' apparent seems to take into account the contribution of the KC bulk reduced by the contribution of the span layer. This can be written as

$$K^s\text{' apparent (hard/soft)} \approx K^s\text{'(KC)} - K^s\text{'(span layer)}$$

$$K^s\text{' apparent (hard/soft)} \approx K^s\text{'(bulk gel)} - K^s\text{'(soft layer)}$$

The opposite takes place when the drop covered with a hard silica layer oscillates in a continuous gel phase. A hard/hard interaction comes into play. An enhancement of the apparent interfacial modulus is obtained. K^s'apparent includes the contribution of the KC bulk and the silica layer. In that situation, the apparent elasticity reads as:

$$K^s\text{' apparent (hard/hard)} \approx K^s\text{'(KC)} + K^s\text{'(silica layer)}$$

$$K^s\text{' apparent (hard/hard)} \approx K^s\text{'(bulk gel)} + K^s\text{'(hard layer)}$$

6.8. Conclusions

In this chapter we explored the possibility of measuring the interfacial viscoelasticity of nanoparticle-laden interface without bulk phase contribution, for this reason we used the rising drop method where the nanoparticles were added to the oil phase and left to diffuse to the interface, the chosen silica particles were hydrophobic silica that could disperse well in the drop phase. In actual tests, diffusion was not enough to fix enough NP on the interface because the affinity of the droplets meant they couldn't cross the energy threshold, we couldn't record a significant viscoelastic modulus. To solve this issue, we changed the wetting properties of the drop by adding isopropanol (IPA), which lowered interfacial tension and facilitated NP adsorption near the oil/water interface. With this proof of concept, we can move on to study the structured interface in an adjustable continuous phase: The addition of a thermosensitive hydrogel (KC), which seems to reinforce the elastic monolayer, at least in comparison with a surfactant monolayer. Much work is still needed in this regard, but the topic is quite promising for further research.

References

(1) Roques-Carmes, T.; Lebrun, M.; Wang, Y.; Ramos, D.; Marchal, P.; Sadtler, V. Comparison of Rheological Methods to Obtain a Sufficient Sensitivity with Shear Interfacial Rheology in the Presence of Nanoparticles at Liquid/Liquid Interfaces. *Silicon* **2022**. https://doi.org/10.1007/s12633-022-02138-z.

(2) Barros, F. M. F.; Chassenieux, C.; Nicolai, T.; de Souza Lima, M. M.; Benyahia, L. Effect of the Hydrophobicity of Fumed Silica Particles and the Nature of Oil on the Structure and Rheological Behavior of Pickering Emulsions. *J. Dispers. Sci. Technol.* **2018**.

(3) Velandia, S. F.; Ramos, D.; Lebrun, M.; Marchal, P.; Lemaitre, C.; Sadtler, V.; Roques-Carmes, T. Exploring the Link between Interfacial and Bulk Viscoelasticity in Reverse Pickering Emulsions. *Colloids Surf. Physicochem. Eng. Asp.* **2021**, *624*, 126785.

(4) Ramos, D.; Sadtler, V.; Marchal, P.; Lemaître, C.; Benyahia, L.; Carmes, T. R. Insight into the Emulsification Process Effect on Particles Distribution in Pickering Emulsions: A Series of Rheological and Gravimetric Tests. *Chem. Eng. Trans.* **2021**, *86*, 1291–1296.

(5) Binks, B. P.; Lumsdon, S. O. Pickering Emulsions Stabilized by Monodisperse Latex Particles: Effects of Particle Size. *Langmuir* **2001**, *17* (15), 4540–4547. https://doi.org/10.1021/la0103822.

(6) Young, T. III. An Essay on the Cohesion of Fluids. *Philos. Trans. R. Soc. Lond.* **1805**, No. 95, 65–87.

(7) Tadros, T. F. Emulsion Formation, Stability, and Rheology. *Emuls. Form. Stab.* **2013**, *1*, 1–75.

(8) Deshmukh, O. S.; van den Ende, D.; Stuart, M. C.; Mugele, F.; Duits, M. H. G. Hard and Soft Colloids at Fluid Interfaces: Adsorption, Interactions, Assembly & Rheology. *Adv. Colloid Interface Sci.* **2015**, *222*, 215–227. https://doi.org/10.1016/j.cis.2014.09.003.

(9) Yazhgur, P. A.; Noskov, B. A.; Liggieri, L.; Lin, S.-Y.; Loglio, G.; Miller, R.; Ravera, F. Dynamic Properties of Mixed Nanoparticle/Surfactant Adsorption Layers. *Soft Matter* **2013**, *9* (12), 3305–3314.

(10) Barman, S.; Christopher, G. F. Simultaneous Interfacial Rheology and Microstructure Measurement of Densely Aggregated Particle Laden Interfaces Using a Modified Double Wall Ring Interfacial Rheometer. *Langmuir* **2014**, *30* (32), 9752–9760.

(11) Jaishankar, A. Interfacial Rheology of Globular Proteins, Massachusetts Institute of Technology, 2011.

(12) Thijssen, J. H.; Vermant, J. Interfacial Rheology of Model Particles at Liquid Interfaces and Its Relation to (Bicontinuous) Pickering Emulsions. *J. Phys. Condens. Matter* **2017**, *30* (2), 023002.

(13) Pinaud, F.; Geisel, K.; Massé, P.; Catargi, B.; Isa, L.; Richtering, W.; Ravaine, V.; Schmitt, V. Adsorption of Microgels at an Oil–Water Interface: Correlation between Packing and 2D Elasticity. *Soft Matter* **2014**, *10* (36), 6963–6974.

Annexes

A.1) Macroscopic Aspect of dispersions

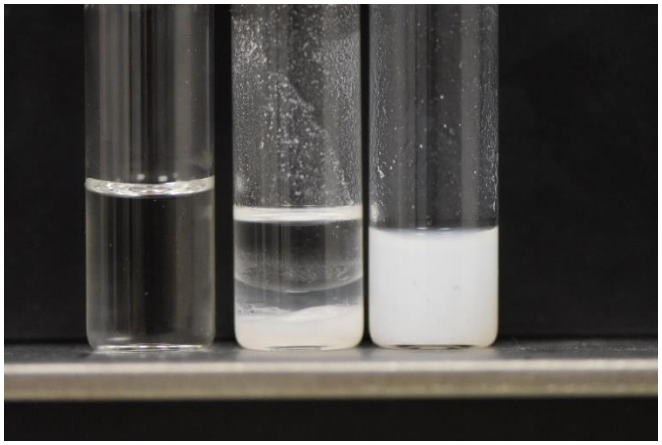

Annex 1: Fumed silica R816 nanoparticles in water, from left to right: 0%, 1% and 5% w/w%. A few hours after preparation.

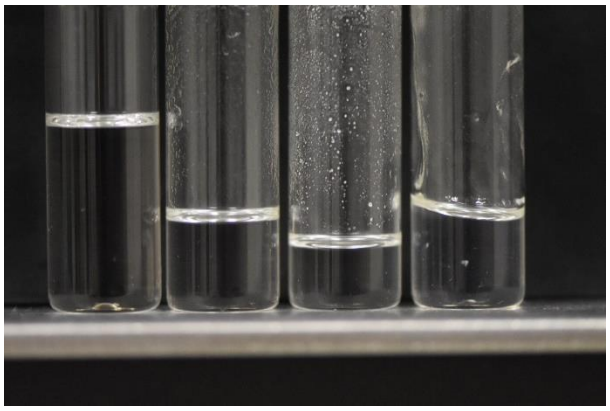

Annex 2: Fumed silica R816 nanoparticles in Indopol oil, from left to right: 0%, 1%, 4%, 5% w/w%.

General Conclusion

This work focused on the interfacial rheology of an oil/water interface in the presence of an adjustable continuous phase to deconvolute the viscoelasticity of complex systems where the effect of the bulk and interface go hand-in-hand.

In chapter IV, we presented our model system for the oil/water phase with an adjustable viscoelastic continuous phase in the form of thermo-reversible cross-linking polysaccharide: k-carrageenan known for having no surface activity. Shear rheology with a stress-controlled rheometer was used to follow the temperature dependence of sol-gel transition and the evolution of the viscoelasticity of the bulk KC for concentrations between 2 to 6g/L. Then static tensiometry was used followed by dilatational interfacial rheology using the same conditions for shear 3D rheology. As results we found that samples prepared from KC were liquid at T > 25°C and weak gels at 20°C for concentrations starting at 4g/L marked by G' plateaus at less than 1Pa. The gel transition was found to be reversible with noticeable hysteresis feature when we compared frequency sweeps curves for the same temperature for 4-6g/L. Static tensiometry with the rising drop method proved that KC was not surface active ruling out any possible contribution from adsorbed layers. Meanwhile, dynamic dilatational rheology revealed an apparent increase in the elastic moduli K^s' upon the sol-gel transition and hysteresis feature during a cooling-reheating cycle. Upon comparison between the tensiometry and shear rheology curves we found similar viscoelastic behavior of KC gel in reflected in our results meaning which means that the manifestation of interfacial viscoelasticity does not necessarily mean the existence of an interfacial layer with a mechanical character but may come from the volume contribution.

In chapter V, we studied the effect of the KC gel on a surfactant-laden oil/water interface with the same goal to check the interference of the continuous phase on the interfacial rheology, therefore we chose Span 80 because it is a liposoluble surfactant that can adsorb to the interface from the drop phase, avoiding any possible interaction with KC in the bulk phase. First, we traced the adsorption isotherms of Span 80 for various concentrations to find the CMC. With the highest possible surface coverage for our setup at 0.05% and 0.1% Span 80, we conducted dynamic drop measurements with KC at various concentrations and temperatures to evaluate the

effect of KC in both liquid and gel states. To complement the interfacial rheology findings, emulsions were prepared at 60/40 and 70/30 water/oil ratios only with a vortex shaker, the macroscopic and microscopic structure were examined visually and using confocal microscopy and shear rheology.

In results, we found that in our setup we could reach a surface coverage of $\Gamma = 2.13.10^{-6}$ mol/m^2 with Span 80 concentration of 0.1% with γ = 4.78mN/m. The drop would detach at this concentration due to low interfacial tension vs gravity so we conclude it is not the CMC yet. Since it is sufficient to study the viscoelasticity of the adsorbed layer, we chose to work with 0.05% and 0.1% Span 80. Next, we used the various KC solutions as the bulk phase. We found that for KC liquid + Span 80 the combined signature was dominated by the Span 80 layer at ~10mN/m but for KC gel + Span 80 the stronger elasticity of the gel dominates with a recurring trend where K^s' reaches a lower value (~30mN/m) than the pure oil/KC gel interface (~40mN/m). The exact cause of this drop in K^s' is still not perfectly clear but we believe it is caused by strain-like banding where the surfactant the layer would slip vis-à-vis the hard gel surrounding. Emulsions were prepared by adding water to the oil+Span 80 phase then mixing with a vortex shaker, for emulsions with KC the same procedure but the gel is liquified at 60°C for easier mixing. The emulsions were visually water-in-oil and showed a gel-like behavior when tilted, confocal microscopy revealed they were densely packed W/O emulsions and shear rheology showed their G' plateau at 10Pa and as a densely packed emulsion this elasticity is mostly attributed to the elasticity of interfaces. The addition of KC gel increases the moduli of the emulsion contrary to the interfacial rheology measurements where a decrease of elasticity is observed, we acknowledge that the conditions in both setups are not the same: In drop experiments we measure a signle drop with a soft interface in dilatation surrounded by a hard gel, in shear 3D rheology it is the entire bulk was deformed.

Finally, chapter VI is an exploratory study of the effect of the KC gel on a nanoparticle-laden interface where nanoparticles are meant to adsorb from the drop to the interface with the same gel. First, we started with amphiphilic Aerosil fumed silica nanoparticles modified with alkyl groups to be more hydrophobic R816 and R202, they did not result in a strongly elastic interface with little modification of the interfacial tension due to their affinity and the adsorption energy barrier. To solve this we tried amorpheuous silica nanoparticles dispersed in isopropanol (IPA),

the isopropanol lowered for 30s the oil/water interfacial and allowed nanoparticles to adsorb more readily as evidenced by K^s' at 30mN/m, similar results were observed when we mixed Aerosil fumed silica nanoparticles with IPA, finally we tested NP-laden interface in presence of KC and we found an increase of the modulus from 30mN/m to 91mN/m. These results serve as proof of concept that we can cover an interface with NP by using IPA as a co-solvent and that we can measure an increased interfacial elastic modulus in presence of KC.

Our last observation was the contrast between the Span 80-gel ("soft" molecular layer/hard gel) and NP- gel (hard spheres layer/hard gel) combinations. In the former there was a noticeable increase of the gel elastic modulus whereas in the latter a cumulative effect is observed.

$$K^s\text{'apparent (hard/soft)} \approx K^s\text{'(bulk gel)} - K^s\text{'(soft layer)}$$

$$K^s\text{'apparent (hard/hard)} \approx K^s\text{'(bulk gel)} + K^s\text{'(hard layer)}$$

This contrast is quite interesting because the trend with Span 80 was surprising, more work is needed on this subject.

Perspectives

This thesis provides guidelines for measuring the viscoelasticity of interfaces laden with surface active molecules in the presence of weak gels representing complex systems to be deconvoluted. It is a novel multi-scale approach to link 2D interfacial rheology and 3D rheology with many possible future perspectives.

For starters, we only used the oscillating drop method for interfacial rheology measurements in conjecture with shear 3D rheology. It would be interesting to use shear dilatational rheology (double wall ring for example) for a more direct 2D-3D comparison as the modes of deformation are the same, it is also known interfaces exhibit both shear and dilatational viscoelasticity when the bulk is deformed.

In chapter V, we used Span 80 as the surfactant as it is soluble in oil but there the rapid decrease of interfacial tension and detachment of the drop limited the Span 80 concentration to 0.1% w/w%, the static tensiometry showed it is not the CMC. It could be possible to perform the measurements with a complete monolayer by changing the type of surfactant for brij for example (figure 1) or trying another oil phase (PDMS). A more in-depth study of adsorption kinetics could also help in better understanding the relaxation processes of the expanding/compressing interface.

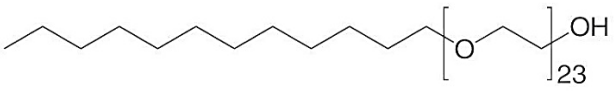

Figure 1: Chemical formula of Brij® 35

Emulsions were also attempted in this study. We aimed to prepare densely packed emulsion for a direct assessment of the interfacial contribution as discussed previously and preferably the emulsions would be O/W to be more comparable with drop profile tensiometry especially when KC is added. It can also be done with the W/O emulsions we have here while taking into account the gel within the droplets.

Chapter VI serves as a proof of concept and shows promising signs as the elastic modulus increased upon adding KC. However further testing is needed with the oscillating drop to confirm the trend with different concentrations of KC and NP while also varying the type of NP and oil phase (different viscosities…). Another aspect is the emulsion which we did not have enough time to explore.

Finally, numerical simulation and modelling could be very helpful to generalize the study starting with the pure Oil/KC interface as we know the physical parameters both in interfacial rheology and bulk rheology. It would also help in understanding more clearly the reason behind the decrease of K^{s}' upon the addition of Span 80 as well as the contrast between the Span 80-KC

and Silica NP-KC systems to confirm our hypothesis regarding the soft/hard and hard/hard interfaces. All of these fundamental concepts are a step towards a complete deconvolution of complex emulsion systems and highlighting the role of interfacial viscoelasticity and a potential relationship with bulk 3D rheology.